Primary production in shallow freshwater systems amid a rapidly changing world

D i s s e r t a t i o n

zur Erlangung des akademischen Grades

d o c t o r r e r u m n a t u r a l i u m

(Dr. rer. nat.)

im Fach Biologie

eingereicht an der

Lebenswissenschaftlichen Fakultät

der Humboldt-Universität zu Berlin

von Garabet, Kazanjian

Präsidentin der Humboldt-Universität zu Berlin

Prof. Dr.-Ing. Dr. Sabine Kunst

Dekan der Lebenswissenschaftlichen Fakultät

Prof. Dr. Bernhard Grimm

Gutachter/innen:
1. PD Dr. Sabine Hilt
2. Prof. Dr. Kurt Zoglauer
3. PD Dr. Irmgard Blindow

Tag der mündlichen Prüfung: 12. September 2019

PREFACE

The majority of this work was conducted at the Leibniz-Institute of Freshwater Ecology and Inland Fisheries, Department of Ecosystem Research, Müggelseedamm 301, 12587, Berlin, Germany. The experiments involving the limnotrons were carried out at the Netherlands Institute of Ecology (NIOO-KNAW), Droevendaalsesteeg 10, 6708 PB, Wageningen, Netherlands. My work was funded by the Landscales Project (http://igb-berlin.de/projekt/landscales) and was under the supervision of Drs. Sabine Hilt, Jan Köhler, Katrin Premke, and Sarian Kosten.

This thesis is based on the following manuscripts that are referred to in the text by their Roman numerals:

I. **Kazanjian, G.**, S. Flury, K. Attermeyer, T. Kalettka, A. Kleeberg, K. Premke, J. Köhler, & S. Hilt, 2018. Primary production in nutrient-rich kettle holes and consequences for nutrient and carbon cycling. Hydrobiologia 806: 77–93. doi: 10.1007/s10750-017-3337-6.

II. **Kazanjian, G.**, M. Velthuis, R. Aben, S. Stephan, E. T. H. M. Peeters, T. Frenken, J. Touwen, F. Xue, S. Kosten, D. B. Van De Waal, L. N. De Senerpont Domis, E. Van Donk, & S. Hilt, 2018. Impacts of warming on top-down and bottom-up controls of periphyton production. Scientific Reports 8: 1–12, doi:10.1038/s41598-018-26348-x.

III. **Kazanjian, G.**, S. Brothers, J. Köhler, & S. Hilt. Resilience of a temperate shallow lake to a brownification event. *Submitted*. Preprint DOI: doi.org/10.1101/658591.

TABLE OF CONTENTS

SUMMARY

Small, shallow freshwater ecosystems (kettle holes, ponds, small lakes) are now considered hotspots of primary production and carbon sequestration. Yet till recently they've been mostly neglected in ecological research. This humble thesis aims at filling a much-needed gap in literature to quantify primary production and explain the underlying mechanisms affecting carbon cycling in these systems, particularly focusing on how contemporary global changes alter these mechanism and ecological equilibria.

In the first section, using a compartmental approach, I thoroughly study primary production in small, temporary ponds (kettle holes) that are highly susceptible to environmental and anthropogenic disturbances. These ecosystems receive high nutrients from surrounding agricultural fields and undergo significant water level fluctuations. I show that summertime gross primary production (GPP) in kettle holes is exceptionally high, mostly driven by a strong macrophyte production. Outside of the macrophyte growing season, periphyton contributes to the majority of the systems' GPP. We also show high summertime deposition rates – correlated to GPP rates – indicating, that the majority of deposited material comes from autochthonous sources. Despite the high deposition rates, we found sediment mineralization rates to be relatively low due to the long periods of anoxia that the kettle holes undergo. This creates a high potential for carbon burial in the sediments, and thus the kettle holes likely being carbon sinks, as long as they don't fully dry up in warmer and dryer years.

In the second experiment, I test the impact of increased temperatures on benthic (periphyton) production during spring. For this purpose, I make use of eight 1000L mesocosms (limnotrons) running at normal and +4°C temperatures. During the first half of the experiment, I recorded elevated periphyton GPP in the warmed treatment driven by direct temperature effects and indirect effects of higher nutrient availability in said treatment. However, by early June, the trend is reversed due to increased grazing pressure in the warm treatment. I discuss the repercussions of these changes in potential future global warming scenarios, leading to food web mismatches and changes in the lakes' stable states. The studied period is very important to the growth of macrophytes in lakes, which might be overshadowed by increased periphyton production in the future.

In the third and last study, I aim to investigate a lake's resilience to a sudden brownification event (reported in Brothers et al. 2014). I highlight changes in the water quality parameters and aquatic primary production of the lake, wherein dissolved organic carbon (DOC) concentrations had increased five-fold. Within three years after peak brownification, the lake DOC and total phosphorous concentrations dropped significantly but seem to have plateaued 1.5 and 2-fold

their pre-brownification levels, respectively. Reflecting these water level parameters, primary production also exhibited only a partial recovery. Benthic primary production, which had collapsed due to light limitation in peak brownification conditions, marked a partial recovery, while phytoplankton (and whole-lake) GPP decreased but remained higher than pre-brownification levels. Thus, phytoplankton and periphyton exhibited an inverse response to DOC and TP concentration. The differential response of primary producers to brownification supports previous models, while also covering a wider DOC concentration range unreported before. I show that a full lake recovery might not occur or would take much longer than the onset of brownification. I argue that the partial return of the lake DOC concentrations might be a component of the long-term increase of DOC concentrations in freshwater ecosystems in the northern hemisphere and predict the effect of expected weather changes to this phenomenon.

ZUSAMMENFASSUNG

Kleine, flache Gewässer (Teiche, kleine Seen) gelten als sogenannte „hotspots“ der Primärproduktion und Kohlenstoffbindung. Dennoch wurden sie in der ökologischen Forschung lange weitgehend vernachlässigt. Diese Doktorarbeit zielt darauf ab, die Primärproduktion verschiedener kleiner Gewässer zu quantifizieren sowie die Mechanismen, die den Kohlenstoffkreislauf dieser Systeme beeinflussen, zu analysieren. Der Fokus liegt dabei auf dem Einfluss globaler Veränderungen, die diese Mechanismen verändern können.

Im ersten Abschnitt wurde die Primärproduktion in kleinen, temporären Söllen untersucht, die sehr anfällig für natürliche und anthropogene Störungen sind. Diese Ökosysteme sind aufgrund der Einträge aus den umliegenden landwirtschaftlichen Flächen sehr nährstoffreich und unterliegen erheblichen Wasserstandsschwankungen. Ich konnte zeigen, dass die Primärproduktion der Sölle im Sommer außergewöhnlich hoch ist, was hauptsächlich auf eine hohe Makrophytenproduktion zurückzuführen ist. Außerhalb der Wachstumsperiode der Makrophyten dominiert der Aufwuchs (Periphyton) die Primärproduktion der Sölle. Hohe Kohlenstoff-Ablagerungsraten im Sommer, die positiv mit den Primärproduktionsraten korreliert sind, deuten auf ein Überwiegen autochthoner Quellen im abgelagerten Material. Trotz der hohen Ablagerungsraten waren die Mineralisierungsraten des Sediments aufgrund der langen anoxischen Perioden in den Söllen relativ niedrig. Dies führt zu einem hohen Ablagerungspotential von Kohlenstoff in den Sedimenten. Somit sind die Sölle wahrscheinlich Kohlenstoffsenken, solange sie nicht vollständig austrocknen.

Im zweiten Teil zeige und analysiere ich die Ergebnisse eines Experiments zum Einfluss erhöhter Temperaturen auf die benthische Primärproduktion kleiner Gewässer im Frühjahr. Acht Mesokosmen mit Sediment und 1000 Liter Wasser wurden bei normalen und um 4 °C erhöhten Wassertemperaturen gemäßigter Breiten betrieben. In der ersten Hälfte des Experiments konnte ich eine erhöhte benthische Primärproduktion in den erwärmten Mesokosmen feststellen, die auf direkte Temperatureffekte und indirekte Auswirkungen einer höheren Nährstoffverfügbarkeit zurückzuführen war. Anfang Juni stieg jedoch der Einfluss der Makroinvertebraten auf das Periphyton in den erwärmten Mesokosmen, so dass keine Unterschiede in der Primärproduktion mehr auftraten. Die Auswirkungen dieser Veränderungen auf potenzielle zukünftige Szenarien der globalen Erwärmung, die zu Verschiebungen im Nahrungsnetz und zu Veränderungen in den stabilen Zuständen von Seen führen können, werden diskutiert. Der untersuchte Zeitraum (Frühjahr-Frühsommer) ist entscheidend für das Wachstum von submersen Makrophyten in Seen gemäßigter Breiten, die in der Zukunft bei höheren Wassertemperaturen möglicherweise durch die erhöhte Primärproduktion des Periphytons stärker beschattet werden.

In der dritten Studie untersuche ich die Resilienz eines kleinen Sees gegenüber einem plötzlichen Eintrag gelösten organischen Kohlenstoffs (DOC) aus dem terrestrischen Umland, der zu einer starken Braunfärbung des Wassers führte. Der Fokus liegt dabei auf Veränderungen der Wasserqualität und der aquatischen Primärproduktion des Sees, nachdem sich die DOC-Konzentration verfünffacht hatte. Innerhalb von drei Jahren nach Erreichen der maximalen DOC- und Gesamt-Phosphorkonzentrationen im See sanken diese signifikant, lagen jedoch noch immer 1,5- bzw. 2-fach oberhalb der Ausgangskonzentrationen vor dem DOC-Eintrag. Die benthische Primärproduktion, die aufgrund der verringerten Lichtverfügbarkeit nach den hohen DOC-Einträgen sehr stark reduziert war, zeigte eine teilweise Erholung, erreichte jedoch ebenfalls nicht die Ausgangswerte. Die pelagische Primärproduktion und Gesamt-Primärproduktion waren während des DOC-Eintrags angestiegen und gingen anschließend zurück, lagen jedoch oberhalb der Ausgangswerte vor dem DOC-Eintrag. Pelagische und bentische Primärproduktion zeigten eine inverse Reaktion auf die Veränderungen der DOC- und Phosphor-Konzentrationen im untersuchten See, was theoretische Modelle und Ergebnisse experimenteller Studien bestätigt, jedoch einen größeren DOC-Konzentrationsbereich abdeckt, der zuvor nie erreicht wurde. Ich zeige, dass eine vollständige Erholung des Sees möglicherweise nicht auftritt oder viel länger dauert als die Veränderungen während der Zunahme der DOC-Konzentrationen. Die nur teilweise Rückkehr der DOC-Konzentrationen im See nach dem plötzlichen Anstieg könnte zum aktuell in vielen Gewässern auf der Nordhalbkugel beobachteten langfristigen Anstieg der DOC-Konzentrationen beitragen.

TO SUNSHINE

PROLOGUE

We live in exciting times! A time when a huge portion of available knowledge rests at the tip of our fingertips (assuming they are not behind inaccessible paywalls). A time when we can communicate with many researchers around the world in real time. A time, also, when the planet we live on seems to be changing at an unprecedented pace. Global warming, extreme weather events, floods, flushes and sludge. Does that accurately describe the current environmental developments? Of course not. It's worse! At least that's what we hear in mainstream media.

But I shall not concentrate on the sensational headlines within the world of (social) media. Instead, this humble doctoral thesis will focus on specific factors that might be affecting our environment. Particularly, the aquatic environment. Specifically, freshwater ecosystems. Precisely small, shallow lentic systems. Why? Because they are important. Far more than a first impression would give. The first part of this introduction will aim at convincing you such. The second and third parts will highlight how a few important global changes are significantly altering freshwater ecosystems and the consequences these changes will bring to our environment.

1. INTRODUCTION

1.1 Why are small freshwater systems important?

The global carbon cycle conducts Earth's climate and productivity. In years past, it was believed that freshwater ecosystems only acted as a funnel to transport carbon from terrestrial sources to the oceans. That view has now been debunked. Many recent studies have demonstrated that inland aquatic systems play an active role in global carbon (C) cycling (Cole et al., 2007; Battin et al., 2009; Raymond et al., 2011). In fact, the current estimate is that more than two-thirds of the carbon that enters freshwater systems is either buried in sediments or mineralized and emitted to the atmosphere as carbon dioxide (CO_2) or methane (CH_4) (Fig. 1, Tranvik et al., 2009).

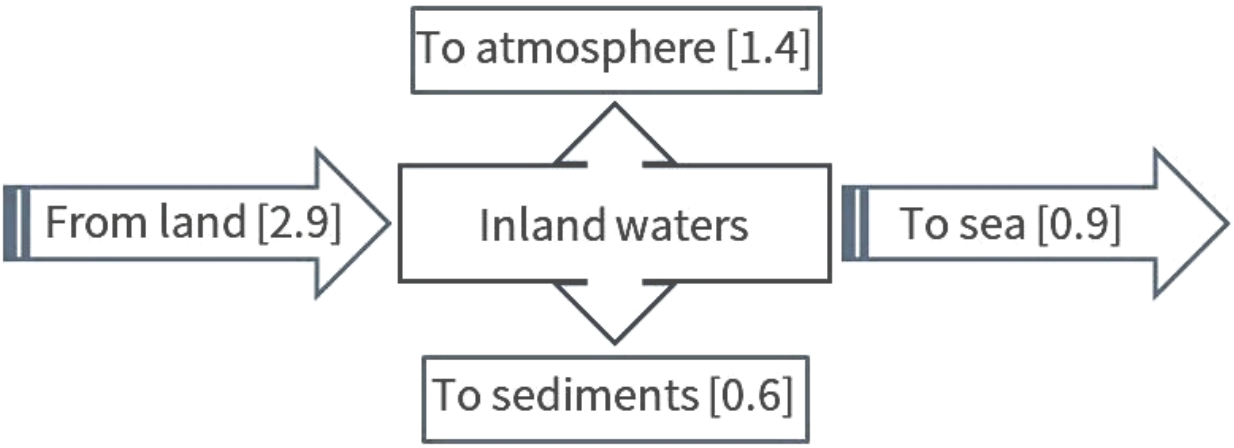

Fig. 1: Illustration adapted from Tranvik et al. (2009), highlighting the revised role that inland waters play in carbon sequestration and transport. Numbers in brackets represent carbon in Pg, 10^{15} g.

The bulk of freshwater systems are shallow, lentic, small water bodies that can be defined by a surface area <0.05 km^2 and a highly variable water depth, mostly resulting in a temporary water regime (Lorenz et al., 2017). Lentic small water bodies <0.1 km^2 add up to a potential 20% of the global surface area of lakes due to their high abundance (Holgerson & Raymond, 2016). As these shallow systems receive plenty of light and nutrients they could be among the most productive systems on Earth (Wetzel, 2001). Staehr et al. (2011) have demonstrated an inverse relationship exists between metabolic rates (gross primary production (GPP) and respiration) and lake area because small water bodies receive larger quantities of allochthonous matter relative to their volume and have a higher probability of being heterotrophic than large ones (Sand-Jensen & Staehr, 2009). Organic C sequestration per unit area of sediment has been

suggested to be at least an order of magnitude higher in small lakes than in larger lakes (Stallard, 1998; Dean & Gorham, 1998; Downing et al., 2008; Heathcote et al., 2016).

Despite the growing evidence that small water bodies are hotspots of carbon turnover, these systems have to date been far less studied than their larger counterparts (Downing et al. 2006) to the detriment of achieving an accurate portrayal of global carbon budgets. For instance, Pace and Prairie (2005) estimated the global GPP of lakes to be 0.65 Pg C yr^{-1}. This figure turned out to be an underestimate as it was based on an approximation of total lake area without attributing the high production of small lakes (Tranvik et al., 2009).

In addition to lake area, C mineralization (and consequently burial) in lake sediments is highly dependent upon oxygen (O_2) availability (Sobek et al., 2009). Isidorova et al. (2016) found that anaerobic conditions reduce C mineralization by roughly 50% compared to aerobic respiration, often resulting in an enhanced C burial in lake sediments. Thus, primary production, through its contribution to C sequestration and O_2 availability in the water column, plays a crucial role in greenhouse gas emissions (Kosten et al., 2010; Yvon-Durocher et al., 2011), C burial (Heathcote et al., 2016) and consumer production (Vadeboncoeur et al., 2002) in small, shallow aquatic systems and the overarching global C cycle.

One very common type of small (<1 ha) lentic water bodies in northern Europe and North America are kettle holes (sometimes referred to as prairie potholes in North America). Most of these ecosystems were formed following the last glaciation (about 12,000–10,000 years ago), when the delayed melting of ice blocks created depressions in the moraine landscape without outlets (Mitsch & Gosselink, 1993; Kalettka et al., 2001; Creed et al., 2013). Anthropogenic influences such as forest clearance and tillage also seem to have enhanced their development (Kalettka et al., 2001). In north-eastern Germany, up to 300,000 kettle holes exist, comprising up to 5% of the arable land (Kalettka & Rudat, 2006). Most of these kettle holes are located within agricultural landscapes. Thus their nutrient concentrations strongly exceed those of shallow lakes of the region (Lischeid & Kalettka, 2012; Eigemann et al., 2016). This potentially promotes primary production (PP) and C turnover (Reverey et al., 2016). Recent case studies indicate that these kettle holes play a significant role in landscape greenhouse gas emissions (Premke et al., 2016). However, to calculate the C budgets of kettle holes, a detailed knowledge of ecosystem processes (PP, sedimentation and mineralization) is needed. Measuring PP in small water bodies could nevertheless be problematic. The standard single-site diel O_2 technique (Staehr et al., 2010) provides unreliable estimates of whole-system GPP because it underestimates benthic GPP (Brothers et al. 2017 and references therein), which can be the most important component of shallow lakes, ponds, and kettle holes due to these systems' high surface area to volume ratios (Vadeboncoeur et al., 2002; Liboriussen & Jeppesen, 2003;

Brothers et al., 2013a). Moreover, a high degree of spatial heterogeneity in summertime diel O_2 curves (Van de Bogert et al., 2012) can occur in macrophyte-dominated water bodies where the benthic zone plays a larger role in whole-ecosystem GPP than phytoplankton (Brothers et al., 2013a, 2017). Long-lasting O_2 depletion may also occur in small aquatic systems (Baird et al., 1987; Prairie et al., 2002), rendering the diel O_2 curve technique altogether impractical. Therefore, other approaches must be pursued to circumvent the problem.

In kettle holes with high nutrient concentrations, emergent, submerged and floating macrophytes are often abundant during the May to September growing season (Lischeid & Kalettka, 2012). It has been long suggested that over a range of nutrient concentrations, shallow lakes can have two alternative equilibria: a clear state dominated by aquatic vegetation and a turbid state characterized by phytoplankton blooms (Scheffer et al., 1993; Zimmer et al., 2016). More recently, free-floating plant dominance has also been proposed as a (third) self-stabilizing ecosystem state (Scheffer et al. 2003). In contrast to this theory, phytoplankton rarely dominates in kettle holes during the macrophyte growing season (Lischeid & Kalettka, 2012). Kettle holes dominated by macrophytes and surrounded by reed stands, defined as 'fringe type' (Luthardt & Dreger, 1996), are the most common kettle hole type among intensively used agricultural landscapes of north-eastern Germany.

Despite the abundance of fringe-type kettle holes within these landscapes, the specific contributions of various primary producer groups (phytoplankton, periphyton, rooted and free-floating macrophytes) to C dynamics (including C sediment deposition and mineralization) within these systems are poorly understood (Vis et al., 2007), even though these processes play a pivotal role in landscape C budgets.

1.2 Global and regional factors impacting shallow freshwater system productivity

Most small systems are easily impacted by their surroundings. Having grown up in a small country, I can anecdotally vouch for that. In the case of small, shallow freshwater systems, their large surface area to volume ratio often implies they receive ample nutrients from surrounding terrestrial sources, are easily impacted by atmospheric and temperature changes, and, lacking a volumetric buffer, could be very harshly disturbed (or entirely dry up) by extreme weather events. Here, I focus on two prominent trends that have been impacting freshwater systems over the past few decades.

1.2.1 Climate change

With our planet rapidly changing there are far too many continuous fluctuations in the environmental homeostasis to count here. But the biggest factor remains climate change. Average global temperatures have risen by 0.6°C during the last century and are predicted to increase by an additional 3-5°C over the next century (IPCC, 2013). Ecological responses to climate change have been reported across various natural systems (Parmesan & Yohe, 2003), including shallow lakes (e.g. Mooij et al., 2007; Sommer et al., 2012).

One of the major processes potentially altered by global warming is primary production. Warming can elevate primary productivity as the rate of most subcellular reactions increase exponentially with temperature following the Van't Hoff-Arrhenius relationship, wherein the calculated activation energy quantifies the change in reaction rate with temperature (Boltzmann 1872, Arrhenius 1889, as described in Allen et al. 2005). Increases in both biodiversity and biomass of planktonic algae in direct response to warming have been reported (Yvon-Durocher et al., 2015a). Temperature-dependent physiological mechanisms also determine the nutrient stoichiometry of algae (Yvon-Durocher et al., 2015b), altering their quality as food for consumers (Moorthi et al., 2016). Several studies have investigated the impacts of global warming on primary producers in shallow lakes either through a space-for-time approach (Bécares et al., 2008; Kosten et al., 2009; Mahdy et al., 2015) or through temperature controlled mesocosm studies (Liboriussen et al., 2005; Feuchtmayr et al., 2009; Lassen et al., 2010; Patrick et al., 2012; Stewart et al., 2013).

However, given the problems associated with quantifying benthic GPP by the common diel O_2 technique discussed above, estimates of periphyton production at the whole lake scale have been hampered by low spatial and temporal resolution of productivity data (Devlin et al., 2016; Fig. 2). Studies on the effects of warming on periphyton GPP are altogether lacking. Available studies on the impacts of temperature on periphyton biomass exhibit contradictory results. These have reported positive (Bécares et al., 2008; Patrick et al., 2012; Mahdy et al., 2015), negative (Shurin et al., 2012; Meerhoff et al., 2012; Rodríguez & Pizarro, 2015) or non-significant effects (Hansson, 1992) of warming on periphyton biomass.

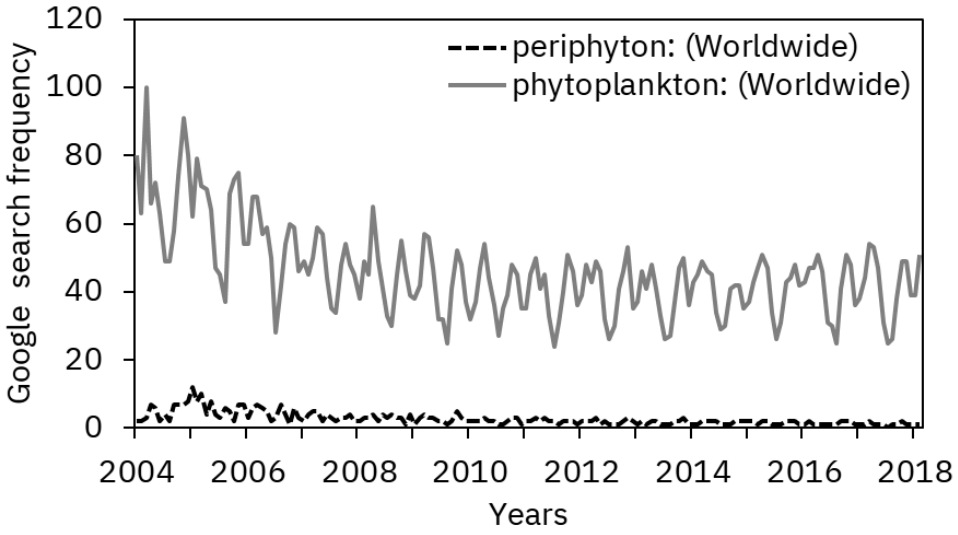

Fig. 2: Google Trends data showing number of monthly searches with keywords of "phytoplankton" and "periphyton".

Warming may affect top-down effects through shifts in periphyton grazer community compositions, abundances, and activity rates (Kishi et al., 2005; Kratina et al., 2012; Shurin et al., 2012). Bottom-up effects may change during warming due to increased nutrient release from sediments (Gudasz et al., 2010; Jeppesen et al., 2009) and increased nitrogen loss by denitrification (Veraart et al., 2011), due to increased macrophyte surface for periphyton colonization (Davidson et al., 2015), and due to decreased light availability by enhanced phytoplankton growth (Mooij et al., 2007). These effects may differ in time leading to contrasting net effects of warming on periphyton biomass and production, yet within-system studies with comprehensive spatial and temporal resolution are lacking.

1.2.2 Increasing allochthonous organic carbon concentrations

Differences in precipitation, among other factors, have altered the amount of organic matter entering lentic systems in the northern hemisphere (Kritzberg et al., 2014). Dissolved organic carbon (DOC) concentrations in lakes and rivers have increased over the past decades in many regions (Evans et al., 2006; Williamson et al., 2015), mostly due to additional terrestrial inputs (Solomon et al., 2015). This has led to brownification becoming a common phenomenon, especially in the northern hemisphere (Roulet & Moore, 2006). Increasing DOC concentrations can significantly impact the chemical, physical, and biological traits of aquatic ecosystems (Jones & Lennon, 2015; Solomon et al., 2015; Hedström et al., 2017). While terrestrial organic carbon (OC) inputs contribute to basal resource availability (Solomon et al., 2011), they can also reduce primary productivity via shading effects on phytoplankton and periphyton (Karlsson et al., 2009). In all but the most oligotrophic systems, the negative influence of DOC shading on

autochthonous primary production usually exceeds the positive effects of DOC on resource availability via direct supply of C and the potential fertilization of autochthonous production (Jones et al., 2012; Seekell et al., 2015). Additionally, increased DOC concentrations can have significant impacts on phytoplankton species composition and diversity (Urrutia-Cordero et al., 2017), which in turn can affect the aquatic food web (McGowen et al., 2005).

Apart from a gradual upward trend in DOC concentrations in many freshwaters, DOC inputs and concentrations can fluctuate significantly on shorter timescales. In lowland river systems, sudden "blackwater" events commonly occur when flooding follows prolonged dry periods, releasing high quantities of accumulated terrestrial organic material. Raymond and Saiers (2010) calculated that 86 % of the annual DOC flux in small forested catchments occurred in association with rising or falling stream-water hydrographs. The released DOC can lead to severe anoxia in streams and rivers, killing aquatic animals (e.g., Hladyz et al., 2011; Ning et al., 2015). Extensive flooding in the Murray–Darling Basin (Australia) after a decade of drought mobilized several hundred thousand tons of DOC and the plume of hypoxic water affected about 2000 km of river channel for up to 6 months (Whitworth et al., 2012). Nonetheless, blackwater events in rivers are often short-lived due to flushing, allowing a rapid recovery of both water quality and the affected fauna (Burford et al., 2008; Kerr et al., 2013).

Post-flooding brownification events can also occur in lakes, although fewer examples have been published. Boreal lakes with a water retention time between one and three years are particularly vulnerable to climate change-induced browning, yet model scenarios based on an expected future increase in precipitation in this region predict that many of these lakes will continue to experience browning (Weyhenmeyer et al., 2016). Brownification in lakes can also lead to anoxia and have strong effects on water chemistry, algal community composition, biomass and productivity, as well as the mortality of macrozoobenthos and fish (Sadro and Melack, 2012; Brothers et al., 2014; Lenard and Ejankowski, 2017). Due to longer water residence time in lakes, the effects on water chemistry and biota are expected to last longer than in rivers. In lakes, DOC removal mainly depends on microbial mineralization, flocculation (von Wachenfeldt & Tranvik, 2008), and photolytic mineralization (Granéli et al., 1996). The resilience of these systems, here defined as the rate of recovery after a disturbance (Tsai et al., 2011), to sudden brownification events (temporary increases to DOC load) remains unknown.

1.3 Thesis aims and hypotheses

Small, shallow freshwater systems are important in global carbon budget calculations but still understudied. This creates a vital gap in literature that needs to be addressed to ensure the validity of regional and global environmental estimates, as well as their future predictions. This problem is compounded due to the uniqueness and unpredictability of these systems. Unlike large lakes, the littoral area of small, shallow lakes usually contributes to the bulk of the total system GPP. The littoral area is usually dominated by periphyton and/or macrophytes. Given that large lakes have historically attracted more research, it is no surprise that benthic production has been much less studied than the pelagic (phytoplankton) one. This represents a second important gap in available literature that this thesis aims to alleviate. To address these two concerns, in study I (Fig. 3), I applied a compartmental approach, calculating the contribution of phytoplankton, periphyton, floating, submerged and emergent macrophytes to determine whole-system GPP during one year in two typical temperate, nutrient-rich, fringe-type kettle holes in north-eastern Germany. **We hypothesized that summer time (macrophyte growing season) GPP in the kettle holes would be comparable to very productive, temperate eutrophic aquatic systems**, due to the high abundance of macrophytes during this period. Outside the macrophyte growing season, **we expected periphyton to contribute significantly to GPP due to the high colonizable surface area to volume ratio of these systems**. In addition, **we hypothesized that high GPP would result in high sediment deposition rates, but low sediment mineralization rates due to significant periods of anoxia common in such systems** due to a high share of emergent macrophytes not releasing O_2 into the water. This study was part of a larger effort (the Landscales project; Premke et al., 2016) aimed at investigating the terrestrial-aquatic linkages driving the landscape carbon dynamics.

Furthermore, given how important, unique, yet "volatile" we found these systems to be, we wanted to investigate how future warming scenarios would affect primary production within them (Fig. 3 Study II). For this aim, we used a very controlled environment that we could easily manipulate: 1000 L fishless indoor mesocosms with sediment, programmed to follow a temperate temperature regime (control) and a warm (+4 °C) treatment. **We hypothesized that warming positively affects whole system and periphyton GPP during spring due to enhanced algal physiological rates. We expected warming to have an indirect positive bottom-up effect on periphyton GPP** due to earlier nutrient recycling from fungal parasites facilitating advanced grazing of phytoplankton as shown in parallel studies (Frenken et al., 2016; Velthuis et al., 2017) and from higher mineralization rates in the sediment of the warm treatment. **We also investigated, whether enhanced invertebrate grazing on periphyton in**

warmed treatments can reverse this trend leading to seasonally changing net effects of warming on GPP within the measurement period. Other doctoral students were also involved in this project to investigate the effects of warming on phytoplankton (Velthuis et al., 2017) and macrophyte dynamics (Velthuis et al., 2018), fungal parasites (Frenken et al., 2016), sedimentation and decomposition rates (Velthuis 2018) and greenhouse gas emissions (Aben et al., 2017).

Lastly, since shallow freshwater systems are known to exhibit shifts from one stable state to another by extreme weather events, I aimed to investigate whether they would eventually return to their original condition given a sufficient time for recovery (study III). To do so, I analyzed the resilience of a small, temperate, shallow lake to a sudden natural brownification event previously described by Brothers et al. (2014). Due to high precipitation and naturally rising water levels, the DOC concentrations in this lake had increased five-fold, from ~12 mg L^{-1} in 2010 to a maximum of about 60 mg L^{-1} by 2012. Concurrently with increasing DOC concentrations, total phosphorus (TP) and iron (Fe) concentrations had risen dramatically. Primary producers had shown opposing responses with an increase in phytoplankton GPP due to increased nutrient availability and thermal stratification, while periphyton biomass strongly declined due to shading (Brothers et al., 2014). I continued the examination of lake water quality and primary production for three years following peak DOC concentrations, to investigate their potential recovery. Along with declining water levels after 2012, I anticipated a reduction of external and internal DOC loading, producing a gradual decrease in lake DOC and TP concentrations. Accordingly, **I hypothesized that pelagic GPP would return to pre-brownification rates, driven by decreasing nutrient concentrations and deeper mixing levels, while benthic primary production would recover due to increased light availability**. I also investigated whether phytoplankton group composition differed during the years of increased DOC concentrations.

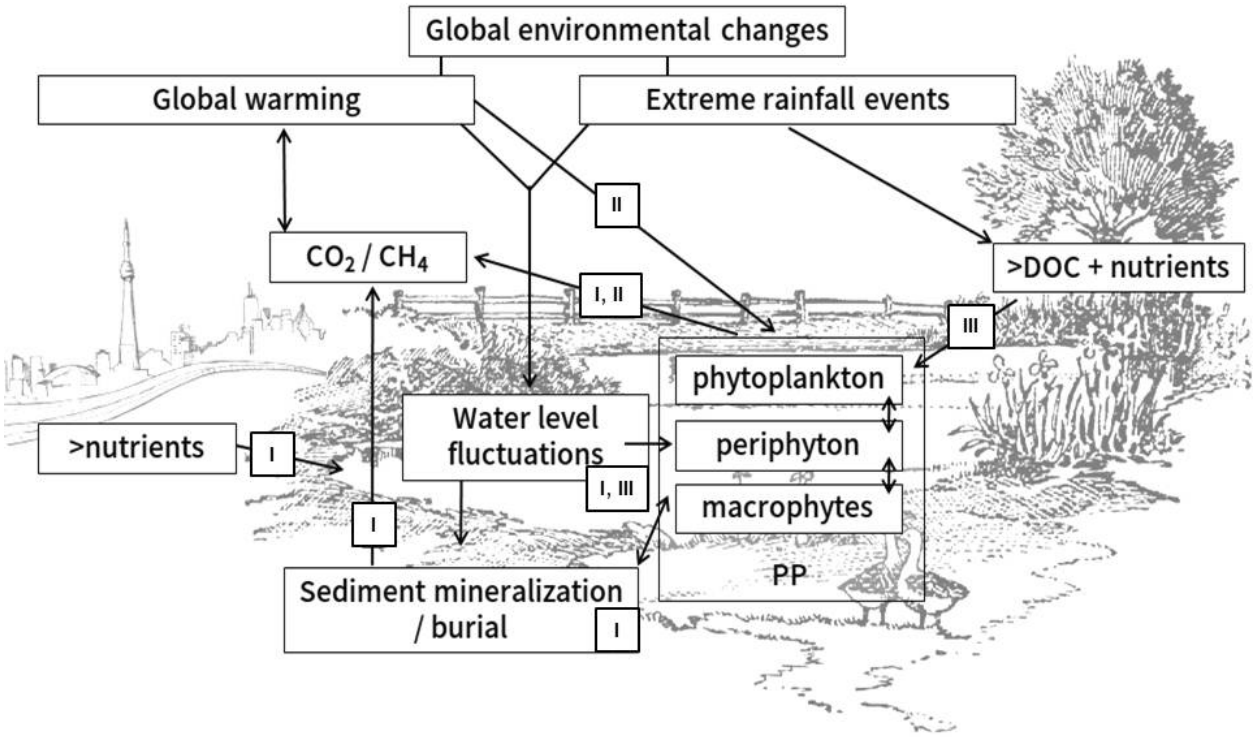

Fig. 3: Schematic representing the biotic and abiotic factors driving carbon cycling in shallow freshwater ecosystems. Interactions between factors are represented by directional arrows. Roman numerals indicate the specific studies in this thesis investigating these interactions.

2. MATERIALS AND METHODS

2.1 Study sites

2.1.1 Field studies in kettle holes

For study I, two kettle holes were selected from the Uckermark region in Brandenburg, north-eastern Germany. A detailed description of the location and bathymetric maps are reported elsewhere (Nitzsche et al., 2016; Kleeberg et al., 2016). Kettle hole Kraatz (N 53°25′05′′ E13°39′48′′) was surrounded by a few *Salix cinerea*, L. shrubs and populated by a mixture of submerged, emergent and floating macrophytes (Fig. 4a; Table 1). Kettle hole Rittgarten (N 53°23′22′′ E 013°42′09′′), situated 5 km southeast of Kraatz, was sheltered by a reed belt (*Phragmites australis* (Cav.) Trin. ex Steud.) and fully covered by non-rooted submerged (*Ceratophyllum submersum* L.) and floating (*Lemna minor* L., *Spirodela polyrhiza* (L.) Schleid) macrophytes during the summer months (Fig. 4b; Table 1). Both kettle holes belong to the most common vegetation type in German kettle holes (fringe type according to Luthardt & Dreger, 1996), which are commonly characterized by permanent or perennial flooding (Kalettka, 1996).

Both kettle holes are surrounded by arable land and are heavily exposed to agricultural practices such as tillage and fertilizer addition, leading to high nutrient concentrations (Table 2). Both kettle holes are sheltered from strong winds (mean ± SE = 1.8 ± 0.01 m s^{-1}), with Kraatz located in a depression while Rittgarten surrounded by a dense reed belt. Neither of the kettle holes was observed receiving continuous surface runoff during the study period. Input of terrestrial particulate organic matter (POM) was limited to extreme winter weather events when there was no significant vegetation and was observed to be higher in Kraatz than in Rittgarten due to sharper surrounding inclines (C. Hoffmann, pers. comm.), in addition to a potential POM input from the surrounding bushes.

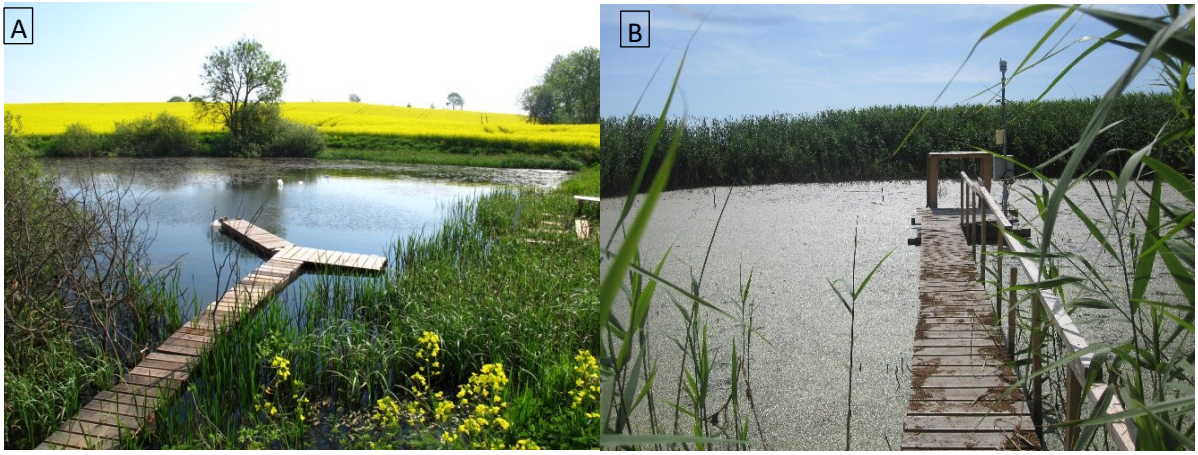

Fig. 4: Pictures of the kettle holes: Kraatz (A) and Rittgarten (B).

Table 1: Sampled standing stock of biomass and coverage of emergent, submerged and floating plant species in in two kettle holes with different vegetation types in June 2013.

Kettle hole	Type of vegetation	Species	Sampled standing biomass (g dry weight m^{-2})	Coverage (% kettle hole surface area)	Quadrat size used (m^2)
Kraatz	Emergent	*Carex acutiformis*	221.3 (± 54.7)	20	0.16
		Sparganium erectum	19.7 (± 2.0)	10	0.16
	Submerged	*Potamogeton natans*	24.5 (± 6.7)	20	0.36 m^3
		Potamogeton acutifolius *Polygonum amphibium*	36.0 (± 5.3)	5	0.36 m^3
	Floating	*Lemna minor, Spirodela polyrhiza, Lemna trisulca*	4.6 (± 1.4)	1	0.09
			4. 8 (± 0.5)	15	0.09
Rittgarten	Emergent	*Phragmites australis*	232.1 (± 2.2)	35	1
	Submerged	*Ceratophyllum submersum*	64.1 (± 6.1)	55	0.36 m^3
	Floating	*Lemna minor, Spirodela polyrhiza*	45.0 (± 18.2)	70	0.09

Table 2: General characteristics and water chemistry of sampled kettle holes from May 2013 to April 2014. Data represent annual means (from 12 monthly samples, except for dissolved manganese where n = 9).

Parameters	Kraatz	Rittgarten
Area (m^2)	1510	1453
Mean depth (m)	0.6 ± 0.3	1.22 ± 0.3
Water temperature (°C)	10.3 ± 6.1	9.1 ± 4.5
pH	7.1 ± 0.3	6.8 ± 0.3
Total nitrogen (TN, mg L^{-1})	0.9 ± 0.2	2.0 ± 0.6
Total phosphorus (TP, µgL^{-1})	116.3 ± 78.4	256.5± 221.6
Soluble reactive phosphorus (SRP, µg L^{-1})	27.9 ± 22.6	150.3 ± 172.7
Total dissolved nitrogen (TDN, mg L^{-1})	0.9 ± 0.2	1.8 ± 0.5
Dissolved silica (mg L^{-1})	0.4 ± 0.3	4.1 ± 1.0
Dissolved manganese (mg L^{-1})	0.2 ± 0.3	0.7 ± 0.6
Dissolved organic carbon (DOC, mg L^{-1})	10.1 ± 1.2	19.6 ± 2.2
Dissolved inorganic carbon (DIC, mg L^{-1})	23.5 ± 2.9	57.7 ± 6.7
Total organic carbon (TOC, mg L^{-1})	10.7 ± 1.6	20.5 ± 2.4
Total inorganic carbon (TIC, mg L^{-1})	25.1 ± 3.5	65.1 ± 10.3

2.1.2 Limnotron experiments

The experiment aimed to investigate the effects of global warming on aquatic primary production (Study II) was performed in eight indoor limnotrons (mesocosms; Fig. 5) of 1.37 m depth and 0.97 m diameter at the Netherlands Institute of Ecology (NIOO) in Wageningen. The full description of these mesocosms is reported in Verschoor et al. (2003). The limnotrons were filled in February 2014 with 908 L of tap water in addition to 80 L of pre-sieved sediment (5 mm mesh size to exclude large invertebrates) collected from a mesotrophic shallow pond (>90% volume) and an eutrophic pond (<10% volume) in Wageningen, The Netherlands. Each limnotron was spiked with a concentrated natural plankton assemblage (≥30 µm) retrieved from ~300 L water from the same pond as where the sediment was derived from. In addition, a small amount of plankton inoculum (<15% of spiked inoculum volume) and sediment (<1% of total sediment) was derived from another, more eutrophic pond (coordinates in DMS: 51°58056.7″N 5°43034.5″E) to allow for a more diverse plankton community resembling different trophic states. Nutrients were added to each limnotron to ensure final concentrations of 86 ± 19, 2.4 ± 0.8 and 152 ± 37 (mean ± SD) µM of NO_3^-, PO_4^{3-} and Si, respectively. Light of constant intensity (175 ± 25 µmol photons m^{-2} s^{-1}) was provided by two HPS/MH lamps (CDM-

TP Elite MW 315-400 W, AGRILIGHT B.V., Monster, The Netherlands) for each limnotron and followed the typical Dutch light : dark annual cycle.

The limnotrons were randomly divided into two groups of distinct temperature treatments (n = 4). The control treatment followed the average seasonal water temperature of Dutch lakes, while the warm treatment was 4°C warmer in accordance with the IPCC RCP8.5 scenario that predicts a global temperature increase of 2.6 to 4.8 °C by the end of the 21st century (IPCC, 2013). The initiation of the experiment was on March 3, 2014.

Fig. 5: Picture of the mesocosms (limnotrons) and the polypropylene strips hung in the limnotrons at 3 different depths for periphyton cultivation.

2.1.3 Field studies in Lake Gollinsee

To study the resilience of a small, shallow lake to increases in DOC concentration (Study III), I continued the examination of water quality and primary production of the same lake that had undergone a natural, two-year brownification event previously reported by Brothers et al. (2014). Kleiner Gollinsee (hereafter referred to as Gollinsee) is a small (0.03 km^2), shallow (Z_{mean}: 1.7 m, Z_{max}: 2.9 m; 2010 values), eutrophic lake located in north-eastern Germany (53°01'N, 13°35'E). The lake lacks any in- or outflows and is protected from strong winds by a reed-dense shoreline (*Phragmites australis* Trin. ex Steud.) and surrounding alder trees (*Alnus glutinosa L.*). Given its eutrophic state and low water clarity, the lake does not contain submerged macrophytes (Brothers et al., 2013a).

From November 2010 to November 2014, as part of an unrelated experiment tracing terrestrial particulate organic carbon within the aquatic food web (Attermeyer et al., 2013; Scharnweber et al., 2013), Gollinsee was fully divided into two similarly sized basins using a plastic curtain (Fig. 6). In this study, we present whole lake averages for the years 2010 and 2015 and separate averages for each basin during the years the lake was split (2011 – 2014). Water quality parameters in 2010 reflect the lake's pre-brownification state, 2011 marks the onset of the brownification event which reaches its maximum in summer 2012 (Brothers et al., 2014), and 2013 sets the beginning of the lake's recovery period from elevated DOC concentrations.

Fig. 6: Picture of Gollinsee separated into two similarly sized basins by a plastic curtain.

2.2 Measurements of physical parameters

In the two kettle holes (Study I), O_2 concentrations in the water column were measured every 30 min throughout the sampling period (May 2013 to April 2014) via a Yellow Springs Instruments monitoring probe (YSI; Xylem Inc., Yellow Springs, OH, USA) hanging initially at a depth of 1 m in the middle of the kettle hole and later raised to the middle of the water column when the water level dropped below 1 m. Due to a breakdown of the YSI at Kraatz, O_2 data were unavailable between 29 August and 18 October. Five additional O_2 probes (MiniDOT loggers, PME, USA) were placed randomly in each kettle hole to investigate spatial O_2 heterogeneity by recording O_2 concentrations and temperature at 30 min intervals from August 8 to October 17, 2013.

Water level fluctuations were measured by water depth loggers (CS451 Pressure transducer, Campbell Scientific, USA) installed in the center of the kettle holes. Water volume, area and mean water depth (Z mean) were calculated using water level fluctuations and tachymetry data collected in June 2013. In Rittgarten, global radiation (in W m^{-2}) and wind speed (in m s^{-1}) were measured every 30 min at a weather station located directly by the kettle hole using a CMP3 pyranometer (Kipp and Zonen, Delft, The Netherlands) and a MeteoMS multisensor (ecoTech Bonn, Germany), respectively. Mean light attenuation (ε) was calculated by measuring light intensity captured by two Underwater Spherical Quantum Sensors (LI-193, LI-COR BioSciences, Lincoln, NE, USA) fixed vertically 0.5 m apart, measured from just below the water surface, then lowered gradually till the lower bulb hit the sediment. When the water levels dropped during summer, only 1–2 measurements were possible. Photosynthetically active radiation (PAR) at depth *Z* was calculated from global radiation (in W m^{-2}) and light attenuation using the Lambert-Beer equation:

$$I_z = I_0 \times e^{-\varepsilon \times z}, \qquad [eq.1]$$

where I_z represents irradiance (in µmol m^{-2} s^{-1}) at depth *Z* and I_0 represents irradiance on the surface of the water.

In the limnotrons (Study II), water temperature was automatically recorded and controlled by a custom-made climate control system (SpecView 32/859, SpecView Ltd., Uckfield, UK). In addition, vertical profiles of each limnotron (temperature, light availability, turbidity and pH) were measured on a weekly basis (WTW Multi 350i, Geotech Environmental Equipment Inc., Colorado, US). Two oxygen loggers (HQ40d Portable probe, Hach, Colorado, United States) were circulated among the eight limnotrons to measure 24-hour oxygen diel curves.

At Gollinsee (Study III), mixing depths were determined using vertical profiles of dissolved oxygen (O_2) concentrations, pH, and water temperature, measured by a Yellow Springs Instruments (YSI) multi-probe sonde. Another YSI sonde was fixed to a weather station near the centre of the lake (in the northern basin) at a depth of 1 m. This lake-centre sonde measured dissolved O_2, water temperature, and conductivity every 30 minutes (from May 2011 to September 2014). In addition, the weather station recorded and transmitted global radiation, wind speed, and air temperature data every 30 minutes over the same time period. Due to technical problems with the weather station, data from the beginning till mid-September of 2013 and for the whole of 2015 were unavailable. For these dates, we used data from the weather station of nearby Döllnsee (approximately 3.5 km south-east of Gollinsee).During every campaign, water column light attenuation was measured using two Underwater Spherical Quantum Sensors (LI-193, LI-COR) deployed 50 cm apart. Water level fluctuations were measured monthly by the local authority (data were kindly provided by R. Michels, Biosphärenreservat Schorfheide-Chorin).

2.3 Measurements of water chemistry parameters

For the measurement of water chemistry parameters in the first study, I took depth-integrated 2 L water samples from the center of the kettle holes every four weeks from May 2013 until April 2014, using a Limnos water sampler (LIMNOS, Turku, Finland). Water samples were filled in separate vials and transported in dark coolers to the laboratory, where a number of water chemistry parameters (listed in Table 2) were analyzed following German standard procedures (DEV, 2009).

Similarly in the limnotron experiment (Study II), depth integrated water samples were taken twice a week using a tube sampler (1m high; 3.5 L) and filtered over prewashed GF/F filters (Whatman, Maidstone, U.K.) to determine dissolved inorganic phosphorus (DIP) and nitrogen (DIN). Thereafter, concentrations of dissolved nutrients (PO_4^{3-}, NO_2^-, NO_3^- and NH_4^+) were measured by a QuAAtro39 Auto-Analyzer (SEAL Analytical Ltd., Southampton, U.K.). When the concentration of nutrients measured was below the detection limit, I used a value equivalent to half the minimum detection concentration for each respective test. Here, I only show inorganic nutrient values of every two weeks on dates that are closest to periphyton sampling days.

To determine sediment P release, intact sediment cores (± 6 cm) from all limnotrons were incubated in dark aquariums for one month, using temperature treatments of 6, 12, 22 and 30 °C. The cores were carefully supplemented with filtered limnotron water. The cores were subdivided to oxic and anoxic treatments (n = 3), which were purged with nitrogen gas until oxygen saturation dropped below 10%. After a settling period of one week, surface water

samples were collected using Rhizon pore water samplers (Rhizon MOM, 0.15 µm pore size; Rhizosphere Research Products, Wageningen, The Netherlands) at five different times at day 0, 6, 10, 13 and 17 of the experiment. Water samples were analyzed for phosphate by an auto-analyzer (Skalar Sanplus Segmented Flow Analyzer, Skalar Analytical BV Breda, The Netherlands), and for TP by an ICP-OES (ICP-OES iCAP 6000 (Thermo Fisher Scientific, Waltham, USA).

At Gollinsee (Study III), integrated water samples (every 0.5m from the water surface to just above the sediment) were retrieved using a Ruttner-like water sampler about every three months from spring 2013 to summer 2015, and water chemistry parameters (listed below) were analyzed on the following day. During stratified periods, separate integrated samples were collected from the epilimnion and hypolimnion.
We analyzed the water samples for concentrations of TP, total dissolved phosphorus (TDP), soluble reactive phosphorus (SRP), and dissolved nitrogen (DN) following German standard procedures (DEV, 2009). We calculated particulate P by subtracting the values of TDP from TP. Dissolved organic phosphorus (DOP) was calculated by subtracting SRP from TDP values. DOC concentrations were measured with a total organic carbon (TOC) Carbon-Analyzer (TOC 5000, Shimadzu), while iron (Fe) concentrations were analyzed using an inductively-coupled plasma optical emission spectrometer (ICP-OES) with an inductively-coupled argon plasma (iCAP 6000-Duo, Thermo Fisher Scientific). Furthermore, to explore any effects of DOC and humic substances on light attenuation in the water column, we compared the fluorescence of filtered lake water at 470 nm that we measured using a pulse amplitude modulated fluorometer (Phyto-PAM, Walz, Effeltrich, Germany) with lake water DOC concentrations.

2.4 Measurements of gross primary production

2.4.1 Periphyton

Periphyton was collected from transparent polypropylene strips with textured surfaces (IBICO, GBC, Chicago, IL, USA). In the kettle holes (Study I) I deposited four large (15 × 2 cm) and four small (4.5 × 1.3 cm) plastic strips 10 cm below the water surface and subsequently every 50 cm till the sediment was reached. These were harvested every month and replaced by new ones. The large strips were transported to the laboratory in plastic cylinders deposited in dark and humid coolers, whereas the small ones were stored in 15 mL plastic tubes filled with filtered kettle hole water to avoid zooplankton grazing during transportation. The same approach was followed at Gollinsee (Study III, n = 3 strips for every depth) for a month between June and July from 2010 to 2014 to measure (maximum summer) periphyton biomass accumulation and GPP rates. In the limnotrons (Study II), I used only one set of the same polypropylene strips (10 x 2.2 cm), hung on plexiglass rods on 16 March at three different depths below the water surface: 10

cm, 60 cm, and just above the sediment at 110–120 cm. This date marks the onset of our periphyton experiment when the polypropylene strips had no periphyton biomass (first timepoint, chl-*a* = 0). Four plastic strips from each depth were harvested first on 9-Apr and thereafter every two weeks until the end of June (n harvest= 7).

Periphyton on the smaller strips (and the ones deposited in the limnotrons) was dark adapted for at least 15 min and used to measure rapid photosynthesis–light curves by a Phyto Pulse Amplitude Modulation (PAM) Emitter Detector Fiberoptics (EDF) unit (Heinz Walz GmbH, Effeltrich, Germany). Periphyton hourly GPP was calculated following Brothers et al. (2013a), using the equation:

$$P_z = P_{max} \bullet \text{chl-}a\ (1 - e^{-\alpha \bullet Iz \bullet Pmax\text{-}1}) \qquad [eq.\ 2]$$

Where P_z is the production at depth *z*, P_{max} and α represent PAM-measured light-saturated photosynthesis and photosynthetic efficiency at low light, respectively, and I_z is photosynthetically active radiation at depth *z*, calculated for every 10 cm depth using equation 1 stated earlier. Total periphyton GPP was obtained by multiplying P_z with the calculated surface area available to epipelon (periphyton growing on sediment) and epiphyton (periphyton growing on submerged surfaces of macrophytes) in each corresponding depth. Epipelon was assumed to grow on all water-covered surfaces within the kettle holes (determined by tachymetry techniques), whereas the surface area of macrophyte leaves (on which epiphyton could grow) was calculated following methods described in the subsequent section (2.4.3) for the kettle holes and taken from Brothers et al. (2013a) for Gollinsee. Daily biomass and light attenuation values were extrapolated using linear equations between monthly measurements.

For total limnotron periphyton GPP estimations (Study II), values from the rapid photosynthesis-light curves and chl-*a* of the strips deposited on the two higher depths (10 and 60 cm) were averaged to estimate wall GPP, whereas the lowest strips deposited on the sediment were used to estimate epipelon chl-*a* and GPP. Daily GPP was derived by multiplying calculated hourly GPP by the number of light hours.

Periphyton on the large strips (and the ones deposited in the limnotrons after utilizing them for measuring rapid photosynthesis-light curves) was brushed off in the laboratory using a toothbrush and filtered lake or limnotron water. The suspension was then filtered onto GF/F Whatman (Maidstone, U.K.) to determine chl-*a* concentrations and pre-washed, pre-ashed MicroTech GravityFlo Filters (MGF) to determine C and N contents. We used chl-*a* values as a proxy for biomass of periphyton. In the case of the limnotron chl-*a* samples, the filters were freeze-dried and stored at -80 °C till further analyses. All chl-*a* analyses were done by High Performance Liquid Chromatography (HPLC, Waters, Millford, MA, U.S.A.) following the

procedure described in Shatwell et al. (2012). To determine the elemental composition of the periphyton, filters were dried at 60 °C. We measured the C and N content of the kettle holes and Gollinsee periphyton samples using a Vario EL Elemental Analyzer (Elementar Analysensysteme GmbH, Germany). As for the limnotron samples (Study II), a subsample of approximately 13% of the filtered surface area on the GF/F filter was folded in a tin cup (Elemental Microanalysis, Okehampton, UK) and analyzed for C and N on a FLASH 2000 NC elemental analyzer (Brechbueler Incorporated, Interscience B.V., Breda, The Netherlands). The remainder of the filter was combusted in a Pyrex glass tube at 550 °C for 30 minutes. Subsequently, 5 mL of persulfate (2.5%) was added and samples were autoclaved for 30 minutes at 121 °C. Digested P (as PO_4^{3-}) was measured on a QuAAtro39 Auto-Analyzer (SEAL Analytical Ltd., Southampton, U.K.).

2.4.2 Phytoplankton

In all the studies, phytoplankton fluorescence and biomass (chl-*a*) were measured from the integrated water samples (for sampling details see 2.3). In the limnotron experiment (Study II), water samples were additionally filtered over a 220 µm mesh. Fluorescence was measured on an aliquot of water using the Phyto-US measuring unit of a pulse amplitude modulated fluorometer (Phyto-PAM, Walz, Effeltrich, Germany) after a dark adaptation period of at least 15 min. Measurements were corrected by subtracting background fluorescence from lake water filtered through 25 mm diameter Whatman Glass Fibre Filters (GF/F). Another aliquot of lake water was filtered through a 25 mm diameter Whatman GF/F filters to measure chl-*a* concentrations by High Performance Liquid Chromatography (HPLC, Waters, Milford, MA, USA) following the procedure described in Shatwell et al. (2012). Carbon and N contents of phytoplankton were measured following filtration through pre-washed, pre-ashed MicroTech GravityFlo Filters (MGF) and analysed on a Vario EL Elemental Analyser (Elementar Analysensysteme GmbH, Germany).

Similar to the periphyton GPP calculations described in the previous section, phytoplankton GPP was estimated following Brothers et al. (2013a) using fluorescence-based rapid photosynthesis–light curves, phytoplankton chl-*a* concentrations, photosynthetically active radiation (PAR, calculated as 46% of global radiation) at water surface and light attenuation at every 10 cm depth, multiplied by the corresponding water volume at each depth. P_Z was calculated separately for each 10 cm layer using Eq. 2 with I_Z calculated for every 10 cm depth. Thereafter, total system phytoplankton GPP was calculated by summing up P_Z of all the separate layers. Daily rates, where reported, were calculated by interpolating monthly chl-*a*, fluorescence and light attenuation values using linear relations between monthly samples. Particularly for the limnotron samples, fluorescence measurements were calibrated by ethanol pigment

extractions (by Mandy Velthuis), followed by measurements with a photo-spectrometer (PerkinElmer, Groningen, The Netherlands). Linear regression of the ethanol extraction data and chlorophyll fluorescence (R^2 = 0.60; n = 189) yielded a conversion factor of 0.87 to calculate chl-*a* concentrations from the fluorescence signal. Furthermore, using PhytoPAM calibration files based on pre-determined monocultures of specific algal groups, we used fluorescence measurements to identify the contribution of various algal groups (diatoms, green algae, and cyanobacteria) to the total pelagic biomass.

2.4.3 Macrophytes

I sampled macrophytes only in the first study. We identified all macrophytes at the two kettle holes to the species level and visually estimated the percent surface cover of each species to the nearest 5% during field surveys and via monthly aerial pictures. I sampled macrophyte biomass in both kettle holes in the third week of June 2013, when standing stock is usually greatest based on previous observations and studies done on similar systems within the same region (e.g. Pätzig et al., 2012). I sampled each species at four random locations in each kettle hole that were fully covered with vegetation using quadrats of varying sizes (Table 1) depending on the growth form and species size. I collected the submerged species with a volumetric sampler (V = 0.36 m^3) to allow for depth-integrated measurements. In the laboratory, I dried the biomass samples at 60°C for seven days to obtain dry weight (DW). Dried samples were ground and aliquots weighed into tin cups for C and N analysis (Vario EL Elemental Analyzer). I estimated minimum standing stock to be negligible prior to May and after September (for submerged and floating macrophytes) or October (for emergent macrophytes), while maximum standing stock was achieved around the time of sampling in late June. Temporal fluctuations in standing stock and GPP (in g C m^{-2} day^{-1}) of each macrophyte species during their growth period (May to September/October) were calculated by fitting a polynomial curve that included the aforementioned minimum and maximum standing stock estimations and their C content on a DW basis. I calculated GPP by multiplying the maximum–minimum biomass by a gross production rate-to-harvest ratio of 1.5 for submerged and floating macrophytes (Best, 1982 and references within) and *P. australis* (Hocking, 1989), and estimated for an active growing period of six months of the year (following observations).

I estimated the total leaf area (LA) of submerged surfaces on macrophytes (available for epiphyton colonization) using the equation:

$$LA = DW \times A \qquad [eq.3]$$

with DW as the dry weight in g and A as the area in cm^2 g^{-1} DW. Values of A are known to differ (by a range of 500–1500) among species (Filbin & Hough, 1983; DVWK, 1990; see Körner &

Kühl, 1996). Submerged, highly branched species tend to have higher A values, while macrophytes with simple structures have low A values (Pettit et al., 2016). For this reason, grouping of morphologically similar plants has been shown to be a viable approach in the absence of measurements for particular species (Armstrong et al., 2003). Here, we used A values for *P. pectinatus* L. (Börner) (A = 1068 $cm^2 g^{-1}$; Fischer & Pusch, 2001), *P. richardsonii* (Benn) Rydb. (A = 766 $cm^2 g^{-1}$), *Ceratophyllum demersum* L. (A = 427 $cm^2 g^{-1}$; Armstrong et al., 2003) instead of *P. acutifolius* Link ex Roem. & Schult., *P. natans* L., and *C. submersum* L., respectively.

In Kraatz, emergent macrophytes such as the *Carex* spp. bushes and *Sparganium erectum* L. were not included in these calculations as the sharp water level decrease during the summer months led to these plants to be outside the submerged area, and their surface area therefore is unavailable for periphyton colonization. In Rittgarten, a small portion (~20%) of *Phragmites australis* remained within the submerged area. To calculate the additional surface area provided by *P. australis* for periphyton colonization, we measured density (within four random 1 m^2 quadrats) and average circumference of each stem. Colonizable reed surface area (CRSA) was then calculated as

CRSA = reed density × average circumference × average water depth of submerged part [*eq. 4*]

2.4.4 Total areal GPP and aquatic (autochthonous) GPP calculations

In the first study, in order to make broad comparisons with other freshwater ecosystems in available literature, system GPP was calculated in two distinct manners: total GPP and aquatic GPP. I estimated Total GPP by summing the GPP of all primary producer groups, including the allochthonous production of emergent macrophytes (species sequestering atmospheric C), as well as the autochthonous production (assimilating aquatic C) of phytoplankton, periphyton, and submerged and floating macrophytes (the latter group is reported to use both sources of C; Filbin & Hough, 1985). For areal total GPP, I divided total GPP by the static kettle hole area (designated by the circumference at the top shoreline), irrespective of water level fluctuations throughout the year. This step was necessary to ensure the inclusion of all emergent macrophytes that were likely connected to the water column via their roots, despite falling outside the water column boundaries aboveground when the water volume receded in the warm summer months.

I calculated aquatic GPP (e.g. Hagerthey et al., 2010) by summing only autochthonous GPP values, thus excluding emergent macrophytes from these calculations. Alternatively, areal aquatic GPP was calculated by dividing the above value by the daily-varying kettle hole surface area, which was derived from daily measurements of water level fluctuations. Therefore, while total areal GPP gives a more accurate indication of overall C sequestration (both allochthonous

and autochthonous) within the boundaries of the kettle hole, aquatic GPP calculations can be used to directly compare our calculations to gross aquatic production (GAP) rates in literature (Hagerthey et al., 2010), obtained using different methods.

Additionally, to test for potential GPP of phytoplankton in the absence of light restricting floating vegetation, we performed a manipulative experiment at Rittgarten in July 2014. Duckweed and hornwort cover was harvested using nets, thus facilitating the penetration of sunlight into the water column. Concentration of chl-*a* was measured in water samples taken before and two weeks after cover clearance. Simultaneous O_2 concentrations in the water column were monitored by the YSI probe.

2.5 Sediment deposition rates

Sediment deposition rates were measured in the first study by Dr. Andreas Kleeberg. Pairs of sediment traps, acrylic glass tubes 56 cm in height and 6 cm in diameter, were deployed in a north–south transect at three sites of each kettle hole. Each pair of traps was exposed on vertical tubing directly on the sediment surface and emptied biweekly between June to November 2013, and between April to June 2014. Given the brevity of the second sampling phase, we did not include these results in our statistical tests but still present them in our figures. The sedimentation rate was calculated as the mean for the three trap sites representing the mean pond-specific flux (n = 6). Since the downward flux of matter is closely coupled to the prevalent water level, the measured pond-specific rates were normalized to 1 m of water depth. A more detailed description of the method can be found elsewhere (Kleeberg et al., 2016a).

2.6 Sediment respiration

In this thesis, I show sediment respiration measurements only from the first study. Aerobic sediment respiration (R) was determined based on O_2 depletion rates in the overlying water of sediment incubation cores. We took four random sediment cores each month using a sediment corer (inner diameter = 6 cm; Uwitec, Mondsee, Austria). We then transferred the top 10 cm of the sediment (and the overlaying water) at the field into transparent, acrylic incubation cores of 5.3 cm diameter and 30 cm length (total volume ~0.5 L). The incubation cores were closed with a rubber stopper, transported in a cooler to the laboratory, placed into a dark chamber and kept at in situ temperatures overnight. In order to avoid O_2 depletion, we kept the cores open overnight. The next morning, we closed the cores with a gas tight stopper, equipped with a floating magnet and incubated them for roughly 3–24 h, depending on the initial O_2 concentrations. We used the magnet to periodically mix the overlaying water column in order to avoid any stratification or the establishment of an O_2 gradient. Oxygen depletion (ΔO_2 in mg L^{-1}) in the overlaying water over time (Δt; in hours) was measured by Drs. Sabine Flurry and Katrin

Attermeyer every two or three hours using a needle-type O_2 microsensor (Optode, PreSens, Regensburg, Germany) inserted about 1 cm above the sediment through the septum. The O_2 sensor was connected to a micro-fiber optic O_2 m (Microx TX3, PreSens, Regensburg, Germany) to log O_2 concentrations.

Oxygen depletion rates were converted to C respiration rates using an empirical conversion factor of 0.85 (Graneli, 1979). Total C mineralization rates were calculated as follows:

$$R = \Delta O_2 \times Vw \times \frac{1}{As} \times \frac{1}{\Delta t} \times 0.85 \times \frac{MWc}{MWO_2} \quad [eq.\ 5]$$

where V_w denotes the volume of the sediment overlaying water (in L), A_s is the sediment surface area (in m^{-2}) and MW represents the molecular mass of C and O_2 (in g mol^{-1}), respectively.

2.7 Sampling of macroinvertebrates

We only sampled macroinvertebrates in the limnotrons (Study II). Multiplates and gravels baskets (Brock et al. 1992) were used for collecting macroinvertebrates. On 13 May 2014, the gravel baskets were placed on the sediment while the multiplates, each consisting of 10 layered hardboard plates (7.5 x 7.5 cm) with interspaces ranging from 0.5–1.5 cm, were hung halfway the water column against the walls of the limnotrons. On 25 June, each multiplate and gravel basket was carefully removed and extensively washed under running tap water over a sieve of 500 µm to remove the animals. All macroinvertebrates were identified alive by E. Peeters to the highest possible taxon and counted. After identification, they were released in their respective limnotrons.

2.8 Statistical analyses

The effects of water nutrient concentrations in the kettle holes on aquatic GPP (Study I) were tested by repeated measures ANOVA, after log transformation of the parameters that did not exhibit normality. Shapiro–Wilk and Bartlett tests were respectively used to confirm the normality and homogeneity of variances of the concerned parameters. Correlation between GPP and both sediment deposition rates and aerobic mineralization rates were tested with Spearman's rank correlation coefficients.

In the limnotron experiments (Study II), treatment (+4 °C), time and their interaction effects on total and specific primary producer (wall periphyton, epipelon, and phytoplankton) biomass and GPP, in addition to DIP and DIN concentrations and light attenuation, were tested by repeated measures (RM) ANOVA, after checking for normality and homogeneity of variances in the samples and residuals (Shapiro-Wilk and Levene's test, respectively). Throughout the study n = 8, with the first timepoint (16 March) signifying the start of periphyton colonization (chl-*a* =

0), followed by seven harvests. Uncertainties are reported as standard errors, unless stated otherwise. Additionally, to identify differences in seasonal timing, periphyton biomass and GPP calculated for each limnotron were analyzed with a Weibull function. We used the fitweibull6 function from the cardidates package (Rolinski et al. 2007) of R (R Core Team), which fits a six-parameter Weibull function. These parameters are the offset before increase, inflection points of increase and decrease, slopes of increase and decrease and the maximum peaks. Each of these parameters was tested for significant differences between treatments using Welch tests. To check differences in elemental composition of periphyton between the two treatments, paired-sample Wilcoxon tests were used.

To test whether differences in periphyton GPP between the two treatments were proportional to temperature-related increase in subcellular reactions, the Van't Hoff-Arrhenius relationship $e^{-Ea/(kT)}$ was fitted for the period of enhanced periphyton growth (April–May, 4 time points) and used to calculate the activation energy (E_a, in eV) observed under different temperature conditions, where k is the Boltzmann constant (8.61 x 10-5 eV K^{-1}) and T is the residing temperature of the limnotrons at any given time (in Kelvin)6. Under optimal growth temperatures, E_a of GPP for both cells and ecosystems is reported to be 0.32 eV (Allen et al. 2005). The Arrhenius plots of the two treatments were fitted by least square regression lines, and their slopes were tested for significant differences using analysis of covariance (ANCOVA). Periphyton nutrient stoichiometry differences between treatments were tested by Wilcoxon paired tests. The differences in abundance (log (abundance+1)) of different groups of macroinvertebrates between both treatments were tested by univariate general linear models (GLM) using SPSS.

Lastly, in study III, Spearman's rho correlation indices were used to compare background Gollinsee water fluorescence and its DOC concentrations, in addition to comparing primary producer biomass and production to DOC and TP concentrations in the water column. Unless otherwise mentioned, all statistical analyses were performed using various versions of R (3.2.2–3.4.2, R Core Team). Graphs were made using R or Origin Pro (versions 8.5 and 9).

3 RESULTS

3.1 Primary production in small, shallow freshwater systems: GPP and carbon cycling dynamics in kettle holes

3.1.1 Water level and chemistry

Small aquatic systems often witness significant annual water-level fluctuations, which might further influence their water chemistry. During the period we sampled the kettle holes (Study I), the water level in Kraatz dropped significantly from a mean depth of 1.2 to 0.4 m, and from 1.8 to 0.9 m in Rittgarten, decreasing the submerged area by 67 and 50%, respectively. Water chemistry parameters showed strong temporal variations in both kettle holes. Total nitrogen (TN) remained high (≥1.1 mg L^{-1} in Kraatz and ≥2.3 mg L^{-1} in Rittgarten) throughout the summer months but decreased slightly thereafter. Total P (TP) was highest in June in both kettle holes (Fig. 7) and notably a sharp increase in both TP and soluble reactive P (SRP) between May and August (especially in Rittgarten) coincided with the prevailing anoxic conditions in the water column (Fig. 7). Mean dissolved organic carbon was higher in Rittgarten than in Kraatz (Table 2) and was slightly higher within both kettle holes during the summer and autumn months before declining in winter. Both kettle holes froze for a period of about ten weeks between December 2013 and February 2014.

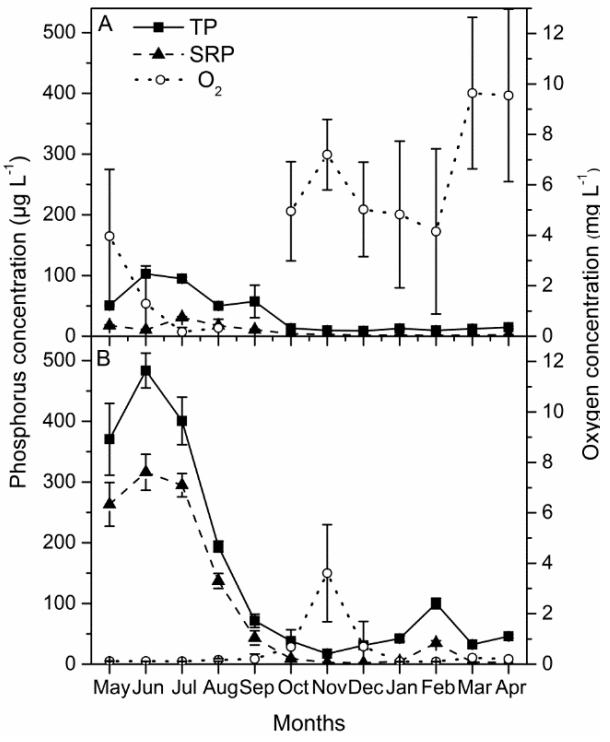

Fig. 7: Temporal fluctuations of total phosphorus (TP), soluble reactive phosphorus (SRP) concentrations (µg L^{-1}) and oxygen concentrations (mg L^{-1}) throughout the sampling period (May 2013 to April 2014) in two kettle holes **A)** Kraatz and **B)** Rittgarten.

3.1.2 Gross primary production

Annual total GPP was 956 and 914 kg C a^{-1} in Kraatz and Rittgarten, respectively. Areal daily GPP rates averaged 1.77 ± 2.2 g C m^{-2} day^{-1} (mean ± SD) in Kraatz and 1.83 ± 1.9 g C m^{-2} day^{-1} in Rittgarten. Macrophytes constituted a significant portion of the total production, accounting for 90 and 81% of the GPP in Kraatz and Rittgarten, respectively. Emergent macrophytes contributed nearly half of the total GPP in both kettle holes (Table 3). Periphyton comprised the majority of the remaining GPP, contributing 10% in Kraatz and 19% in Rittgarten (Table 3). Phytoplankton production was limited in both kettle holes (representing <1% of total annual GPP). During summer (peak macrophyte growing months; June–August) mean GPP rates were 5.1 ± 0.1 g C m^{-2} day^{-1} (mean ± SD) and 4.5 ± 0.6 g C m^{-2} day^{-1} in Kraatz and Rittgarten, respectively (Fig. 8; Table 4). System GPP rates dropped considerably throughout the remaining seasons (Fig. 8; Table 4).

Table 3: Mean total (allochthonous + autochthonous) and aquatic (only autochthonous) areal gross primary production (GPP ± SE in mg C m^{-2} day^{-1}) rates of the different primary producer groups and their contribution to overall GPP inside parentheses (in percent) in the two studied kettle holes from May 2013 to April 2014.

	Kraatz		Rittgarten	
	Total	Aquatic	Total	Aquatic
Phytoplankton	0.5 ± 0.2 (0.04 %)	0.5 ± 0.2 (0.01 %)	0.7 ± 0.02 (0.05 %)	0.7 ± 0.2 (0.1 %)
Periphyton	184 ± 30 (11 %)	284 ± 39 (23 %)	348 ± 146 (19 %)	533 ± 200 (43 %)
Submerged macrophytes	727 ± 288 (41 %)	910 ± 354 (75 %)	261 ± 115 (14 %)	410 ± 179 (33%)
Floating macrophytes	17.3 ± 7.6 (1 %)	19.9 ± 8.5 (2 %)	185 ± 80 (10 %)	289 ± 124 (24 %)
Emergent macrophytes	837 ± 319 (47 %)	---	1036 ± 372 (57%)	---

Table 4: Total GPP (in g C m^{-2} d^{-1}) ± SD per season in the two studied kettle holes in northeastern Germany.

Season	Kraatz	Rittgarten
Spring	1.01 ± 1.11	0.93 ± 1.48
Summer	5.11 ± 0.98	4.54 ± 0.61
Autumn	0.85 ± 1.03	1.40 ± 1.34
Winter	0.09 ± 0.09	0.47 ± 0.47

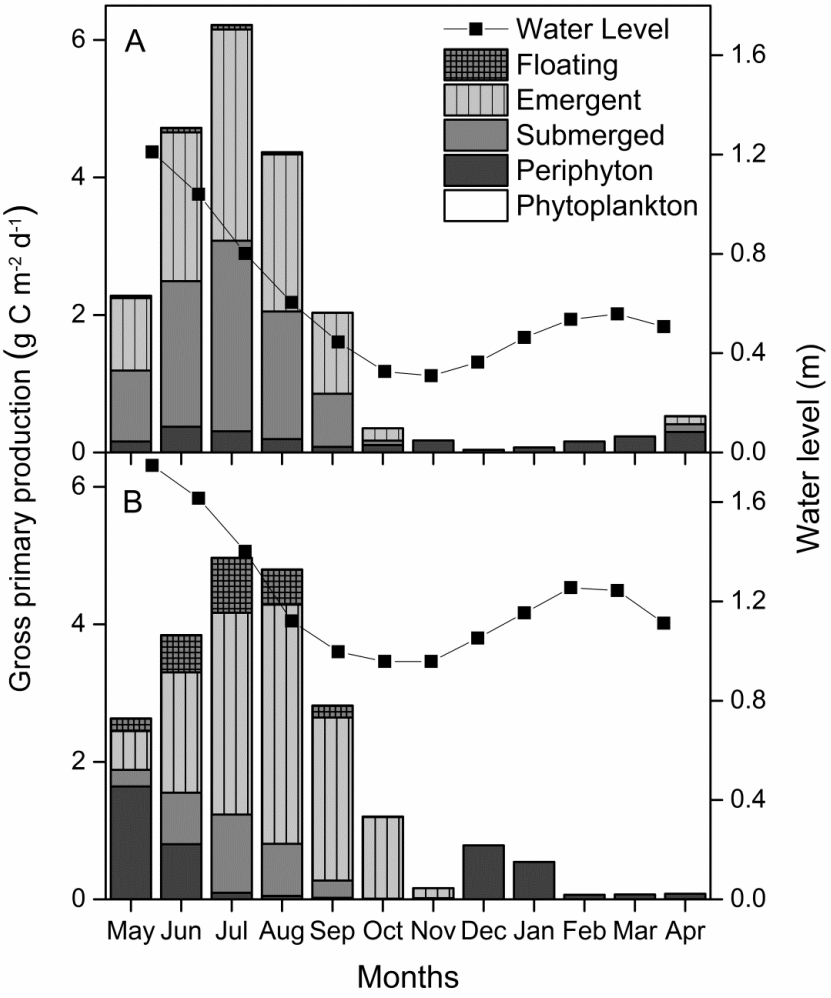

Fig. 8: Monthly gross primary production (GPP, g C m^{-2} day^{-1}) including the contributions of different primary producer groups in two kettle holes: **A** Kraatz **B** Rittgarten

A decline in water levels during the summer of 2013 reduced the surface area available to aquatic GPP calculations (Fig. 8). Annual aquatic GPP averaged 1.2 ± 1.3 g C m^{-2} day^{-1} in Kraatz and 1.2 ± 1.4 g C m^{-2} day^{-1} in Rittgarten (Table 3). Aquatic GPP rates were highest during summer months and averaged 3.2 ± 0.7 and 2.8 ± 0.5 g C m^{-2} day^{-1} in the two kettle holes, respectively. Despite the differences in water nutrient concentrations between the kettle holes (Table 2), only SRP was shown to effect system GPP in both kettle holes (repeated measures ANOVA, $P < 0.05$, Table 5).

Table 5: *F* and *P* values of repeated measures ANOVA investigating the effects of chemical parameters on aquatic GPP.

Kraatz	*F* value	*P*
SRP	9.19	0.029*
TP	0.95	0.375
TN	0.17	0.701
TDN	0.1	0.765
DOC	0.42	0.547
DSi	0.06	0.823

Rittgarten	*F* value	*P*
SRP	15.97	0.01*
TP	5.19	0.07
TN	0.22	0.66
TDN	2.95	0.15
DOC	0.06	0.82
DSi	1.39	0.29

3.1.3 Temporal dynamics of different primary producer groups

Phytoplankton GPP rates were highest in May and June 2013 in both kettle holes, after which they gradually decreased. Periphyton GPP was relatively uniform in Kraatz. In contrast, GPP in Rittgarten was highest in May before declining sharply during summer, likely in response to shading by duckweed (Fig. 8). Periphyton areal GPP increased during winter, but a declining water level led to lower colonization area (Fig. 8). Periphyton GPP contributed 43% to the annual aquatic GPP in Rittgarten and contributed to the majority of the kettle hole's total GPP outside of the macrophyte growing season.

Daily macrophyte (floating, submerged and emergent) GPP between May and October (macrophyte growth season) was 3.1 ± 2.1 g C m^{-2} day^{-1} (mean ± SD) in Kraatz and 2.9 ± 1.7 g C m^{-2} day^{-1} in Rittgarten. Among the submerged macrophytes in Kraatz, *Potamogeton natans* and *P. acutifolius* contributed most to system GPP (Table 1). *Carex acutiformis* Ehrh., *Sparganium erectum* represented the greatest share of emergent macrophytes (Table 1), but following the initial decline in water levels in early July, they occupied an area beyond the aquatic zone. Floating plants (Table 1) altogether covered 16% of the surface area of Kraatz. In contrast, duckweed (a mixture of *Lemna minor* L., *Spirodela polyrhiza* L.) covered 100% of the water surface of the other kettle hole. *Ceratophyllum submersum* L. formed a 10 cm dense mat beneath the duckweed, covering roughly 55% of the kettle hole area. At their peak, the submerged parts of the macrophytes created additional surface area for periphyton colonization, amounting to 7710 m^2 in Kraatz and 6880 m^2 in Rittgarten.

3.1.4 Manipulative experiment of duckweed harvesting

The manipulative experiment in Rittgarten resulted in an increase in phytoplankton chl-*a* concentration from 3.2 (SD: ±0.1) µg L^{-1} to 45 (±0.9) µg L^{-1} two weeks after the harvest of the duckweed and Ceratophyllum cover. Simultaneously, the water column transitioned from anoxia to >30% O_2 saturation. During that period, phytoplankton GPP increased 92% (up to 0.02 mg C m^{-2} day^{-1}). Duckweed returned to cover 100% of the water surface area three weeks after the manipulative experiment and subsequently phytoplankton chl-*a* concentration reverted to 5 µg L^{-1}.

3.1.5 Sediment deposition

Sediment deposition rates from June to November 2013 amounted to 0.84 g C m^{-2} day^{-1} in Kraatz (range: 0.24–3.09 g C m^{-2} day^{-1}) and 1.88 g C m^{-2} day^{-1} in Rittgarten (range: 0.5–3.77 g C m^{-2} day^{-1}) (Fig. 9). The highest sediment deposition rates were recorded in June in Kraatz and in August in Rittgarten. Sediment deposition rates showed a strong correlation to GPP in Rittgarten (Spearman $\rho = 0.89$, $P = 0.034$), but not in Kraatz (Spearman $\rho = 0.49$, $P = 0.36$). From June until the end of November 2013, the cumulative mass of C settled represented 63% of the organic C produced by GPP in Rittgarten and 29% in Kraatz (Fig. 10).

3.1.6 Aerobic sediment mineralization

Aerobic sediment mineralization rates ranged between 0.1 to 0.15 g C m^{-2} day^{-1} in Kraatz and 0.05 to 0.09 g C m^{-2} day^{-1} in Rittgarten (Fig. 9). The highest rates were recorded in December in Kraatz and in June in Rittgarten. During several summer months sediment respiration (SR) measurements using dissolved O_2 were not possible due to the prevailing anoxia above the sediments during these months. Aerobic mineralization rates were not correlated to GPP (P = 0.25) or sedimentation rates (P = 0.1) (Fig. 9).

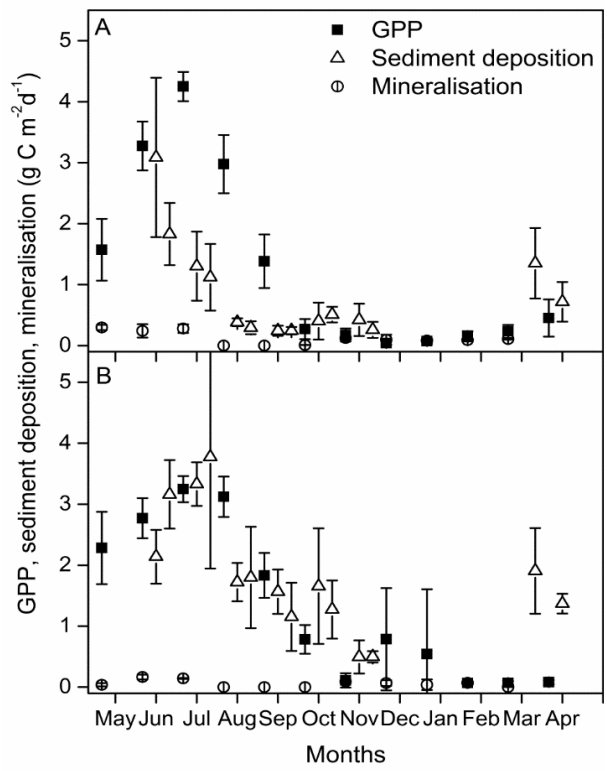

Fig. 9: Temporal variations of total gross primary production (GPP), sediment deposition rates and sediment aerobic mineralization rates in two kettle holes: **A** Kraatz and **B** Rittgarten from May 2013 to April 2014.

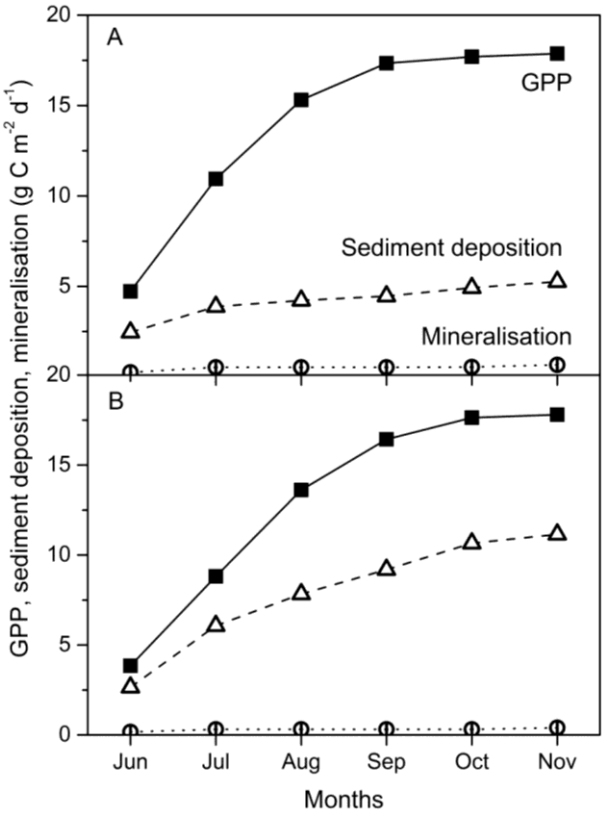

Fig. 10: Cumulative gross primary production (GPP) vs. cumulative sedimented material in **A** Kraatz and **B** Rittgarten from June to November 2013.

3.2 Impacts of warming on primary production in freshwater ecosystems

3.2.1 *GPP and biomass of primary producers*

In the second study, total limnotron GPP was not significantly different between the control and warmed treatments during the investigated period (Fig. 11, Table 6). A maximum total GPP of 3.0 ± 0.7 g C limnotron^{-1} day^{-1} was recorded on 2 June in the warmed limnotrons, while the maximum was lower (2.4 ± 0.1 g C limnotron^{-1} day^{-1}) and two weeks later in the controls (Fig. 11).

Overall, periphyton attached to the walls of the limnotrons (subsequently termed wall periphyton) contributed to 82%–91% of the total limnotron GPP in the control and warm treatment, respectively during the investigated period (Fig. 11). The share of phytoplankton to overall limnotron GPP was low (17% and 8% in the control and warm treatment, respectively). Wall periphyton GPP increased until the beginning of June in both treatments. Similar to total GPP, the maximum of 3 ± 0.65 g C limnotron^{-1} day^{-1} was recorded on 2 June in the warm treatment and 2.2 ± 0.1 g C limnotron^{-1} day^{-1} two weeks later in the control (Fig. 11). Subsequently, wall periphyton GPP decreased in both treatments. Throughout the sampling period, wall periphyton GPP varied 0.8–1.9 fold between the treatments and was significantly higher in the warmed limnotrons (mean = 1.5 ± 0.4 g C limnotron^{-1} day^{-1}) compared to the control (1.1 ± 0.3 g C limnotron^{-1} day^{-1}) (Table 6). This warming effect was time-dependent (Table 6). To compare temporal trends between the two treatments, I plotted Weibull curves which showed that the warm treatment had a significantly earlier inflection point of increase as compared to the control (Table 7). Epipelon GPP, quantified by strips that rested on the sediment, was much lower than GPP produced by wall periphyton and showed no distinct temporal dynamics (Fig. 11). Epipelon GPP (about 1% of total GPP) was significantly lower in the warm treatment compared to the control (Table 6), averaging 0.015 ± 0.005 g C limnotron^{-1} day^{-1} and 0.020 ± 0.008 g C limnotron^{-1} day^{-1}, respectively. Phytoplankton GPP was highest in March in both treatments and decreased henceforth, with an earlier decline in the warm treatment, which coincided with an advanced activity by fungal parasites (Frenken et al. 2016; Velthuis et al. 2017). Overall, phytoplankton GPP was significantly lower in the warm treatment (Table 6).

Total biomass of primary producers, expressed in chl-*a,* was not significantly different between treatments (Table 6). Wall periphyton biomass exhibited similar patterns to its GPP rates described above (Fig. 11), and was significantly higher in the warm treatment, but was also time dependent (Table 6). Epipelon biomass showed less distinct dynamics, as its maximum values were lower than those of wall periphyton, and not different between the two treatments during

the investigated period (Table 6). Phytoplankton biomass was significantly lower in the warm treatment between mid-March and end of June (Table 6).

Table 6: Results of repeated measures ANOVA on the effects of treatment (+4°C), time, and treatment x time interaction on periphyton biomass and GPP during the period of sampling (April till end of June). Plus (+) and minus (-) signs indicate the positive and negative effects of warming, respectively.

Total PP		Biomass		GPP	
	df	*F*-value	*P*-value	*F*-value	*P*-value
Treatment	1	0.0	0.987	2.851	0.097
Time	7	22.42	1.38e-05 ***	36.572	1.38e-05 ***
Treatment x Time	7	0.003	0.956	0.209	0.649
Wall periphyton					
Treatment	1	4.488	0.0383* (+)	7.297	0.0095** (+)
Time	7	53.832	6.65E-10**	15.167	2.35E-10**
Treatment x Time	7	0.509	0.478	2.218	0.0492*
Epipelon					
Treatment	1	0.417	0.521	0.996	0.0323* (-)
Time	7	12.915	0.001**	2.003	0.0741
Treatment x Time	7	7	0.484	0.490	0.65
Phytoplankton					
Treatment	1	7.366	0.009** (-)	13.52	0.0006** (-)
Time	7	47.784	3.53E-09**	14.32	7.07E-10**
Treatment x Time	7	0.153	0.697	1.05	0.411

Table 7: P-values of the Welch tests comparing the Weibull6 fit parameters between the control and warm (+4°C) treatments. Values in bold indicate a significant difference between the treatments.

	Value before increase	Point of increase	Slope of increase	Peak value	Point of decrease	Slope of decrease	Area
Biomass wall	0.23	0.12	0.09	**0.03***	0.51	0.14	0.37
GPP wall	0.88	**0.02***	0.17	0.14	0.21	0.49	0.27

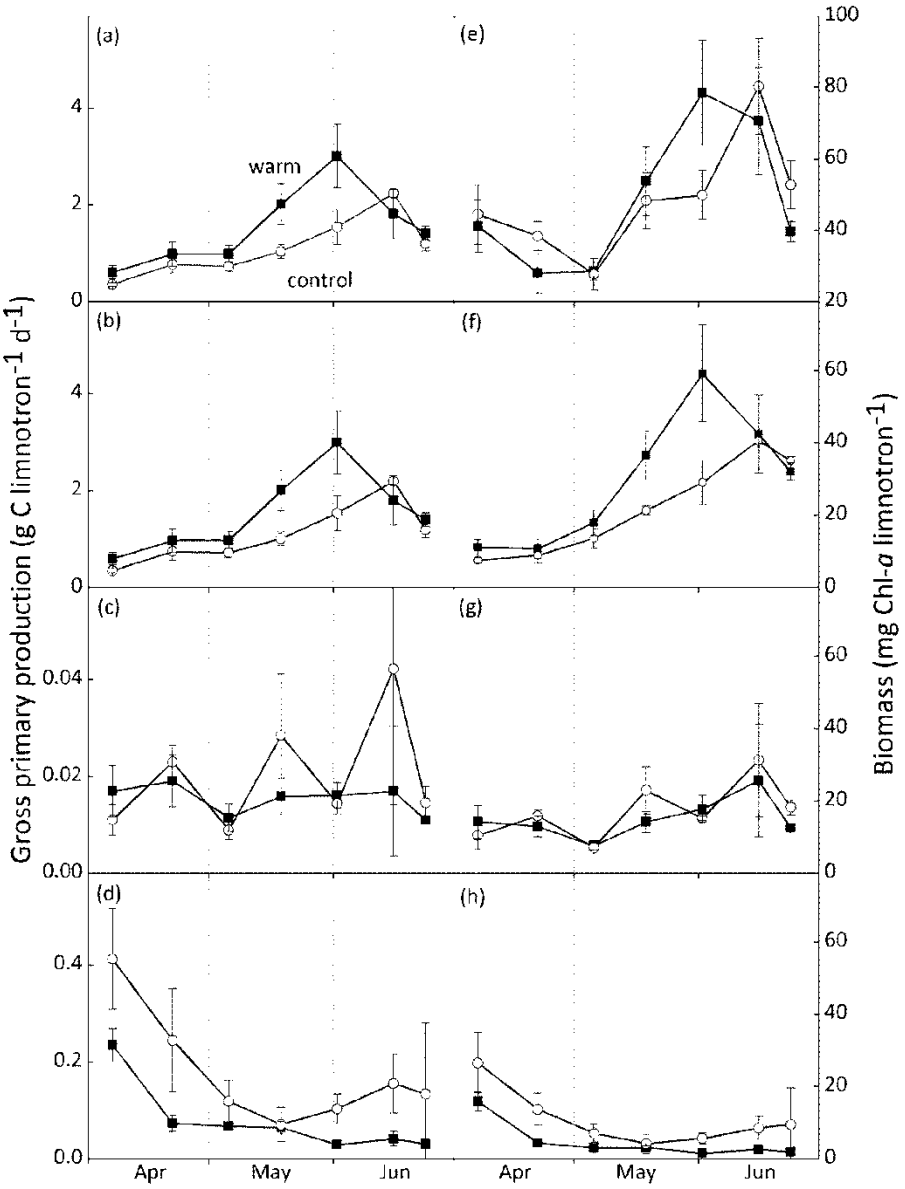

Fig. 11: Gross primary production (GPP, left column) and biomass (chlorophyll-*a*, right column) of total primary producers (a,e), periphyton attached to the limnotron walls (b,f), epipelon (c,g), and phytoplankton (d,h) in control and warm (+4°C) treatments. Values denote mean ± SE (n = 4).

3.2.2 Effects of temperature on bottom-up control and stoichiometry of periphyton

During the investigated period, water temperatures rose from 5.8 to 17.5 °C in the control (average 10.8 °C) and 8.6 to 21.3 °C (average 14.5 °C) in the warm treatment (Fig. 12). To quantify the effect of temperature on gross photosynthetic rates we calculated the apparent activation energy (E_a). Arrhenius plots focusing only on the initial period till early June, which depicted an increase in wall periphyton GPP, were similar for the control and warm treatment (Fig. 13). Specifically, the slopes of the regression lines fitted to this response were not significantly different (ANCOVA, P = 0.37, Fig. 13) and calculated activation energies (E_a) were comparable, with 0.53 and 0.56 eV in the control and warm treatment, respectively.

Table 8: Results of repeated measures ANOVA on the effects of treatment (+4°C), time, and treatment x time interaction on dissolved inorganic phosphorus (DIP), dissolved inorganic nitrogen (DIN), and light attenuation during the period of sampling (April till end of June).

	df	*F*-value	*P*-value
DIP			
Treatment	1	0.111	0.74
Time	7	11.895	6.13e-16 ***
Treatment x Time	7	1.053	0.41
DIN			
Treatment	1	1.172	0.2818
Time	7	30.559	<2e-16 ***
Treatment x Time	7	1.839	0.0399 *
Light attenuation			
Treatment	1	2.834	0.0988
Time	7	2.731	0.0181 *
Treatment x Time	7	1.361	0.2436

Light attenuation (and thereby residual light availability) was not significantly different between temperature treatments (Table 8) and did not show drastic temporal fluctuations until June (Fig. 12). Dissolved inorganic phosphorus (DIP) concentrations were below detection limits in April and early May but increased in the second half of May and June (Fig. 12). Overall, DIP concentrations were not significantly different between treatments during the investigated period (Table 8). Dissolved inorganic nitrogen (DIN) concentrations were also not significantly different between the two treatments, though a marginal treatment and time interaction was detected (Table 8).

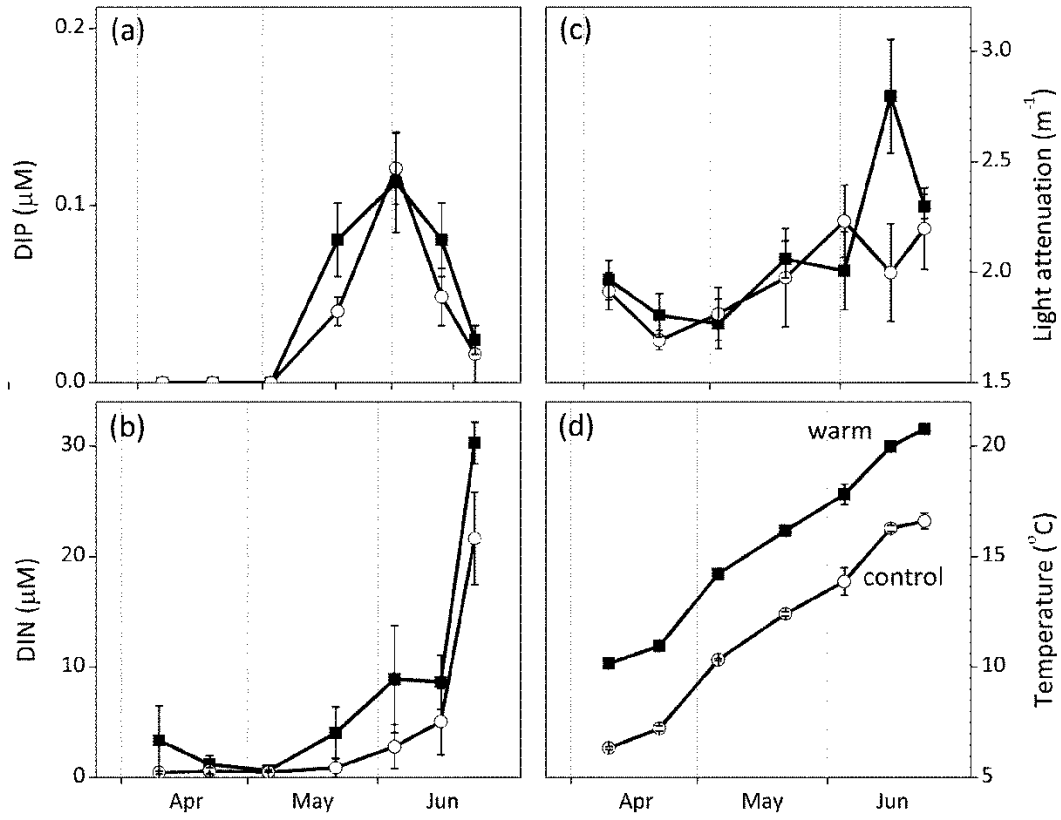

Fig. 12: Concentrations of dissolved inorganic phosphorus and nitrogen (DIP, DIN), light attenuation, and water temperature in control and warm (+4°C) treatments Values denote mean ± SE (n = 4).

Periphyton elemental composition of carbon (C), nitrogen (N), and phosphorus (P) (C:N, C:P, N:P ratios) showed no significant differences between treatments during the investigated period (Fig. 14, paired Wilcoxon tests, $df = 6$, $P > 0.05$). C:N ratios showed a decline over time, but there were no clear trends in C:P and N:P ratios apart from a peak mid-May. Lower periphyton biomass buildup in the control treatment led to less P stored in wall periphyton and epipelon as compared to the warm treatment (Student's *t*-test, $P = 0.02$; Fig. 15a, b). Total limnotron P stored in all primary producers also showed a higher peak in the warm treatment over the same period (Fig. 15c).

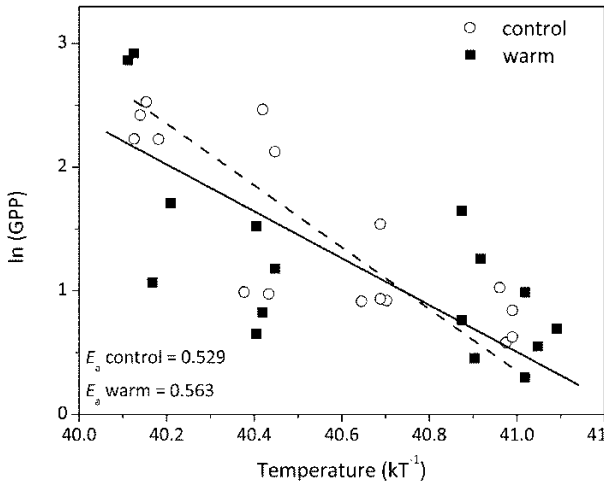

Fig. 13: Arrhenius plots indicating temperature dependence of wall periphyton GPP between 7-Apr and 2-Jun, plotted as the relationship between log transformed GPP (originally measured in mg C m^{-2} d^{-1}) and inverse temperature (kT^{-1}), where k signifies the Boltzmann constant (8.61 10^{-5} eV K^{-1}) and T denotes temperature in Kelvin.

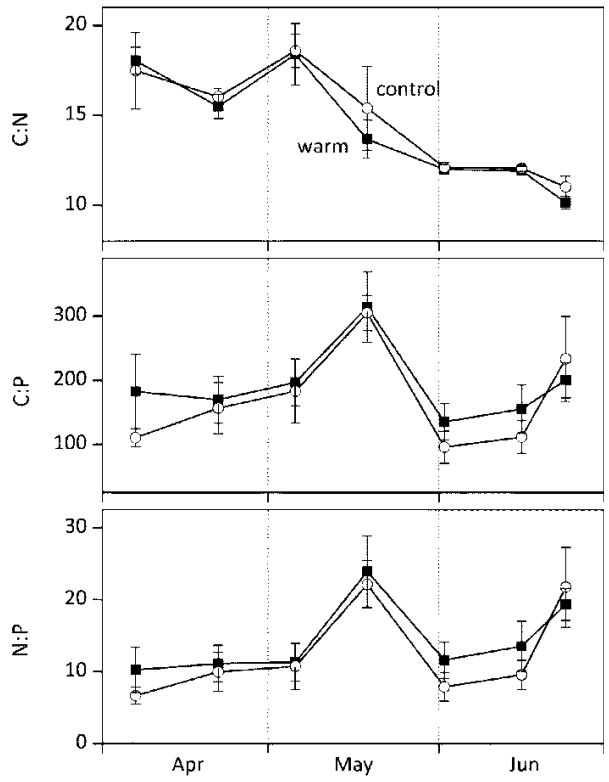

Fig. 14: Periphyton elemental composition with C:N, C:P, and N:P molar ratios in control and warm (+4°C) treatments. Values denote mean ± SE (n = 4).

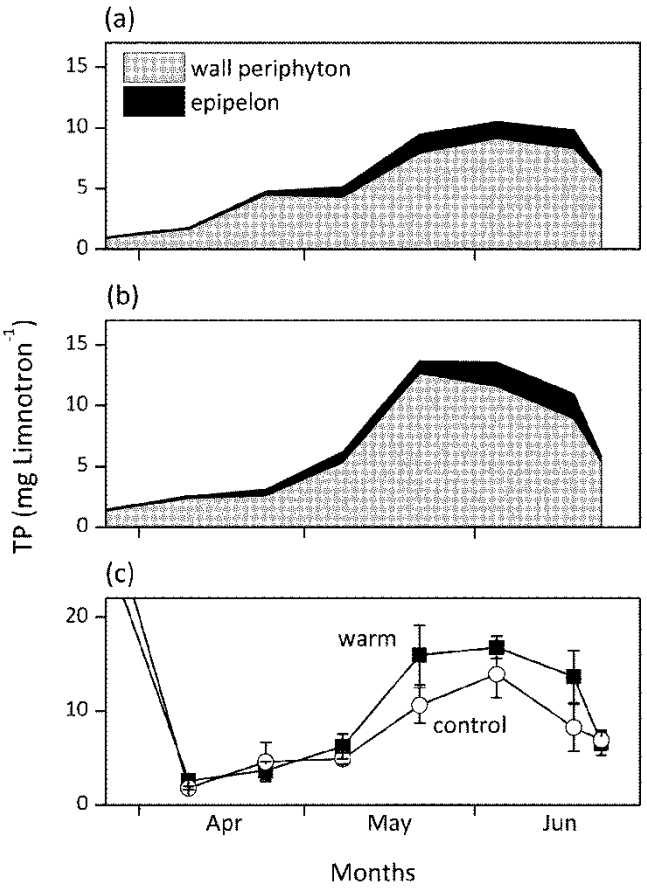

Fig. 15: Total phosphorus (TP) stored in wall periphyton and epipelon in the (a) control and (b) warm (+4°C) treatments. (c) pelagic-TP in the limnotrons of both treatments, calculated by summing up total dissolved inorganic phosphorus (DIP) in the water column and P content of all primary producers: wall periphyton, epipelon, and phytoplankton.

3.2.3 *Effects of temperature on top-down control of periphyton*

The periphyton-grazing macroinvertebrates, consisting of oligochaetes, snails, and mayflies (*Caenis*) and their predator leeches (*Erpobdella octoculata* and *Helobdella stagnalis*) (Fig. 16) were sampled in June. The most abundant snail genus was *Valvata*. In addition, single individuals of the species *Armiger crista* and the genus *Bithynia* were captured only in the warm treatment. The warm treatment had significantly lower abundance of *Caenis* ($F_{1,7}$ = 6.416, P = 0.044 for gravel baskets, $F_{1,7}$ = 4.837, P = 0.070 for multiplates) and abundances of *Valvata* tended to be slightly higher ($F_{1,7}$ = 4.129, P = 0.088, n.s. for multiplates). Abundances of oligochaets were not significantly different between treatments ($F_{1,7}$ = 2.298, P = 0.18 for gravel baskets, $F_{1,7}$ = 2.042, P = 0.203 for multiplates). The abundance of leeches (both *E. octoculata* and *H. stagnalis*) was higher in the warm treatment (Fig. 16).

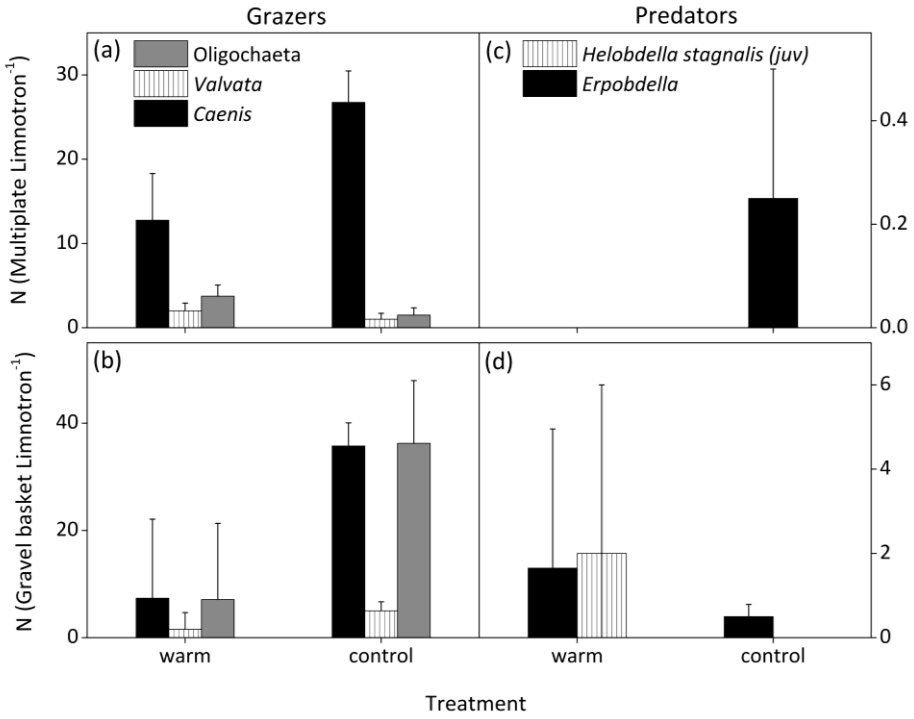

Fig. 16: Most abundant herbivorous macroinvertebrates and their predators, sampled on 25-Jun from (a, c) multiplates and (b, d) gravel baskets in control and warm (+4°C) treatments. Values denote mean ± SE (n = 4).

3.3 The resilience of a shallow lake to a sudden brownification event

3.3.1 Lake water parameters and quality

In the third study, after a strong increase in the water level of Gollinsee between 2011 and 2012, a gradual decline post summer 2013 had returned the water surface to roughly pre-flood levels by the summer of 2015 (Fig. 17). Lake water DOC concentrations, having also reached a maximum during the summer of 2012, decreased more rapidly (Fig. 18A). In fact, by the summer of 2013, DOC concentrations were already reduced by about 40% of the previous measurements in 2012, even though water levels decreased only marginally (5%) over that same period. Thereafter, the decline in DOC concentrations slowed down (29% annual drop till summer of 2014) despite a stronger concurrent water level decline (19%), while in the last year of sampling, the concentration appeared to level off at about 17.5 mg L^{-1}, roughly 1.5-fold that of 2010 pre-brownification values. Concentrations of TP fluctuated greatly from 2012 until the end of 2013, but were generally lower thereafter (Fig. 18B) and seemed to have stabilized by the end of 2014 at concentrations around double those measured prior to brownification (127 µg L^{-1} in July 2015, compared to 58.5 µg L^{-1} in 2010).. Concentrations of SRP (Fig. 19A), which had remained relatively low till summer 2012, exhibited a sharp peak in autumn 2013 (261 µg L^{-1} and 152 µg L^{-1} in the southern and northern basins, respectively). This peak was preceded by

peaks in PP (Fig. 19B), and in DOP concentrations (Fig. 19C) in summer 2013, albeit peak DOP concentrations coincided with the highest DOC concentrations (summer 2012). Concentrations of DN and Fe (Fig 19D, F) also exhibited a similar trend to DOC, while trends in ammonium concentrations followed those of SRP concentrations (Fig. 19E). Concentrations of Mn increased significantly with maxima recorded in summer 2012 (Fig. 19G). Furthermore, all of SRP, PP, DN, NH_4, Fe, and Mn concentrations exhibited peaks at least in one of the basins in autumn 2013 (Fig. 19). In general, the two lake basins showed comparable dynamics for all parameters with only slight differences in peak concentrations. To establish a longer term view of the water quality in Gollinsee prior to the brownification event, we also report here data from a prior sampling conducted in 2007 (Table 9).

Table 9: Mean (+SD) concentrations of dissolved organic carbon (DOC, mg L^{-1}), total phosphorus (TP, µg L^{-1}), soluble reactive phosphorus (SRP, in µg L^{-1}), total particulate phosphorus (PP = TP – TDP, in µg L^{-1}), total nitrogen (TN, in mg L^{-1}), and ammonium (NH_4^+, in mg L^{-1}) measured monthly in Gollinsee from March to October 2007 (n = 8).

DOC	TP	SRP	PP	TN	NH_4^+-N
12.91 ± 0.56	53.13 ± 16.31	4.25 ± 1.89	38.25 ± 12.9	1.42 ± 0.31	0.15 ± 0.16

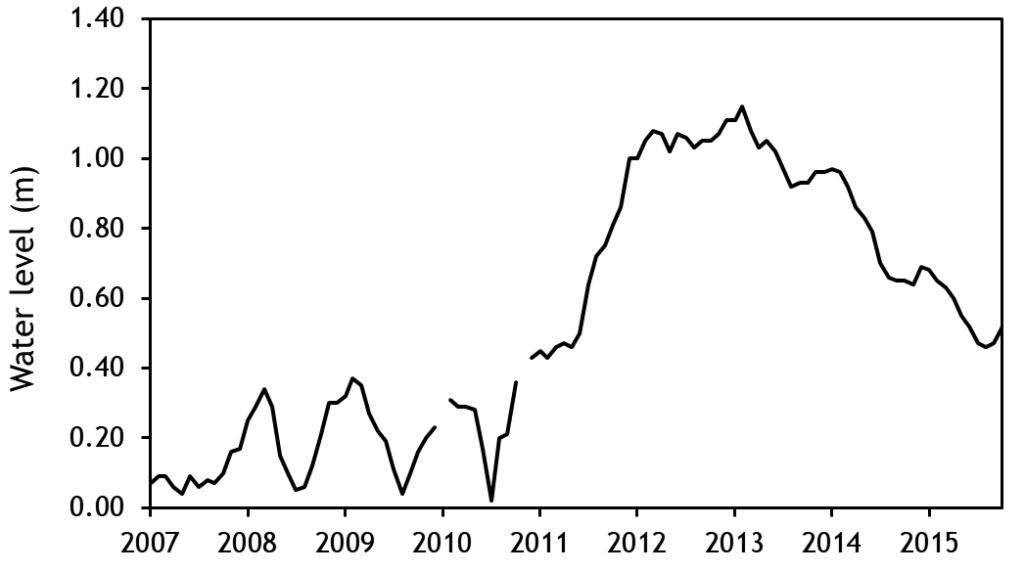

Fig. 17: Water level fluctuations at the measuring gauge level in Gollinsee between 2007 and 2015.

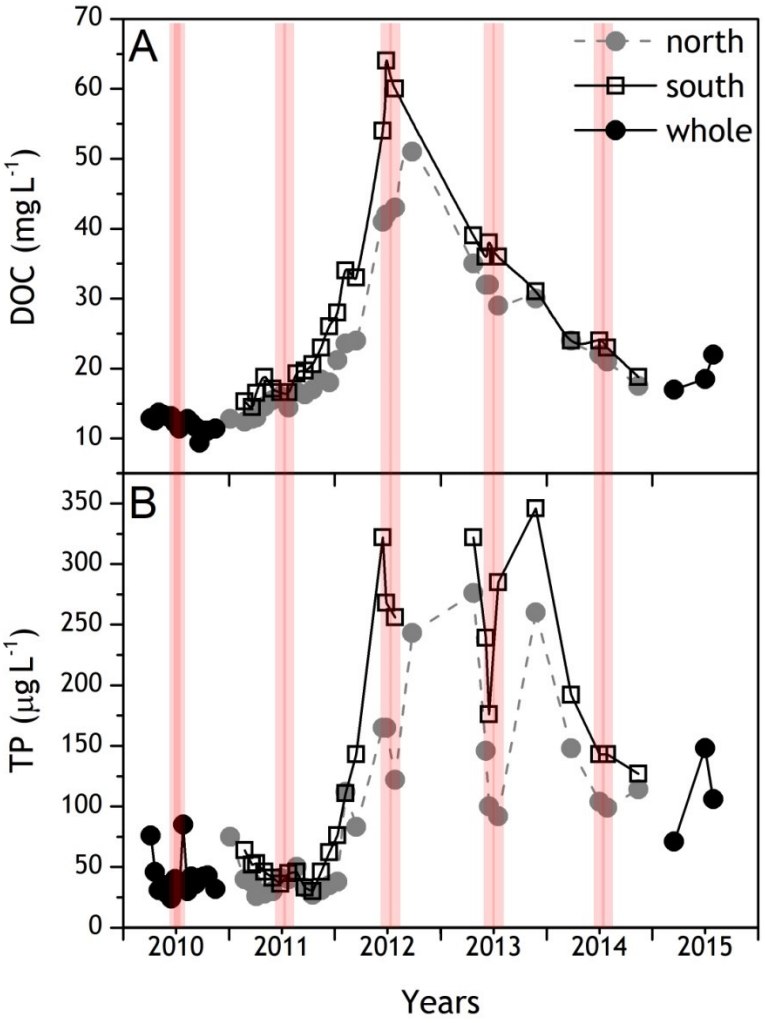

Fig. 18: Dissolved organic carbon (DOC, mg L^{-1}) and total phosphorus (TP, µg L^{-1}) concentrations in Gollinsee, from 2010 to 2015. 2010 and 2015 values represent that of the whole lake, whereas 2011-2014 values are shown for the two sides when the lake was split in half. Vertical bars indicate annual benthic production sampling times. Data from 2010-2012 are taken from Brothers et al. (2014).

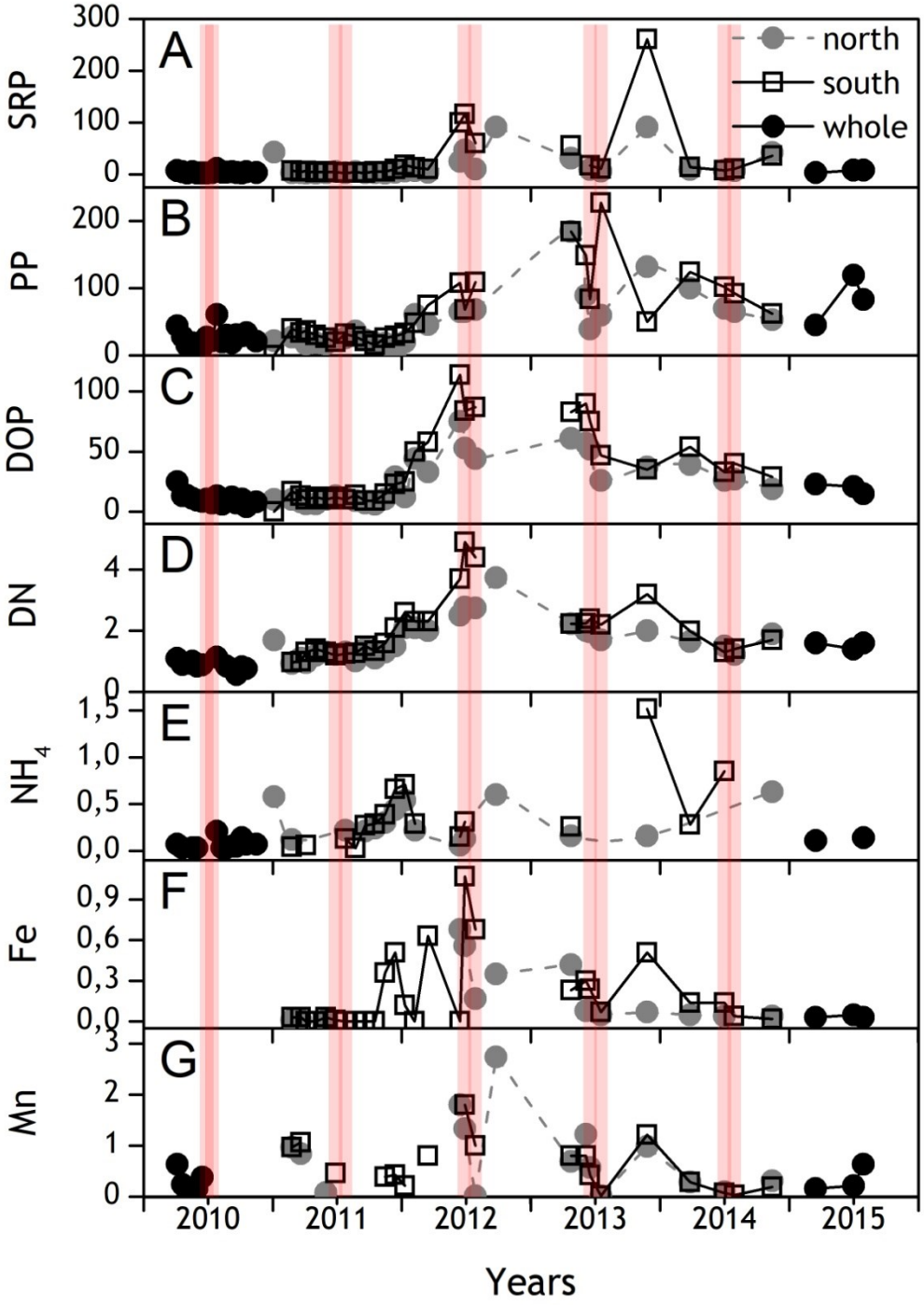

Fig. 19: Concentrations of (A) soluble reactive phosphorus (SRP, in µg L^{-1}), (B) total particulate phosphorus (PP = TP – TDP, in µg L^{-1}), dissolved organic phosphorus (DOP = TDP -SRP, in µg L^{-1}), dissolved nitrogen (DN, in mg L^{-1}), ammonium (NH_4^+, in mg L^{-1}), iron (Fe, in mg L^{-1}), and manganese (Mn, in mg L^{-1}) in Gollinsee from 2010 to 2015. 2010 and 2015 values represent that of the whole lake, whereas 2011-2014 values are shown for the two sides when the lake was split in half. Vertical bars indicate annual benthic production sampling times.

3.3.2 Light availability

Mean global radiation values measured at the surface of Gollinsee during our periphyton study periods (June-July) dropped in 2011 but increased gradually every year from 2011 to 2014 (Fig. 20A). Light attenuation values were highest in 2012 (Fig. 20B), leading to the lowest euphotic zone depth during that same year (Fig. 20C). Thereafter, despite increasing light conditions every year, the water column did not fully return to its pre-brownification light attenuation levels (1.8 m^{-1} in 2010 *vs* 2.9 m^{-1} in 2015) and euphotic zone depth (2.6 m in 2010 *vs* 1.6 m in 2015) (Figs. 20B, C).

The light extinction coefficient (K_D) showed a linear relationship to DOC concentrations (Fig. 21). The background fluorescence of filtered water (i.e. likely caused by colored humic substances) was higher in 2012 and 2013 than in previous years, but values in 2014 were similar to those in 2011, and values had returned to pre-brownification levels by 2015. Background fluorescence and DOC concentrations were strongly correlated (Spearman's rho = 0.958, P = 0.0002, Fig. 22).

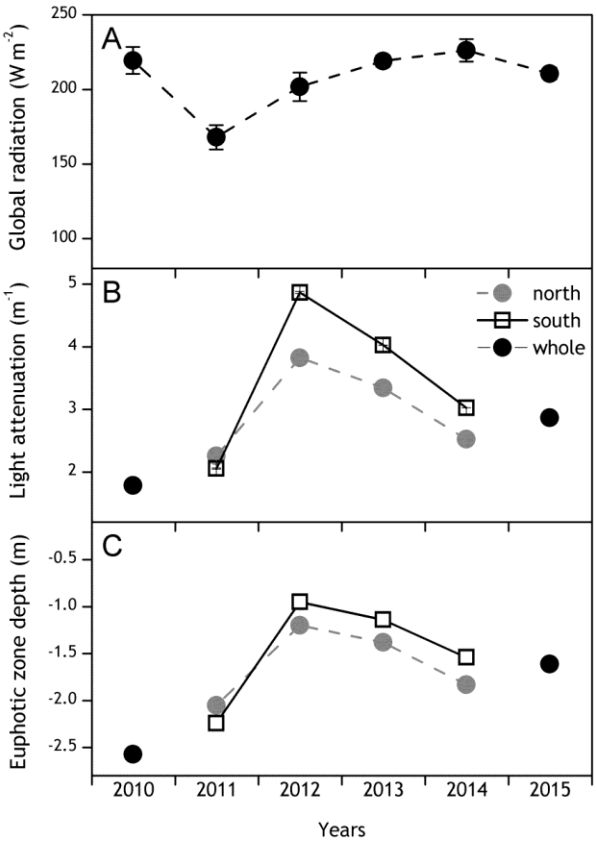

Fig. 20: Differences in global radiation at the water surface (A, ± standard error), water column light attenuation levels (B, ± standard error) and euphotic zone depth, defined as 1% of PAR (C) at Gollinsee in June and July between 2010 and 2015. Global radiation was measured continuously at regular intervals of 10 minutes in 2011, hourly in 2012, and every 30 minutes in 2014. On-site 2013 and 2015 data are lacking due to weather station malfunction, and we thus show global radiation measurements from Döllnsee instead (3.5 km from Gollinsee). Light attenuation values represent the average of two direct measurements per year, at the start and end of the studied period.

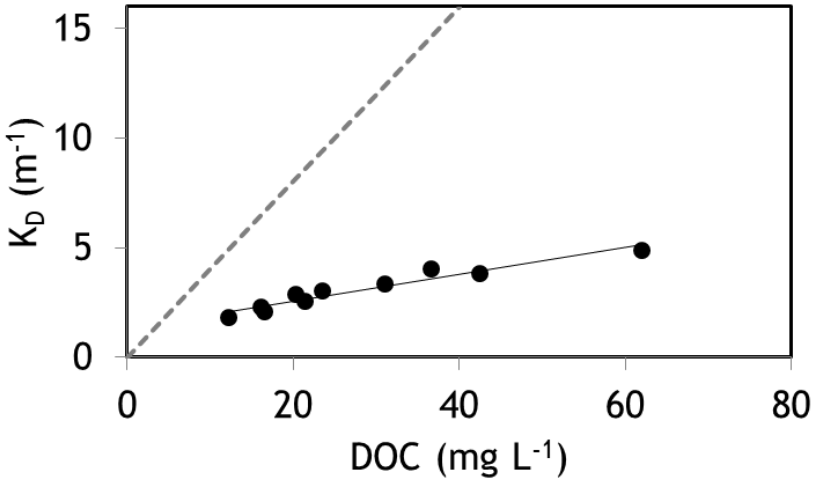

Fig. 21 The light extinction coefficient (K_D in m^{-1}) in Gollinsee as a function of different DOC concentrations (black circles, mg L^{-1}). The dotted line represents K_D used in the model of Kelly et al., 2018.

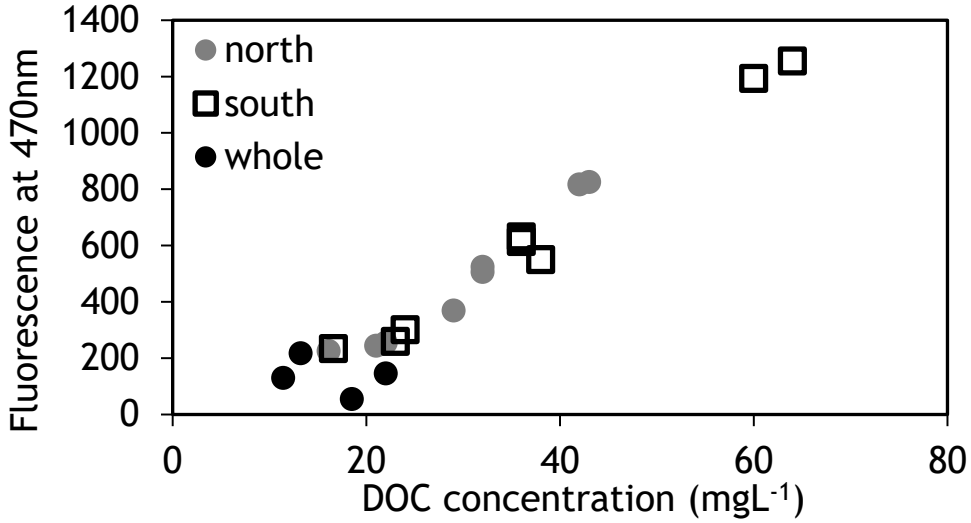

Fig. 22: Correlation between DOC concentrations and background water column fluorescence at 470nm in the whole lake (2010 and 2015) and in two lake sides of split Lake Gollinsee from June and July of 2011 to 2014.

3.3.3 Biomass and production of phytoplankton and periphyton

Throughout the study, Gollinsee was dominated by phytoplankton production, though the biomass and GPP of the primary producers varied between years and with changes in DOC and TP concentrations (Fig 23). Phytoplankton biomass reached its peak in 2013 (191 mg chl-*a* L^{-1} in the epilimnion of the southern basin), before decreasing to pre-brownification (2010) levels by 2014. Phytoplankton GPP rates peaked at 4.9 g C m^{-2} d^{-1} in the southern basin in 2013 and dropped three-fold the following year. Phytoplankton biomass was positively correlated with TP. In contrast, periphyton biomass and GPP showed an inverse relationship to DOC and TP concentrations (Table 10; Fig. 23) and thus were at their lowest during peak brownification. Phytoplankton community composition exhibited annual changes with relatively similar trends in the two basins of the lake (Fig. 24). Diatoms dominated the phytoplankton community before the brownification event. During the first summer after the onset of brownification (2011), green algae represented more than three-quarters of the phytoplankton biomass in the two basins of the lake. In the two subsequent years, diatoms established the majority of phytoplankton biomass, followed by a more heterogeneous composition in 2014. During the summer of 2015, after the removal of the curtain splitting the lake, the phytoplankton community was dominated by cyanobacteria.

Table 10: Spearman's correlation indices and *P*-values of phytoplankton and periphyton biomass and GPP values with water DOC and TP concentrations in Gollinsee between 2010 and 2015. Significant values are represented in bold.

	DOC		**TP**	
	Spearman's rho	*P*-value	Spearman's rho	*P*-value
Phytoplankton biomass	0.527	0.123	0.748	**0.013**
Phytoplankton GPP	0.236	0.514	0.300	0.403
Periphyton biomass	-0.745	**0.018**	-0.651	**0.042**
Periphyton GPP	-0.721	**0.024**	-0.784	**0.007**

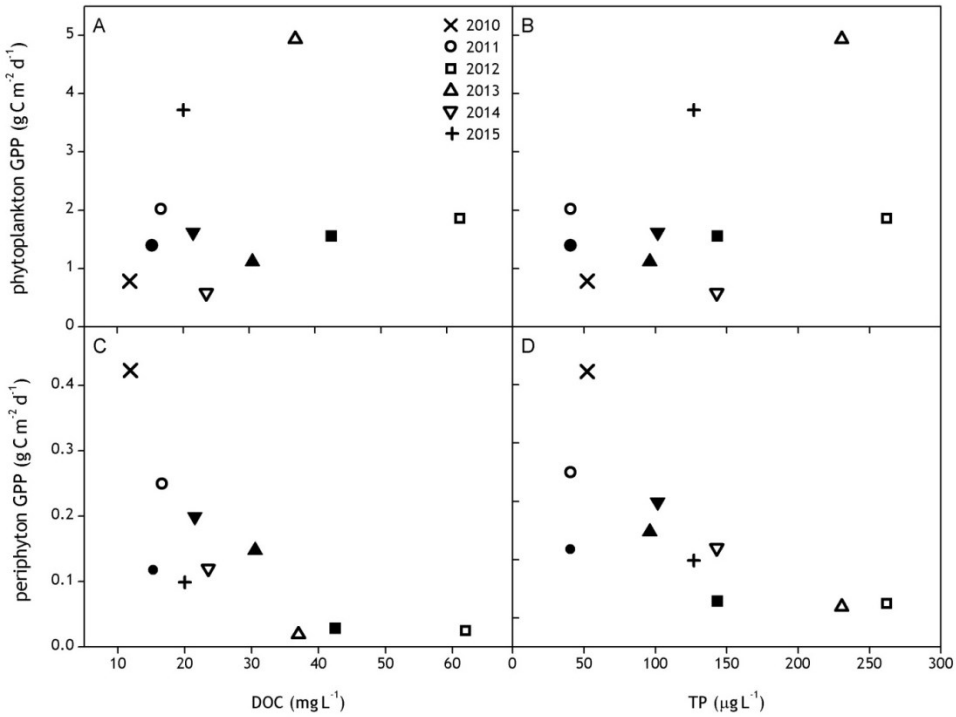

Fig. 23: Summer GPP (phytoplankton in top row and periphyton GPP in bottom; in g C m^{-2} d^{-1}) and water DOC (in mg L^{-1}) and TP (in µgL^{-1}) concentrations in Gollinsee from 2010 to 2015. Filled symbols represent values from the northern basin, empty symbols correspond to values from the southern basin. A single symbol from each of 2010 and 2015 represents whole-lake calculations.

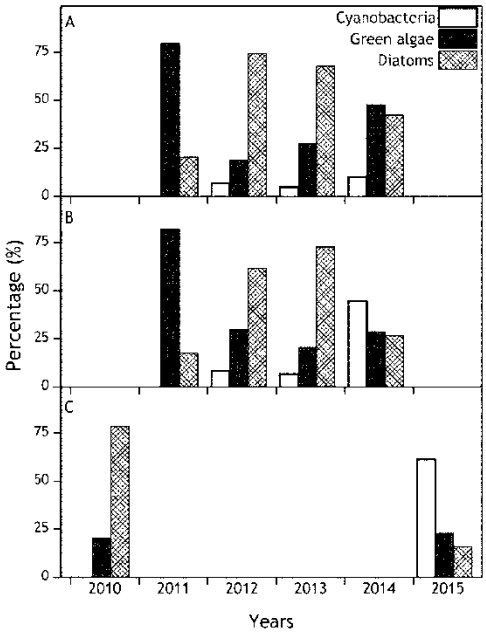

Fig. 24: Percentage contribution (average summer values) of the different phytoplankton groups (cyanobacteria, green algae, and diatoms) to phytoplankton chl-*a* (PhytoPAM measurements) in the northern basin (A), in the southern basin (B), and in the whole lake (C).

4. DISCUSSION

4.1 Small, shallow aquatic systems are C turnover hotspots

The first investigation highlighted the importance of small, shallow systems in primary productivity and carbon cycling. Summer daily GPP rates of the studied nutrient-rich, temperate kettle holes were high and comparable to the most productive natural eutrophic temperate freshwater ecosystems (Fig. 25; Table 11). Emergent macrophytes dominated in the summer and accounted for about half of the annual GPP in both systems (47% in mixed vegetation and 57% in full duckweed cover). The duckweed cover and related anoxia in Rittgarten led to a strong redox-controlled P release from the sediments (Fig. 26). Furthermore, summer sediment deposition rates were high and were strongly correlated to GPP in Rittgarten. Despite the availability of organic material, aerobic sediment mineralization was low in both kettle holes, but specifically in Rittgarten due to prolonged periods of anoxia. Thus, the type of primary producers notably affected nutrient cycling and organic C processing, highlighting the structuring role of the plant communities on biogeochemical processes in the studied kettle holes (Fig. 26). The relatively high temporal resolution of this investigation, a rarity when looking at available literature, make it a valuable contribution to understanding how primary producers affect C dynamics and the uniqueness kettle holes pose compared to other aquatic ecosystems.

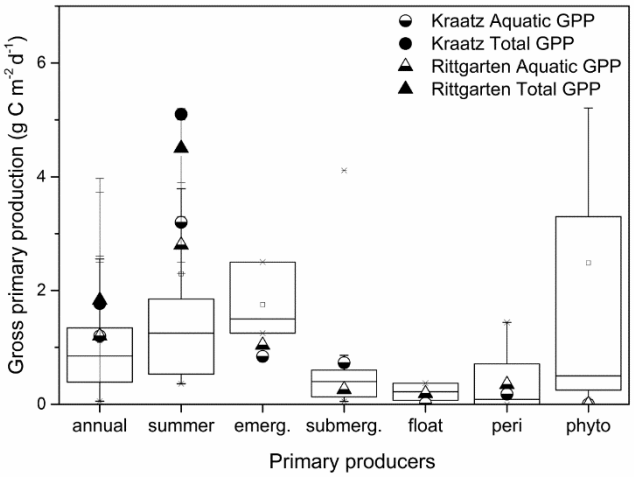

Fig. 25: Annual and summer total (allochthonous + autochthonous) and aquatic (autochthonous) gross primary production (GPP) rates, in addition to annual GPP rates from distinct primary producer groups (emergent, submerged and floating macrophytes, periphyton and phytoplankton) measured in two eutrophic kettle holes (Kraatz and Rittgarten) compared to equivalent GPP rates from other freshwater, temperate shallow systems previously reported in literature (boxplots). Data used from literature are detailed in the supplementary table.

Table 11: Comparison of gross primary production (GPP) of different primary producer groups in freshwater ecosystems (reported values converted to g C m^{-2} d^{-1}). O_2 to C conversion was done applying a 1:1 molar ratio. When not reported, %C was estimated at 45% of dry weight.

Primary producer group	Calculated GPP (g C $m^{-2}d^{-1}$)	Reported GPP	Method	Period	System	Reference
Whole system	1.77-1.83		Compartmental	Annual	Eutrophic kettle hole	This study
	0.36-3.79	30-316 (mmol O_2 $m^{-2}d^{-1}$)	O_2 sondes + in situ mesocosm and bottle incubations	May - Sep	Charophyte dominated shallow pond in SE Sweden	Christensen, Sand-Jensen & Staehr, 2013
	1.12 - 1.61	408-586 (g C $m^{-2}a^{-1}$)	Compartmental (PAM, Biomass)	Annual	Eutrophic, shallow, temperate lakes	Brothers et al., 2013a
	1.2 -1.8	100-150 (mmol O_2 $m^{-2}d^{-1}$)	O_2 sondes	Various	Various stratified lakes	Obrador, Staehr & Christensen, 2014
	6.03	502.1 (mmol O_2 $m^{-2}d^{-1}$)	O_2 sondes	Jul - Nov	Eutrophic, agricultural pond	Klotz, 2013
	1.85	154.2 (mmol O_2 $m^{-2}d^{-1}$)	O_2 sondes	Jul - Nov	Oligotrophic pond in a forest	Klotz, 2013
	1.71 - 9.6	143-800 (mmol O_2 $m^{-2}d^{-1}$)	O_2 sondes	Summer	Eutrophic prarie pot holes	Domine, 2011
	0.38 - 0.52	31-43 (mmol O_2 $m^{-2}d^{-1}$)	^{13}C	May - Sep	Unproductive lakes	Carpenter et al., 2005
	1.25	104.5 (mmol O_2 $m^{-2}d^{-1}$)	^{13}C	May -Sep	Enriched lake	Carpenter et al., 2005
	0.39 - 0.46	11.9 - 14.1 (mol O_2 $m^{-2}a^{-1}$)	O_2 sondes	Annual	Danish lakes	Sand-Jensen & Staehr, 2009
	0.53 - 0.8	44-67 (mmol O_2 $m^{-2}d^{-1}$)	O_2 sondes	10 days mid-summer	Sparkling and Peter Lakes	Van de Bogert et al., 2012
Phytoplankton	0.0005-0.0007		Chl-*a* + PAM	Annual	Eutrophic kettle hole	This study
	5.21	6.95 (g O2 $m^{-2}d^{-1}$)	O_2 sondes	May-Aug	Restored wetlands	Reeder, 2011
	0.39 - 0.499	141- 182 (g C $m^{-2}a^{-1}$)	PAM	Annual	Eutrophic shallow lakes	Brothers et al., 2013
	3.3-11.6		Chamber measurements	Summer	Lake (Michigan)	Althouse et al., 2014
	0.206	206 (mg C $m^{-2}d^{-1}$)	Chl-*a* + light	2 years	Eutrophic shallow lake	Cremona et al., 201
	0.249	249.3 (mg C $m^{-2}d^{-1}$)	^{14}C	Annual	Shallow, saline lake	Wetzel, 1964
	0.08-0.83	29-300 (g C $m^{-2}a^{-1}$)			Eutrophic shallow lake	Mitchell, 1989
Periphyton	0.18 - 0.35	(g C m^{-2} d^{-1})	Chl-*a* + PAM	Annual	Eutrophic kettle hole	This study
	0.732	731.5 (mg C $m^{-2}d^{-1}$)	^{14}C	Annual	Shallow, saline lake	Wetzel, 1964
Epiphyton	0.03-0.09	10-33 (g C $m^{-2}a^{-1}$)	PAM	Annual	Eutrophic, temperate shallow lake	Brothers et al., 2013
	0.086	12.9 (g C m^{-2})		Summer	Eutrophic Shallow lake	Blindow et al., 2006
Epipelon	0.67-0.71	243-258 (g.C.$m^{-2}a^{-1}$)	PAM	Annual	Eutrophic, temperate shallow lake	Brothers et al., 2013
	0.00003 - 0.0071	0.03-7.1 (mg C $m^{-2}d^{-1}$)	Pmax	Jun-Dec	Eutrophic Shallow lake	Liboriussen & Jeppesen, 2003

	0.00002 - 0.0035	0.02-3.5 (mg C $m^{-2}d^{-1}$)	Pmax	Jun-Dec	Mesotrophic, Shallow lake	Liboriussen & Jeppesen, 2003
	1.44	60 (mg C $m^{-2}h^{-1}$)	Pmax		Various US lakes	Vadeboncoeur et al. 2003
	0.84	35 (mg C $m^{-2}h^{-1}$)	Pmax		Various Danish Lakes	
Epixylon	0.03	1.3 (mg C $m^{-2}h^{-1}$)	^{14}C		Reference lake	Vadeboncoeur & Lodge, 2000
	0.10	4.2 (mg C $m^{-2}h^{-1}$)	^{14}C		Eutrophic (fertilized)	
Emergent macrophyte	0.84 - 1.04		Biomass, P/B ratio	Annual	Eutrophic kettle hole	This study
	1.88	1.3 (g C m^{-2} a^{-1})	^{14}C	Annual	Hardwater lake	Gessner et al., 1996
	~2.5	2300 (g DW $m^{-2}a^{-1}$)	Biomass, P/B ratio	Annual	Marsh - Louisiana (*P.australis)*	Sasser & Gosselink, 1984
		2980 (g DW $m^{-2}a^{-1}$)	Biomass	Annual	Former Czechoslovakia ponds (*P.australis)*	Dykyjova, 1967
Submerged Macrophyte	0.26-0.73		Biomass, P/B ratio	Annual	Eutrophic kettle hole	This study
	4.11	5.48 (g O_2 m^{-2} d-1)	O_2 sondes	May-Aug	Restored wetlands	Reeder, 2011
	0.13	49 (g C $m^{-2}a^{-1}$)	Biomass, P/B ratio	Annual	Eutrophic, temperate shallow lake	Brothers et al. 2013
	0.4	400 (mg C $m^{-2}d^{-1}$)	14C	2 years	Eutrophic, large, shallow lake	Cremona et al. 2014
	0.86	(g C m^{-2} d^{-1})	O_2 sondes + chamber measurements	2 years	Shallow lakes	Kenning, 2009
	0.05 - 0.13	17-48 (g C $m^{-2}a^{-1}$)	Biomass, P/B ratio	4 years	Eutrophic, shallow lake	Mitchell, 1989
	0.0765	76.5 (mg C $m^{-2}d^{-1}$)	^{14}C	Annual	Shallow, saline lake (*Ruppia maritima)*	Wetzel, 1964
	~0.6	500 (g DW $m^{-2}a^{-1}$)	Biomass, P/B ratio	Annual	Czech fish pond (*Elodea canadensis)*	Pokorny et al., 1984
Floating macrophyte	0.19		Biomass, P/B ratio	Annual	Eutrophic kettle hole	This study
	0.07	44.5 (g DW m^{-2})	Peak biomass	During peak biomass	Wetlands, Morocco (*L. minor)*	Ennabili et al., 1998
	0.37	300 (g DW $m^{-2}a^{-1}$)		Annual		Wetzel, 2001
	~0.39-0.43	319-348 (g AFDW $m^{-2}a^{-1}$)	Biomass, P/B ratio	Annual	Lake Netherlands (*Nymphaea alba)*	Kok et al., 1990
	~0.13-0.55	108-447 (g AFDW $m^{-2}a^{-1}$)	Biomass, P/B ratio	Annual	(*Nuphar lutea)*	

Pokorny et al., 1984; Kok et al., 1990, and Ennabili et al., 1998 are taken from Wetzel, 2001.
All other full citations are present in the reference list of the thesis.

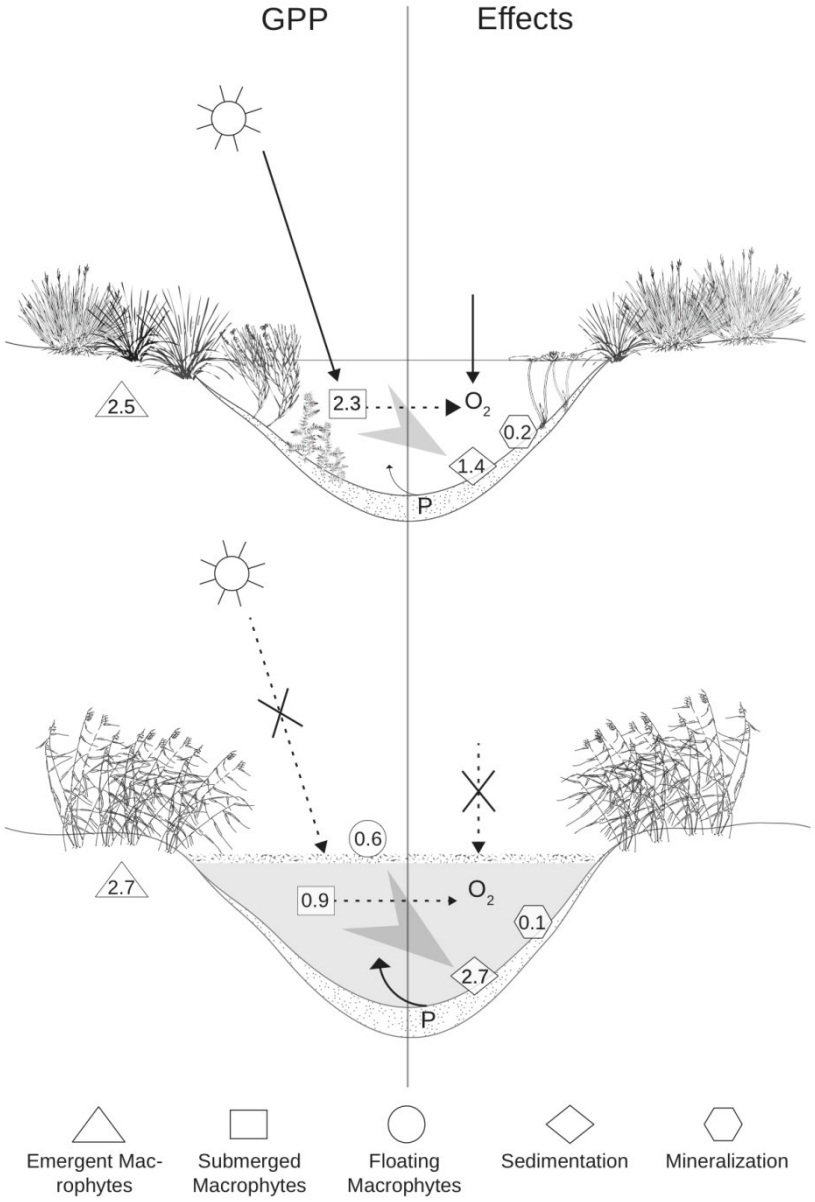

Fig. 26: Gross primary production (GPP) of the different primary producer groups during peak summer months (June to August) and their cascading effects on phosphorus (P) release from sediments and carbon sediment deposition and mineralization (all units in g C m^{-2} day^{-1}) in **A** Kraatz and **B** Rittgarten. Phytoplankton and periphyton constituted <10% of community GPP in the summer and hence were not shown here. Triangles represent emergent macrophyte GPP, rectangles represent submerged macrophyte GPP and circles depict floating macrophyte GPP.

4.1.1 Comparison of kettle hole GPP to other systems

Summer total and aquatic GPP rates of the kettle holes were higher than those reported from other natural temperate lakes and ponds (Hanson et al., 2003; Hoellein et al., 2013; Fig. 25). Due to lower GPP rates recorded throughout the winter months, annual GPP rates were equal or slightly higher than rates reported from similar pothole systems (Badiou et al., 2011; Euliss et al., 2006). Wetland GPP rates have previously been reported to be within the same range as those in these kettle holes (Buffam et al., 2011) or slightly higher (Reeder, 2011; Wagle et al., 2014). In contrast, several studies measured lower GPP values in larger lakes (see Table 11: Carpenter et al., 2005; Coloso et al., 2008; Sand-Jensen & Staehr, 2009; Van de Bogert et al., 2012). However, the different methods used for measuring primary production (including C, DIC consumption, O_2 and fluorescence) and the different units used to report them (i.e. as O_2 production or C fixation) render comparisons between studies difficult. Additionally, depending on the method used, reported values either pertain to GPP, net ecosystem production (NEP), or even, in case of ^{14}C measurements, to a value that lies in between GPP and NEP. Most studies on aquatic GPP have relied on O_2 probes or bottle incubations, making them phytoplankton-centric and excluding the contribution of emergent and floating macrophytes, while studies that adopt a compartmental approach (e.g. Wetzel, 1964; Liboriussen & Jeppesen, 2003; Blindow et al., 2006; Vis et al., 2007; Domine, 2011; Brothers et al., 2013a) are few.

In the first study, the use of multiple O_2 probes revealed a high degree of spatial heterogeneity in O_2 saturation levels (data not shown). However, we were unable to effectively estimate ecosystem metabolism due to extended periods of anoxia or hypoxia throughout the water column. In order to account for high spatial heterogeneity of primary production within systems featuring emergent, submerged and floating vegetation (Hanson et al., 2008; Van de Bogert et al., 2012) and extended periods of anoxia (Baird et al., 1987), we recommend a compartmental approach when determining metabolic rates. A compartmental approach both estimates the contribution of each primary producer group to overall system GPP and avoids limitations pertaining to O_2 unavailability.

Nonetheless, the method is not without limitations. It is laborious, requires frequent sampling efforts and thus does not allow for a high temporal resolution in contrast to in situ continuous measurements. Estimating total system GPP relies on the summation of singular measurements of all PP groups, further increasing uncertainty by incorporating more random and variable measurement error. Standard deviation between sampled replicates of phytoplankton, periphyton and even macrophytes (Table 1) were found to be reasonably low. Instead, the greatest uncertainty within our GPP calculations lies within the biomass to GPP conversion factor chosen while calculating macrophyte GPP. This factor varies greatly (1.2–2.6) within

reported literature (Westlake, 1982 and references within) depending on macrophyte species, season, water and air temperatures, light availability, and state of decay of the plants. In our GPP calculations, we used a conservative biomass to GPP conversion factor of 1.5 and thus might have represented the lower range of GPP estimates from these kettle holes. Another factor of uncertainty lies in macrophyte biomass to leaf area conversion rates (needed to estimate periphyton colonizable area), which can differ in a threefold range among species (Filbin & Hough, 1983) but also depending on environmental conditions (Spence & Chrystal, 1970). Nonetheless, in our study, given the relatively low periphyton biomass during the macrophyte growing season in both kettle holes (and thus its very minor contribution to system summer GPP) this particular uncertainty is not significantly pronounced with regards to the overall GPP calculations.

4.1.2 Contribution of different primary producers to total GPP

Among different autotroph groups, emergent macrophytes contributed most to GPP in our kettle holes, a pattern that has also been observed within small temperate aquatic systems and wetlands (Fig. 26). Despite minimal direct gas exchange with the water column, emergent macrophytes are an important metabolic component of aquatic ecosystems, influencing the availability of organic C and nutrients to other aquatic primary and secondary producers (Wetzel, 2001). GPP of emergent macrophytes is rarely incorporated into terrestrial C balances. Excluding their contribution from aquatic C balances can lead to significant underestimation of C sequestration at the landscape scale (Abril et al., 2014).

Submerged macrophytes are usually less productive than emergent plants, mostly due to effects of self-shading, as well as shading by periphyton, phytoplankton and other macrophytes (Wetzel, 2001). In our study, submerged macrophytes still represented a substantial fraction of the total GPP in Kraatz (Table 3). As with emergent macrophytes, herbivory on submerged macrophytes often leads to underestimated productivity rates. Wetzel (2001) reports that for *C. submersum*, true production rates can be three times greater than those estimated from maximum biomass values. We applied a conservative factor of 1.5 to calculate GPP from maximum standing crop and thus may have underestimated the production of some submerged macrophytes. However, our GPP values are still comparable to those in the literature (Fig. 25; Table 11). In contrast, floating macrophytes constituted a rather small share of the total GPP in both kettle holes (Table 3). Despite this, they had a very significant impact on the nutrient and C dynamics, as described below.

Periphyton was the major contributor to system GPP during periods when the influence of macrophyte shading was negligible. Periphyton biomass in Rittgarten was more than double that of Kraatz, except during periods of complete cover by duckweed. Although potential periphyton colonization area increased due to the spread of the submerged macrophytes, shading (and probably grazing) limited its production in summer. Annual periphyton GPP rates were within the same range or higher than those reported for other temperate water bodies (Fig. 25). In contrast, phytoplankton GPP rates in our kettle holes were lower than rates reported from temperate eutrophic shallow lakes (Fig. 25), indicating the minor role that they play in kettle holes (Table 3). Despite the high availability of nutrients, this was expected due to the low water depth of the kettle holes, shading and potentially allelopathy by macrophytes. Although not measured, the grazing potential on phytoplankton and periphyton by zooplankton and invertebrates was likely high due to the absence of fish (Jones & Sayer, 2003). The higher areal phytoplankton GPP and biomass in Rittgarten can be partially attributed to the initial 48% greater mean depth of that kettle hole compared to Kraatz. The low contribution of phytoplankton to aquatic GPP explains the lack of correlation between phytoplankton chl-*a* concentrations and aquatic GPP in the kettle hole with mixed vegetation. Shading effects of floating vegetation on phytoplankton were verified with the manipulative experiment in Rittgarten wherein the removal of duckweed and *Ceratophyllum* led to a brief phytoplankton bloom and the oxygenation of the water column. On the longer term, however, grazing by zooplankton might have also played a significant role in limiting phytoplankton production and biomass.

4.1.3 Primary production drives nutrient cycling, sediment deposition and benthic mineralization rates

The effects of a given primary producer group on a system's nutrient and C dynamics were not proportional to the group's contribution to total GPP. Free-floating macrophytes (duckweed) in Rittgarten constituted only 9% of the system's total GPP but triggered substantial cascade effects on several ecosystem processes. A full surface cover of floating plants impeded light penetration into the water column, limiting the growth of planktonic, epiphytic and epipelic algae, and resulting in extended periods of anoxia. In addition, we calculated that a potential O_2 surface influx of 33.5 g O_2 m^{-2} was blocked by the full duckweed cover for roughly 90 days between June to September. A strong increase in SRP concentrations in Rittgarten (Fig. 7; Kleeberg et al., 2016b) was likely due to the release of iron-bound P from settled matter and surface sediments, which can result from hypoxic or anoxic conditions (Gächter & Müller, 2003; Kleeberg et al., 2013). Given the steady-state conditions and assuming that there was no high

external P input into the system during the same period, the increase in SRP concentrations is attributed to the release of P from settled matter and the surface sediments. After the disappearance of the floating vegetation during autumn and the subsequent re-oxidation of the water column, TP and SRP concentrations decreased (Fig. 7). Kleeberg et al. (2016b) reported that the sedimentary molar Fe:P ratio, an indicator of P mobility, was similar in both kettle holes. Nevertheless, as indicated by the molar S:Fe ratio in surface sediments (0–2 m) there was a much lower Fe availability for P binding in Rittgarten (S:Fe = 2.33) than in Kraatz (S:Fe = 0.06). At a S:Fe ratio <1.5, vivianite, an iron phosphate mineral (Fe_3 $(PO_4)_2$ $8H_2O$), can be formed (Rothe et al., 2015). In Rittgarten, O_2 depletion, exacerbated by shading, lead to exceedance of this threshold and promoted effective sulphate reduction (Kleeberg et al., 2016a), consequently leading to the formation of insoluble iron sulphides (FeS_x). Thus, the duckweed dominance represents a self-stabilizing mechanism, achieved through increasing P availability via a dense surface covering that directly lowers the O_2 flux from the atmosphere as well as indirectly by limiting O_2 production by submerged primary producers through shading. The establishment of a P-rich water column favors the annual re-occurrence of duckweed, resulting in a positive feedback between P availability and duckweed cover (Scheffer et al., 2003). Duckweed dominance in Rittgarten thus represents a stable state (Scheffer et al., 2003) that contrasts with patterns exhibited in Kraatz, where short periods of anoxia and low TP concentrations were prevalent.

Cumulative deposited material remained lower than cumulative GPP from June to November (Fig. 10) pointing to a low input of particulate organic matter by erosion or aeolian transport from the terrestrial catchment during this period. A discrepancy between cumulative GPP and sediment deposition rates in Kraatz might be explained by a lower probability of the prevailing species being caught in our traps and the later senescence of emergent macrophytes (6–12 months), while duckweed and *Ceratophyllum* mats were mainly senescing in the measuring period (within 1–3 months) (Twilley et al., 1985). This might also explain the differences in the peaks of aerobic mineralization occurring in June and December in Rittgarten and Kraatz, respectively. Regardless, sediment deposition rates in both systems are high compared to other aquatic systems (Ferland et al., 2014). The effects of primary producers on O_2 availability may also influence C burial rates, which have been shown to be high under anoxic conditions (Bastviken et al., 2004; Brothers et al., 2013b; Isidorova et al., 20156). However, in our study, the low C degradation by aerobic mineralization in Rittgarten was likely compensated by higher methane (CH_4) emissions due to anaerobic C degradation, especially within the reed belt (C. Lisboa, pers. comm.). During the mostly anoxic months of full duckweed cover (May–September), CH_4 emission, measured on a monthly basis by a greenhouse gas analyzer (ABB—Los Gatos Research, San Jose, CA, USA), averaged 0.21 ± 0.1 g C m^{-2} day^{-1} (mean ± SD) above the

water column and 0.52 ± 0.3 g C m^{-2} day^{-1} above the reed belt. During the same period, CH_4 emissions were lower in Kraatz, amounting to 0.14 ± 0.1 g C m^{-2} day^{-1} (mean ± SD) and 0.25 ± 0.2 g C m^{-2} day^{-1} above the water column and surrounding emergent macrophytes, respectively. Anaerobic mineralization is reported to contribute significantly to C loss from small aquatic systems (Holgerson, 2015). Regardless, aerobic and anaerobic mineralization combined still do not add up to GPP or sedimentation rates within these kettle holes, indicating a high potential for C burial, if current conditions prevail.

Kleeberg et al. (2016b) showed lower burial rates in Rittgarten within the past century compared to Kraatz. We assume that this result mainly stems from a higher frequency of drying up of Kraatz during the last century. The assumed lower sediment deposition and higher mineralization rates of buried material during the drying–rewetting period were supported by the molar ratio of the redox-sensitive elements Fe and Mn over the last 100 years from dated sediment cores (Kleeberg et al., 2016b). The data show a stronger variability in Rittgarten (Fe:Mn 86.1 ± 15, n = 622) while being more constant in Kraatz (Fe:Mn 72.9 ± 4.9, n = 1022), which did not dry up due to its location in a deeper depression. Hydroperiod (Rittgarten dries more frequently during summer than Kraatz) may also contribute to lower species richness in Rittgarten, since differences in nutrient profiles alone are unlikely to explain dissimilar plant community structure. Given the laborious methodology involved, our study focused only on two kettle holes. There is a need for further studies of kettle holes with similar characteristics (water levels and fluctuations) in order to more reliably isolate the effects of differences in plant community type. Regardless, this study provides valuable insight into C dynamics within these understudied systems and, in agreement with Carpenter (1989), we believe obtaining ecological knowledge about whole ecosystems is a valid approach even in the absence of sufficient replication.

4.2. Warming has significant, yet complex effects on primary producers, as well as carbon and nutrient turnover in small aquatic systems

In contrast to our hypothesis, average total GPP did not significantly increase in response to 4°C warming in limnotrons where we simulated temperate lentic spring and early summer conditions, even though we recorded a higher peak production in the warm treatment. This was due to the contrasting effects of warming on phytoplankton and periphyton GPP and biomass during this period (Fig. 11, Table 6). Potential positive temperature effects on phytoplankton biomass were offset by an earlier termination of the spring bloom by fungal parasites facilitating zooplankton grazing (Frenken et al., 2016; Velthuis et al., 2017). In contrast,

periphyton development was initially determined by bottom-up processes, while periphyton grazing seems to have significantly impacted its GPP only starting early summer.

4.2.1. The effect of warming on primary production

As expected, periphyton biomass and GPP in warm treatment were strongly enhanced compared to controls in spring (April and May) when water temperatures ranged from 6–16 °C. Higher spring temperatures nearly doubled maximum periphyton GPP, which was likely facilitated by higher P availability for periphyton in the warm treatments (Fig. 15C) originating from an earlier P release from phytoplankton grazing (Frenken et al., 2016) and a stronger P release from the sediment (Fig. 27). After the initial increase, periphyton biomass and GPP declined more rapidly in the warm treatment in June. The decrease in biomass coincided with an increase in the abundance of zooplankton (Fig. 28; Velthuis et al., 2017). This, along with stronger macroinvertebrate grazing pressure indicated by higher snail abundances in the warm treatment, counteracted the positive temperature effects. Consequently, differences in periphyton biomass and GPP between treatments disappeared by mid-June.

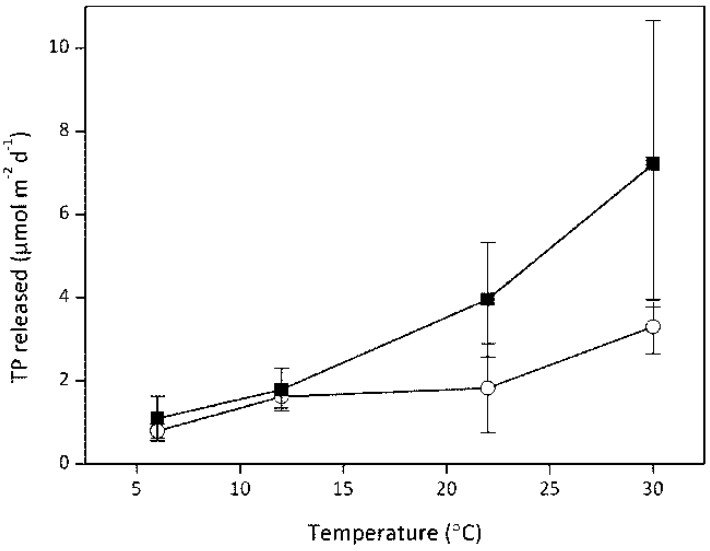

Fig.27: Total phosphorus (in µmol m^{-2} day^{-1}) released from the sediment in oxic and anoxic conditions.

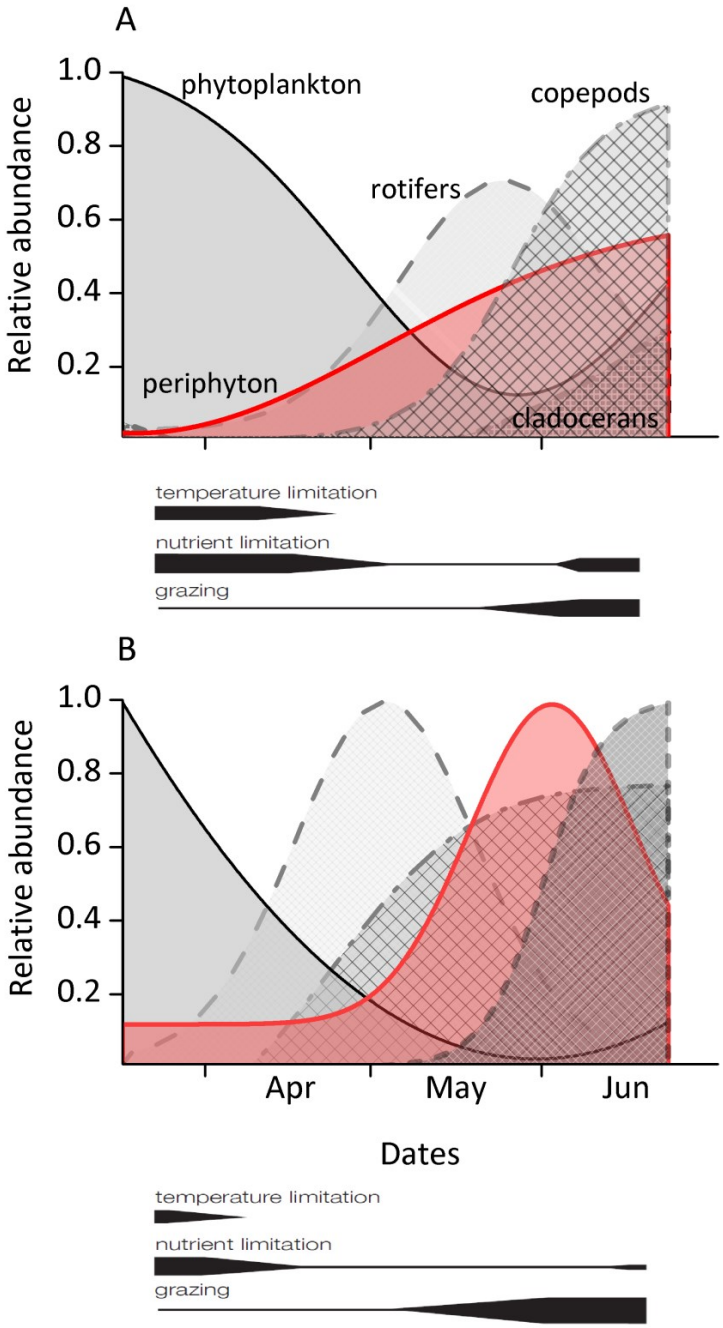

Fig. 28: Dynamics of relative phytoplankton and periphyton GPP and the abundance of their potential zooplankton grazers (from Velthuis et al., 2017) in the (a) control and (b) warm (+4°C) treatment. Data are retrieved from Weibull analyses and scaled to the maximum across treatment and within a group. Width of black bars below each figure indicates potential of limitation on periphyton GPP by each indicated factor. The period shown is extended into March to include the peak of the phytoplankton bloom which was part of another work (Velthuis et al., 2017).

Limnotron primary production was dominated by periphyton due to the systems' high surface to volume ratio, high phytoplankton grazing pressure due to lack of top-down control of fish on zooplankton, and the low light availability at the sediment surface (< 2.5 E m^{-2} day^{-1}) restricting epipelon GPP (Asaeda et al., 2004; Rier et al., 2006).

Periphyton GPP measured in the limnotrons are comparable to rates measured with a similar approach in small, temperate eutrophic lakes during the same seasons (0.7–0.8 g C m^{-2} day^{-1}; Brothers et al. 2013a) and in the previously studied hypertrophic fishless kettle holes (0.3–1.1 g C m^{-2} day^{-1}). The overall high periphyton contribution to total GPP supports recent studies on the importance of periphyton production in both smaller (Liboriussen & Jeppesen, 2003; Brothers et al., 2013a) and larger shallow lakes (Brothers et al., 2016; Devlin et al., 2016).

The fluorescence-based method applied for GPP measurements seems particularly useful for periphyton as it avoids problems of the more common O_2 or ^{14}C techniques. These are assumed to underestimate GPP in periphyton as some of the O_2 produced or ^{14}C fixed in periphyton is respired before reaching the oxygen probe or the end of the incubation period for ^{14}C measurements (Revsbech et al., 1981; Glud et al., 2009; Denis et al., 2012). PAM measurements might also underestimate GPP as fluorescence from deeper portions of thick periphyton layers might not be fully captured; but otherwise it could be argued the method used overestimated GPP as 1) actual light perceived by periphyton on the walls might be lower than light measured by the central flat sensor and 2) due to the direct inflection of excitation light in the PAM fluorometer as opposed to *in-situ* light scatter.

Arrhenius' plots for the period of enhanced periphyton growth (April–May) showed that periphyton GPP responded to temperature following a similar pattern in both treatments, indicating that differences in periphyton growth between the two treatments might simply reflect the two-week lag of temperature in the control treatment. However, calculated apparent activation energy (E_a) for periphyton GPP were 1.65 (control) and 1.75 (warm treatment) times higher than values predicted by the Metabolic Theory of Ecology (MTE[6]) explaining the relationship between temperature and biomass production at the ecosystem level. This disproportional increase in GPP likely points at a co-alleviation of another limiting factor in both treatments, further enhancing the temperature-driven periphyton production. The most likely factor is a higher P availability indicated by 1) declining periphyton C:P and N:P ratios in mid-May despite an increase in periphyton biomass and 2) by a slight increase in DIP concentrations during the same period (Fig. 2). However, P availability was likely higher in the warm treatment, stemming from an earlier termination of a phytoplankton spring bloom (Frenken et al., 2016; Velthuis et al., 2017) and a higher sediment P release during the investigated period (4–6 and 3.2–4.5 mg P $limnotron^{-1}$ for the warm and control treatment, respectively). Differences in oxygen availability at the sediment surface[53] and/or temperature-dependent mineralization rates (Jeppesen et al., 2009; Gudasz et al., 2010; Liboriussen et al., 2011) could explain this TP discrepancy.

4.2.2 Higher grazing pressure counterbalances the positive effects of warming on periphyton GPP

It has been shown that macroinvertebrates and zooplankton can both exert strong grazing pressure on periphyton. In our study, the stronger decrease of periphyton biomass and GPP in the warm treatment in June might be attributed to a higher abundance in periphyton grazing snails (*Valvata*), a two week advanced temperature optimum for snails (Kairesalo & Koskimies, 1987), and an advanced increase in zooplankton abundance (Fig. 28). Oviposition of *V. piscinalis* has been shown to occur between May and June (Mouthon & Daufresne, 2008) suggesting a strong increase of their grazing impact after this period. As periphyton stoichiometry, and thereby their putative nutritional value (Sterner & Elser, 2002), did not differ between treatments (Fig. 14), periphyton quality is not assumed to have led to differences in grazing pressure. Furthermore, algal group composition was found to be similarly dominated by diatoms (HPLC analyses showed high pigment concentrations of fucoxanthin, data not shown) in both treatments in the beginning of June, when grazing started significantly reducing periphyton biomass.

Zooplankton can feed on periphyton, especially when phytoplankton abundance is low (Hann, 1991; Duggan, 2001; McIntyre et al., 2006; Feuchtmayr et al., 2009; Masclaux, 2012). Zooplankton data (Velthuis et al., 2017) show an advanced increase in rotifer abundance in May, and copepods and cladocerans in June in the warm treatment, coinciding with the decline in periphyton biomass (Fig. 28). As a result, zooplankton grazing pressure, expressed by the ratio of zooplankton biovolume to total chl-*a* values (phytoplankton and periphyton), increased from April to June in both treatments. The maximum ratio, however, was higher in the warm treatment (9.1 *vs* 5.7).

Other studies support the notion that warming affects grazer-periphyton interactions. For instance, positive impacts of temperature on periphyton were dampened - or altogether absent - in the presence of snails (Cao et al., 2015) and the impact of grazing was stronger than nutrient availability (McIntyre et al., 2006). Shurin et al. (2012) showed that the presence of planktivorous fish had a positive effect on periphyton, indicating that the decline in periphyton biomass in warmer temperatures was due to increased grazing activity. Similarly, Elster et al. (2001) reported decreased periphyton biomass with elevated temperature, likely due to increased consumption by chironomids. We thus conclude that the occurrence and the termination of an initially positive effect of warming on periphyton biomass and GPP in spring depend on type and phenology of periphyton grazers and their response to warming. The pattern observed in our experiment could be a likely scenario for temperate, fishless

waterbodies (such as kettle holes and temporary ponds) and has important implications for their ecosystem functioning.

4.2.3 Ecosystem consequences of seasonally distinct warming effects on periphyton

Recent evidence shows that European lakes are warming up most significantly during spring (Rier et al., 2006). Our results suggest that in spring, warming may facilitate a stronger periphyton biomass build-up (Figs. 11 and 28) which can hamper both phytoplankton through nutrient competition and macrophytes through shading (Phillips et al., 1978; Jones & Sayer, 2003; Roberts et al., 2003). In shallow lakes, losses of macrophytes induced by periphyton shading have been shown to result in regime shifts (Scheffer et al., 1993) with potentially severe consequences for several important ecosystem processes, such as habitat provision, greenhouse gas emissions, C burial, nutrient retention and consumer production (Hilt et al., 2017). Depending on the type and phenology of the prevailing periphyton grazers, a facilitating effect of warming on periphyton grazers may not be enough to fully counterbalance the spring warming effects on periphyton, cascading to other ecosystem components. The temporal dynamics of warming effects on periphyton and their bottom-up and top-down control factors will thus be decisive for future ecosystem functioning of many temperate shallow water bodies. While climate induced changes in the phenology and subsequent mismatches in species interactions have often been studied in plankton communities (Adrian et al., 2006; Nicolle et al., 2012), benthic communities deserve more attention to arrive at a comprehensive assessment of global change effects in aquatic ecosystems.

4.3 The resilience of a shallow lake to a brownification event

In the third study, the shallow, temperate lake we monitored for five years did not exhibit a full recovery from a strong, flood-induced one-year brownification event. Three years after reaching peak levels (60 mg L^{-1}), DOC concentrations were still 1.5-fold greater than pre-brownification values. The decrease of TP concentrations was even less pronounced, remaining at more than double the baseline concentrations by the end of this study. Consequently, summer phytoplankton biomass and GPP remained higher, while periphyton biomass and GPP, being negatively correlated with both DOC and TP concentrations, were lower than pre-brownification levels.

4.3.1 DOC and TP dynamics

Along with the water-level rise at Gollinsee (Fig. 17), the sharp five-fold increase in DOC concentrations (from early 2011 to the summer of 2012) was attributed to DOC leaching from the surrounding flooded degraded peatlands (through most of 2011 and early 2012), followed by an internal loading due to the reductive dissolution of iron-bound DOC in the lake sediments by mid-2012 (Brothers et al., 2014). The subsequent decrease in DOC concentrations, roughly by 30 mg L^{-1} a^{-1} in the first year after peak DOC concentrations (2012-13), was faster than the gradual water-level drop. This was likely due to bacterial (von Wachenfeldt & Tranvik, 2008) and photolytic mineralization (Granéli et al., 1996; Bertilsson & Tranvik, 2000), as well as flocculation resulting in burial in the sediments (von Wachenfeldt & Tranvik, 2008; Skoog and Arias-Esquivel, 2009). Mineralization and sedimentation can be equally strong forces throughout the year at removing organic carbon from the water column (von Wachenfeldt & Tranvik, 2008). Afterwards DOC concentrations declined at a slower rate and eventually appeared to level out at concentrations which were roughly 1.5 times greater than pre-brownification values. Rising DOC concentrations can increase bacterial DOC consumption rates by up to 68% when nutrients are not limiting (measured in a nearby lake: Schulzensee, see Attermeyer et al., 2014), with consumption rates reaching 87.8 µg C L^{-1} d^{-1} in eutrophic lakes featuring elevated bacterial growth efficiencies (Biddanda et al., 2001). Photolytic mineralization is also known to be an effective pathway for removing terrigenous organic carbon (Obernoster & Benner, 2004), with estimations (based on Bertilsson & Tranvik, 2000) suggesting that it could explain about half of our observed decrease in DOC concentrations (25.7 µg C L^{-1} d^{-1}, using the mean global radiation at Gollinsee for the year 2012 and assuming the top 2 cm water layer to have been subject to photolysis).

Concomitant decreases of DOC and Fe concentrations (Figs. 18A, 19F) indicate that the co-precipitation of DOC with iron-containing minerals (namely iron sulfide) could have also played a major role in DOC removal (Skoog and Arias-Esquivel, 2009). Prevailing anoxic conditions during peak brownification (summer 2012) would have presumably driven sulfide concentrations to increase in the water column, which in turn would have led to iron sulfide precipitation. Although we did not directly measure sulfide concentrations in the water column, the sediment surface in Gollinsee post-brownification was characterized by a fluffy black precipitate (pers. obs.), a known characteristic of sulfide. An increasing proportion of oxic sediment layers during benthic periphyton recovery (see below) might have produced a positive feedback loop inhibiting the re-release of that DOC from the sediments (Peter et al., 2017), while also intercepting the release of nutrients from the sediment (Vasconcelos et al., 2016).

Total phosphorus concentrations exhibited an even longer delay in recovery (Fig. 18B). Phosphorus released from both catchment soils and sediments during anoxic conditions was likely taken up by phytoplankton when pelagic production was boosted during the brownification event. This is corroborated by the highest recorded values of particulate phosphorus (PP) (in 2013 in the southern basin, Fig. 19B) coinciding with the highest phytoplankton GPP (Fig. 23). The assimilation of P in phytoplankton potentially ensured that it did not co-precipitate with iron when the water column became oxic again, as indicated by a lack of correlation between TP and Fe concentrations during the recovery phase. Other recorded peaks during autumn 2013 in concentrations of SRP, Fe, and Mn (Fig. 19) were likely caused by the mixing of the nutrient-rich and anoxic hypolimnion with the epilimnion following a strong summer stratification (Fig. 29).

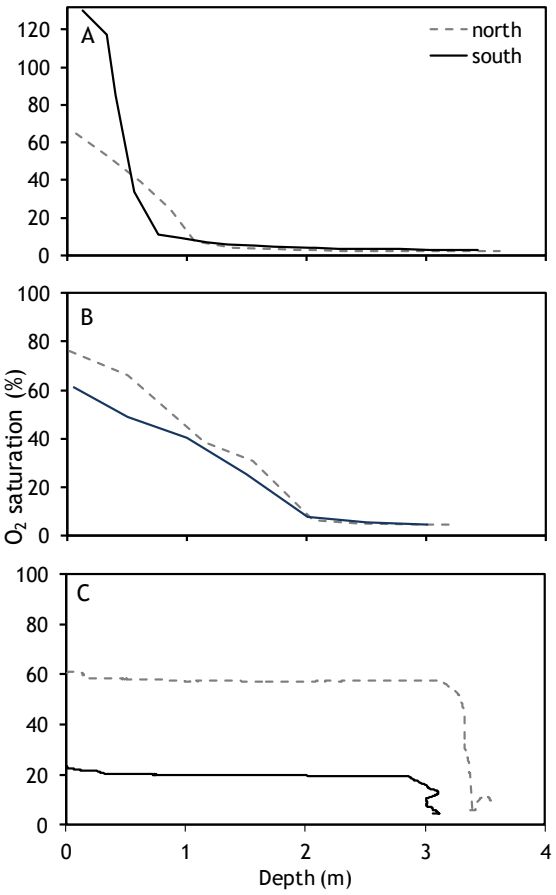

Fig. 29: Vertical oxygen profiles (percentage O_2 saturation) of both basins at Gollinsee on three dates in summer and autumn of 2013 (A: 17.07; B: 25.09; C: 25.11).

4.3.2 Response of primary producers to brownification

Phytoplankton and periphyton biomass and GPP responded in opposing manners to the brownification event and through the lake's recovery. Phytoplankton GPP was enhanced by brownification due to higher TP concentrations and compressed mixing depths, exacerbating the shading of periphyton by DOC and Fe (Jones, 1992; Brothers et al., 2014). Previous studies have reported a similar rise in pelagic GPP during brownification events, likely due to an increase in P availability (Grabowska et al., 2003; Zwart et al., 2016). Browning also alleviates pelagic algal nutrient limitation by shading benthic competitors and preventing them from intercepting the release of nutrients from the sediments (Vasconcelos et al., 2016). Consequently, light extinction (which limits GPP) and nutrient availability (which stimulates GPP) are non-linearly related to DOC concentration (Seekell et al., 2015; Kelly et al. 2018). This is also demonstrated in our results (Fig. 5), which strongly support previous theoretical model predictions on the differential response of pelagic and benthic primary producers to increasing DOC and TP concentrations (Vasconcelos et al., 2016). Higher DOC and TP concentrations coincides with a gradual increase in phytoplankton biomass and production (Fig. 30 A, B), as well as an increasing light attenuation within the water column that diminishes benthic GPP. This trend continues until crossing a threshold (yellow background line in Fig. 30 C, D) beyond which benthic algae are no longer productive. Since light attenuation is driven by both DOC and phytoplankton biomass, which is itself correlated to TP concentrations within the water column (Table 10), this threshold varies along a DOC : TP concentration spectrum. In contrast, if water quality parameters return to pre-brownification levels, the lower DOC and TP concentrations enhance and limit periphyton and phytoplankton GPP, respectively.

But while our study fits published models in theory, it covers a much wider spectrum of DOC concentrations than previously studied. Most studies to date have focused on DOC concentrations up to 20 mg L^{-1}. In our study, and due to the occurrence of the strong brownification event, DOC concentrations had spiked up to almost three-fold those amounts. This provided an excellent opportunity to test these theories further. Most published reports and models suggest that whole-lake GPP drops to negligible levels when DOC concentrations exceed a threshold of 15 mg L^{-1} due to extreme shading effects (e.g. Hanson et al 2003; Seekell et al., 2015; Kelly et al. 2018). In this study, we have shown high pelagic GPP production is still possible at much higher concentrations (Figs. 23 & 30). Light extinction by high DOC concentrations is the underlying reason for limiting GPP (Karlsson et al. 2009), yet DOC can highly differ in its color and light-absorption properties (Pace and Cole, 2002). Veritably, the light extinction coefficient corresponding to the same DOC concentrations in our study was threefold lower than the values reported in Kelly et al. 2018 (Fig. 21).

By the end of study III, the lake had experienced only a partial recovery in most measured water quality parameters. Consequently, periphyton GPP also had not reached pre-brownification (2010) levels (Fig. 23). The increase in phytoplankton biomass in 2015 might have additionally shaded the benthic algae, leading to lower production rates than in the previous year. During recovery from brownification, phytoplankton GPP fluctuated but generally declined in 2014, before again increasing in 2015 (Fig. 23). The increase in 2015 might have been caused by the severe physical disturbance of the sediments during the removal of the lake division barrier in November 2014, potentially releasing nutrients into the water column. However, water column TP concentrations in 2015 were not significantly greater than those at the end of 2014 (prior to the curtain removal), indicating that the increase in 2015 may instead have been a continuation of the previous unstable phytoplankton dynamics.

We cannot yet confirm whether Gollinsee, given more time, will fully return to its pre-brownification state. By the end of this study, the proportion of phytoplankton from the overall lake production GPP remained elevated, supported by DOC and TP concentrations that plateaued higher compared to the years prior to brownification. It has been previously hypothesized that resource pulses can cause transitions between alternative states with long lasting effects on food webs (Holt, 2008). Gollinsee was already a phytoplankton-dominated lake in 2010 (Brothers et al., 2013), but the overall increase in phytoplankton GPP during brownification and the lack of a full recovery led to a higher whole-lake GPP in 2015 compared to 2010. Contrary to the modelled results of Genkai-Kato et al. (2012), the loss in benthic production could not compensate the concurrent increase in pelagic GPP. It appears that oligotrophic, clear lakes characterized by a rich littoral production exhibit a decline in whole-system GPP following an increase in water DOC concentrations (Karlsson et al. 2009; Ask et al. 2009). The slight increase in pelagic GPP remains lower than the overall decrease in benthic GPP, which becomes limited by DOC and phytoplankton shading. In contrast, eutrophic lakes such as Gollinsee, already dominated by phytoplankton, can witness a significant increase in pelagic production generated by brownification-triggered internal nutrient loading and shallower mixing depth (Jones, 1992; Brothers et al., 2014). This can compensate for the decrease (or complete disappearance) of an already-low benthic production and drives an overall rise in whole-system GPP.

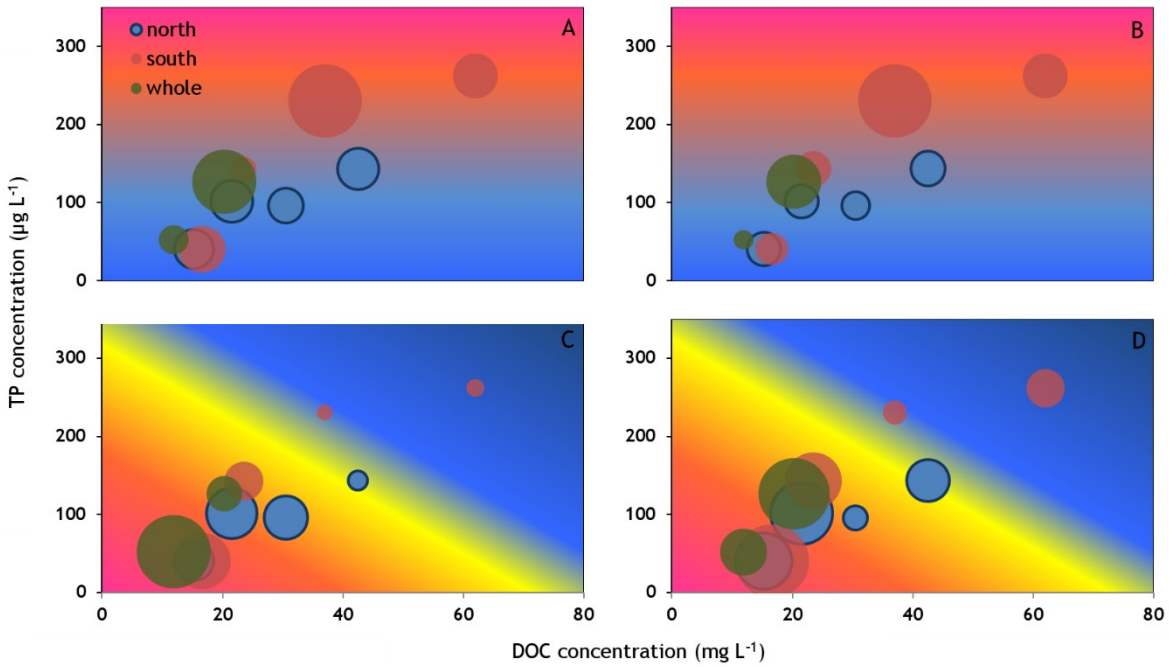

Fig. 30: Hypothesized (background) and measured (circles) summer phytoplankton gross primary production (GPP) (A) and biomass (B) and epilimnetic periphyton GPP (C) and biomass (D) in Lake Gollinsee, in relation to water column DOC and TP concentrations from 2010 to 2015. The colored background (concept taken from the model of Vasconcelos et al, 2016) indicates a gradual (A,B) or sudden (C, D) shift from favorable (red) to limited (blue) growth conditions. The size of the circles corresponds to the relative value of GPP or biomass. Blue circles represent measurements from the northern basin, red circles from the southern basin, and green circles from the whole lake during the years when the curtain splitting the lake was not deployed.

I also recorded annual differences in algal composition (Fig. 24) in study III, though I cannot confirm whether this is strictly due to DOC and nutrient changes. Nonetheless, organic nutrient bioavailability regulates planktonic composition and production (Berggren et al. 2015; Creed et al. 2018). Therefore, the effects of the source, magnitude and timing of terrestrial runoff on the proportion of the algal groups merits further investigation and clarification.

The incomplete return of DOC concentrations to pre-brownification levels might also imply that the long-term effects of extreme rainfall events contribute to the general trend of increasing DOC concentrations in freshwater systems of the northern hemisphere. A study of 120 Swedish lakes predicted that an increase in precipitation would result in greater terrestrially derived DOM concentrations and diminish the influence of in-lake processing on DOM quality (Kellerman et al., 2014). DOC concentrations and its quality can also have significant positive effects on bacterioplankton communities (Crump et al., 2003; Kritzberg et al., 2006) which in turn impact DOC mineralization rates in the system (Attermeyer et al., 2014). With higher frequency of extreme rain events expected in the region (Meehl et al., 2000; van den Besselaar

et al., 2012), the trends and impacts of such brownification events will further intensify (de Wit et al., 2016), increasing carbon export from terrestrial to aquatic sources, altering aquatic primary production and greenhouse gas emissions. It is estimated that an increase of 10% in precipitation could lead to a 30% mobilization of OC from soils to freshwaters (de Wit et al., 2016). The increase in DOC concentration in lakes across recent decades has also led to increases in OC burial rates (Anderson et al., 2014), though such impacts caused by short-term brownification events have yet to be thoroughly studied.

4.4 The larger scope of this work

As mentioned in the aims of this thesis (section 1.3), both studies I and II were part of larger projects. In study I, the efforts of quantifying carbon sequestration by the primary producers were helpful in understanding the underlying mechanisms of the landscape carbon fluxes (Attermeyer et al., 2016; Premke et al., 2016), the drivers of bacterial processes in the water column (Attermeyer et al., 2017), the source of sediment depositions in the kettle holes (Kleeberg et al., 2016a), and finally contributed to the biogeochemical model of the kettle holes (Onandia et al., 2018).

In the second study, the results presented here highlighted the (often neglected) importance of periphyton in 1) its significant contribution to the total mesocosms (limnotrons) GPP and 2) its role in binding the system's available nutrients, thus making it unavailable to other primary producers (*e.g.* phytoplankton). The temporal GPP dynamics helped in understanding the succession of primary producers (via competition) and consumers (as food source) within the system (Fig. 28; Velthuis et al., 2017). The high periphyton biomass was a valuable food source to the macroinvertebrates and some of the larger zooplankton. Furthermore, the GPP dynamics clarified the effects of warming on the systems' greenhouse gas emissions (Aben et al., 2017).

Study III served as a nice follow-up to another sizeable study (Brothers et al., 2013b & 2014) that, as customary, had created as many new questions as the ones it had answered. Monitoring the system for additional three years provided us with valuable insight on its resilience to sudden brownification events, answered our hypotheses, and, of course, produced new questions.

5. CONCLUSIONS AND FUTURE RECOMMENDATIONS

Our investigations revealed that small, shallow, nutrient-rich freshwater systems (kettle holes) in temperate moraine landscapes have relatively high GPP rates during the summer months when they are dominated by emergent plants combined with either mixed or floating vegetation. We could also highlight how primary production produced strong cascading effects on temporal nutrient and C dynamics. It directly affected sediment C deposition, governed the availability of O_2 in the water column (through direct release from primary producers or limiting flux to and from the atmosphere by floating macrophytes) and thus indirectly impacted the aerobic mineralization rates and phosphorus concentrations in the water column. All these processes combined also govern C burial in and greenhouse gas emissions from these systems. Due to our limited sample size, more studies are needed to corroborate these results. Further studies involving kettle holes of different classifications and plant community types are also needed to determine the effects of these different groups on system GPP and C dynamics. Long-term data incorporating the frequency of dry periods and C loss by mechanisms such as CH_4 evasion would be helpful to determine landscape-scale C budgets in areas with abundant ponds and kettle holes. During very warm and dry summers as the current one and with some projections showing lower future precipitation for the region (Germer et al., 2011), there is a higher probability of these systems to dry up, leading to a sharp decrease in their C burial potential (Reverey et al., 2016), leading to higher greenhouse gas emissions. Paradoxically however, despite warmer and dryer periods coupled to global warming, more extreme rain events are expected (Meehl et al., 2000; Van den Besselaar et al., 2012), which would exacerbate the trends and impacts of brownification events in increasing carbon export from terrestrial to aquatic sources, further increasing greenhouse gas emissions. Terrestrial production in arid regions was reported to have already increased by about 12% from CO_2 fertilization in recent decades (Donohue et al., 2013). Moreover, it is estimated that an increase of 10% in precipitation could lead to a 30% mobilization of OC from soils to freshwaters (De Wit et al., 2016). Anderson et al. (2014) have reported that the increase in DOC concentration in lakes across recent decades has also led to increases in OC burial rates, but this might not hold true in small, shallow ponds and kettle holes that are susceptible to drying. This remains a particularly important aspect in need for further clarification.

Unfortunately, despite the uniqueness and importance of such systems, it seems they've been mostly overlooked so far by both researchers and legislators. That might partially be due to the methodological challenges involved in sampling these systems (as discussed above) and partly due to semantics (confusing definition and poor classification of these ecosystems), as they inhabit a transitional zone between terrestrial and aquatic habitats, and are influenced to

varying degrees by both, yet seem to be ignored by studies focusing on either ecology (Del Giorgio & Williams, 2005). Moreover, local and global climate considerations are often not integrated into temporary ponds and wetland management schemes. For instance, the international treaty for the protection of wetlands, The Ramsar Convention, does not include provisions to conserve wetlands as a climate change strategy (Finlayson et al., 2017). This is a critical omission, given their important role in C turnover and climate security that this and other recent studies (Del Giorgio & Williams, 2005; Reverey et al., 2016) have shown. Nonetheless, the large gaps and uncertainties in the processes controlling the C cycle that still exist in our knowledge need to be clarified by further research. Both the limnotron experiments (study II) and the Lake Gollinsee study (III) exhibited the complex and intricate feedback loops that could be triggered by contemporary global changes within the nutrient and carbon fluxes, as well as primary and consumer production. Study III also showed that shallow lakes might either exhibit a partial recovery or require long periods to reach a full recovery following such environmental events. With a projected increase in the number of extreme rainfall events coupled to global change, sudden brownification events might become a common phenomenon. Similar studies are needed to help us better understand the underlying mechanisms driving natural greenhouse gas emissions and ways of circumventing them.

ACKNOWLEDGEMENTS

First and foremost, I would like to extend immense gratitude to my supervisor Dr Sabine Hilt for her guidance, dedication, endless encouragement and patience. Without her this thesis would not have been completed. Further thanks go to my co-supervisors Drs Jan Köhler, Katrin Premke, and Sarian Kosten for sharing their valuable knowledge and experience with me, for their support, and for including me in many interesting discussions.

I'm forever indebted to Søren Brothers for his generous help in acting as my unofficial mentor, teaching me various methods used in this thesis, and engagement in numerous theoretical and technical discussions. Myriad blessings to Cécile Perillon, Sabine Flurry and Katrin Attermeyer for their help and guidance in the field and laboratory. Massive appreciation to all the *limnonauts* (especially Mandy Velthuis, Ralf Aben, Thijs Frenken and Susanne Stephan) for their warm welcome in the Netherlands, being the perfect colleagues and even better friends. Further thanks to all the members of the Hilt-Köhler working group for their support and camaraderie.

Enormous thanks to all the co-authors of the publications included in this thesis (Andreas Kleeberg, Thomas Kalettka, Edwin Peeters, Dedmer Van de Waal, Lisette N. de Senerpont Domis, and Ellen van Donk) for their expert contributions. Without them this work would have had far less depth.

I would like to also thank Thomas Hintze and Reinhard Hölzel for their technical help, Barbara Stein, Grit Siegert, Elke Zwirnmann, Antje Lüder, Hans-Jürgen Exner, Thomas Rossoll and Jörg Gelbrecht for help in laboratory analyses [at IGB], in addition to Nico Helmsing, Suzanne Naus-Wiezer, Erik Reichman for technical assistance at NIOO. Additional gratitude goes to all the students for their helping hands in the field and lab-work. Lastly, sincere appreciation to Iman Charara for her help with graphical software and endless kind support.

DECLARATION OF ACADEMIC INTEGRITY

I hereby declare, that the dissertation entitled "Primary production in shallow freshwater systems amid a rapidly changing world" is my own work. No sources other than those indicated have been used. All collaboration that has taken place with other researchers is indicated. This thesis has not been submitted for a doctoral degree at any other institution.

REFERENCES

Aben, R. C. H., N. Barros, E. van Donk, T. Frenken, S. Hilt, G. Kazanjian, L. P. M. Lamers, E. T. H. M. Peeters, J. G. M. Roelofs, L. N. de Senerpont Domis, S. Stephan, M. Velthuis, D. B. Van de Waal, M. Wik, B. F. Thornton, J. Wilkinson, T. Del Sontro, & S. Kosten, 2017. Cross continental increase in methane ebullition under climate change. Nature Communications 8: 1682.

Abril, G., J. M. Martinez, L. F. Artigas, P. Moreira-Turcq, M. F. Benedetti, L. Vidal, T. Meziane, J. H. Kim, M. C. Bernardes, N. Savoye, J. Deborde, E. L. Souza, P. Albéric, M. F. Landim de Souza & F. Roland, 2014. Amazon River carbon dioxide outgassing fuelled by wetlands. Nature 505: 395–398.

Adrian, R., S. Wilhelm. & D. Gerten, 2006. Life-history traits of lake plankton species may govern their phenological responses to climate warming. Global Change Biology 12: 652-661.

Allen, A. P., J. F. Gillooly & J. H. Brown, 2005. Linking the global carbon cycle to individual metabolism. Functional Ecology 19: 202–213.

Anderson, N. J., H. Bennion, & A. F. Lotter, 2014. Lake eutrophication and its implications for organic carbon sequestration in Europe. Global Change Biology 20: 2741–2751.

Armstrong, N., D. Planas, & E. Prepas, 2003. Potential for estimating macrophyte surface area from biomass. Aquatic Botany 75: 173–179.

Asaeda, T., M. Sultana, J. Manatunge, & T. Fujino, 2004. The effect of epiphytic algae on the growth and production of *Potamogeton perfoliatus* L. in two light conditions. Environmental and Experimental Botany 52: 225–238.

Attermeyer, K., K. Premke, T. Hornick,S. Hilt, & H. P. Grossart. 2013. Ecosystem-level studies of terrestrial carbon turnover reveal contrasting roles for bacterial metabolism in different aquatic habitats. Ecology 94: 2754–2766.

Attermeyer, K., T. Hornick, Z. E. Kayler, A. Bahr, E. Zwirnmann, H.-P. Grossart, & K. Premke, 2014. Enhanced bacterial decomposition with increasing addition of autochthonous to allochthonous carbon without any effect on bacterial community composition. Biogeosciences 11: 1479–1489.

Attermeyer, K., S. Flury, R. Jayakumar, P. Fiener, K. Steger, V. Arya, F. Wilken, R. van Geldern, & K. Premke, 2016. Invasive floating macrophytes reduce greenhouse gas emissions from a small tropical lake. Scientific Reports 6: 20424.

Attermeyer, K., H.-P. Grossart, S. Flury, & K. Premke, 2017. Bacterial processes and biogeochemical changes in the water body of kettle holes - mainly driven by autochthonous organic matter? Aquatic Sciences 79: 675–687

Badiou, P., R. McDougal, D. Pennock & B. Clark, 2011. Greenhouse gas emissions and carbon sequestration potential in restored wetlands of the Canadian prairie pothole region. Wetlands Ecology and Management 19: 237–256.

Baird, D.J., T. E. Gates & R. W. Davies, 1987. Oxygen conditions in two prairie pothole lakes during winter ice cover. Canadian Journal of Fisheries and Aquatic Sciences 44: 1092–1095.

Bastviken, D., L. Persson, G. Odham & L. J. Tranvik, 2004. Degradation of dissolved organic matter in oxic and anoxic lake water. Limnology and Oceanography 49: 109–116.

Battin, T. J., S. Luyssaert, L. A. Kaplan, A. K. Aufdenkampe, A. Richter & L. J. Tranvik, 2009. The boundless carbon cycle. Nature Geoscience 2: 598–600.

Bécares, E., J. Gomá, M. Fernández-Aláez, C. Fernández-Aláez, S. Romo, M. R. Miracle, A. Ståhl-Delbanco, L.-A. Hansson, M. Gyllström, W. J. Van de Bund, E. Van Donk, T. Kairesalo, J. Hietala, D. Stephen, D. Balayla, & B. Moss, 2008. Effects of nutrients and fish on periphyton and plant biomass across a European latitudinal gradient. Aquatic Ecology 42: 561–574.

Bertilsson, S., & L. J. Tranvik, 2000. Photochemical transformation of dissolved organic matter in lakes. Limnology & Oceanography 45: 753–762.

Best, E. P. H., 1982. The aquatic macrophytes of Lake Vechten. Species composition, spatial distribution and production. Hydrobiologia 95: 65–77.

Biddanda, B., Ogdahl, M. & J. Cotner, 2001. Dominance of bacterial metabolism in oligotrophic relative to eutrophic waters. Limnology and Oceanography 46: 730–739.

Blindow, I., A. Hargeby, J. Meyercordt & H. Schubert, 2006. Primary production in two shallow lakes with contrasting plant form dominance: A paradox of enrichment? Limnology and Oceanography 51: 2711–2721.

Bridgeman, T. B., J. D. Chaffin, D. D. Kane, J. D. Conroy, S. E. Panek, & P. M. Armenio, 2012. From River to Lake: Phosphorus partitioning and algal community compositional changes in Western Lake Erie. Journal of Great Lakes Research 38: 90–97.

Brock, T. C. M., M. van den Bogaert, A. R. Bos, S. W. F. van Breukelen, R. Reiche, J. Terwoert, R. E. M. Suykerbuyk, R. M. M. Roijackers, R. Van Wijngaarden, B. J. Budde, J. Tijink, A. Zuppellit, & P. Leeuwangh, 1992. Fate and effects of the insecticide Dursban® 4E in indoor *Elodea*-dominated and macrophyte-free freshwater model ecosystems: II. Secondary effects on community structure. Archives of Environmental Contamination and Toxicology 23: 391–409.

Brothers, S. M., S. Hilt, S. Meyer & J. Köhler, 2013a. Plant community structure determines primary productivity in shallow, eutrophic lakes. Freshwater Biology 58: 2264–2276.

Brothers, S. M., S. Hilt, K. Attermeyer, H. P. Grossart, S. Kosten, B. Lischke, T. Mehner, N. Meyer, K. Scharnweber & J. Köhler, 2013b. A regime shift from macrophyte to phytoplankton dominance enhances carbon burial in a shallow, eutrophic lake. Ecosphere 4: 1–17.

Brothers, S., J. Köhler, K. Attermeyer, H. P. Grossart, T. Mehner, N. Meyer, K. Scharnweber, & S. Hilt, 2014. A feedback loop links brownification and anoxia in a temperate, shallow lake. Limnology and Oceanography 59: 1388–1398.

Brothers, S., Y. Vadeboncoeur & P. Sibley, 2016. Benthic algae compensate for phytoplankton losses in large aquatic ecosystems. Global Change Biology 22: 3865–3873.

Brothers, S., G. Kazanjian, J. Köhler, U. Scharfenberger & S. Hilt, 2017. Convective mixing and high littoral production established systematic errors in the diel oxygen curves of a shallow, eutrophic lake. Limnology and Oceanography: Methods 15: 429–435.

Buffam, I., M. G. Turner, A. R. Desai, P. C. Hanson, J. A. Rusak, N. R. Lottig, E. H. Stanley & S. R. Carpenter, 2011. Integrating aquatic and terrestrial components to construct a complete carbon budget for a north temperate lake district. Global Change Biology 17: 1193–1211.

Burford, M. A., A. J. Cook, C. S. Fellows, S. R. Balcombe & S. E. Bunn, 2008. Sources of carbon fuelling production in an arid floodplain river. Marine Freshwater Research 59 (3): 224–234.

Cao, Y., É. Neif, W. Li, J. Coppens, N. Filiz, T. Lauridsen, T. Davidson, M. Søndergaard, & E. Jeppesen, 2015. Heat wave effects on biomass and vegetative growth of macrophytes after long-term adaptation to different temperatures: A mesocosm study. Climate Research 66: 265–274.

Carpenter S. R., 1989. Replication and treatment strength in whole lake experiments. Ecology 70: 453–463.

Carpenter, S. R., J. J. Cole, M. L. Pace, M. Van De Bogert, D. L. Bade, D. Bastviken, C. M. Gille, J. R. Hodgson, J. F. Kitchell & S. Kritzberg, 2005. Ecosystem subsidies: Terrestrial support of aquatic food webs from 13 C addition to contrasting lakes. Ecology 86: 2737–2750.

Catalán, N., B. Obrador, M. Felip, & J. L. Pretus, 2013. Higher reactivity of allochthonous vs. autochthonous DOC sources in a shallow lake. Aquatic Sciences 75: 581–593.

Christensen, J. P. A., K. Sand-Jensen & P. A. Staehr, 2013. Fluctuating water levels control water chemistry and metabolism of a charophyte-dominated pond. Freshwater Biology 58: 1353–1365.

Cole, J. J., Y. T. Prairie, N. F. Caraco, W. H. McDowell, L. J. Tranvik, R. G. Striegl, C. M. Duarte, P. Kortelainen, J. A. Downing, J. J. Middelburg & J. Melack, 2007. Plumbing the global carbon cycle: Integrating inland waters into the terrestrial carbon budget. Ecosystems 10: 172–185.

Coloso, J. J., J. J. Cole, P. C. Hanson & M. L. Pace, 2008. Depth-integrated, continuous estimates of metabolism in a clear-water lake. Canadian Journal of Fisheries and Aquatic Sciences 65: 712–722.

Creed, I. F., J. Miller, D. Aldred, J. K. Adams, S. Spitale & R. A. Bourbonniere, 2013. Hydrologic profiling for greenhouse gas effluxes from natural grasslands in the prairie pothole region of Canada. Journal of Geophysical Research: Biogeosciences 118: 680–697.

Crump, B. C., G. W. Kling, M. Bahr, & J. E. Hobbie, 2003. Bacterioplankton Community Shifts in an Arctic Lake Correlate with Seasonal Changes in Organic Matter Source Bacterioplankton Community Shifts in an Arctic Lake Correlate with Seasonal Changes in Organic Matter Source. Applied and Environmental Microbiology 69: 2253–2268.

Davidson, T. A., J. Audet, J.-C. Svenning, T. L. Lauridsen, M. Søndergaard, F. Landkildehus, S. E. Larsen, & E. Jeppesen, 2015. Eutrophication effects on greenhouse gas fluxes from shallow-lake mesocosms override those of climate warming. Global Change Biology 21: 4449–4463.

De Wit, H. A., S. Valinia, G. A. Weyhenmeyer, M. N. Futter, P. Kortelainen, K. Austnes, D. O. Hessen, A. Räike, H. Laudon, & J. Vuorenmaa, 2016. Current Browning of Surface Waters Will Be Further Promoted by Wetter Climate. Environmental Science & Technology Letters 3: 430–435.

Dean W. E. & E. Gorham, 1998. Magnitude and significance of carbon burial in lakes, reservoirs, and peatlands. Geology 26: 535–538.

Del Giorgio, P. A. & P. J. le B Williams, 2005. Respiration in aquatic ecosystems. Oxford University Press.

Denis, L., F. Gevaert, & N. Spilmont, 2012. Microphytobenthic production estimated by in situ oxygen microprofiling: short-term dynamics and carbon budget implications. Journal of Soils and Sediments 12: 1517–1529.

DEV, 2009. Deutsche Einheitsverfahren zur Wasser-, Abwasser und Schlammuntersuchung. VCH Verlagsgesellschaft mbH, Beuth Verlag GmbH, Weinheim.

Devlin, S. P., M. J. Vander Zanden & Y. Vadeboncoeur, 2016. Littoral-benthic primary production estimates: Sensitivity to simplifications with respect to periphyton productivity and basin morphometry. Limnology and Oceanography: Methods 14: 138–149.

Domine, L. M., 2011. Mechanisms influencing carbon burial in prairie pothole shallow lakes. PhD Thesis, University of Minnesota.

Donohue, R. J., M. L. Roderick, T. R. McVicar, & G. D. Farquhar, 2013. Impact of CO_2 fertilization on maximum foliage cover across the globe's warm, arid environments. Geophysical Research Letters 40: 3031–3035.

Downing, J. A., Y. T. Prairie, J. J. Cole, et al. 2006. The global abundance and size distribution of lakes, ponds, and impoundments G.E. Likens [ed.]. Limonology and Oceanography 51: 2388–2397. doi:10.4319/lo.2006.51.5.2388

Downing, J. A., J. J. Cole, J. J. Middelburg, R. G. Striegl, C. M. Duarte, P. Kortelainen, Y. T. Prairie, & K. a. Laube, 2008. Sediment organic carbon burial in agriculturally eutrophic impoundments over the last century. Global Biogeochemical Cycles 22.

Duggan, I. C. 2001. The ecology of periphytic rotifers. Hydrobiologia 446-447: 139–148.

Eigemann, F., U. Mischke, M. Hupfer & S. Hilt, 2016. Biological indicators track differential response of pelagic and littoral areas to nutrient load reduction in German lakes. Ecological Indicators 61: 905–910.

Elster, J., J. Svoboda, & H. Kanda, 2001. Controlled environment platform used in temperature manipulation study of a stream periphyton in the Ny-Alesund, Svalbard. Nova Hedwigia, Beiheft 123: 63–75.

Euliss, N. H., R. A. Gleason, A. Olness, R. L. McDougal, H. R. Murkin, R. D. Robarts, R. A. Bourbonniere, & B. G. Warner, 2006. North American prairie wetlands are important nonforested land-based carbon storage sites. Science of the Total Environment 361: 179–188.

Evans C. D., P. J. Chapman, J. M. Clark, D. T. Monteith & M. S. Cresser, 2006. Alternative explanations for rising dissolved organic carbon export from organic soils. Global Change Biology 12: 2044–53.

Ferland, M. E., Y. T. Prairie, C. Teodoru & P. A. Del Giorgio, 2014. Linking organic carbon sedimentation, burial efficiency, and long-term accumulation in boreal lakes. Journal of Geophysical Research: Biogeosciences 119: 836-847.

Feuchtmayr, H., R. Moran, K. Hatton, L. Connor, T. Heyes, B. Moss, I. Harvey, & D. Atkinson, 2009. Global warming and eutrophication: effects on water chemistry and autotrophic communities in experimental hypertrophic shallow lake mesocosms. Journal of Applied Ecology 46: 713–723.

Filbin, G. J. & R. A. Hough, 1983. Specific leaf area, photosynthesis, and respiration in two sympatric Nymphaeaceae populations. Aquatic Botany 17: 157–165.

Filbin, G. J. & R. A. Hough, 1985. Photosynthesis, photorespiration, and productivity in Lemna minor L. Limnology and Oceanography 30: 322–334.

Finlayson, C. M., S. J. Capon, D. Rissik, J. Pittock, G. Fisk, N. C. Davidson, K. A. Bodmin, P. Papas, H. A. Robertson, M. Schallenberg, N. Saintilan, K. Edyvane, & G. Bino, 2017. Policy considerations for managing wetlands under a changing climate. Marine and Freshwater Research 68: 1803–1815.

Fischer, H. & M. Pusch. 2001. Comparison of bacterial production in sediments, epiphyton and the pelagic zone of a lowland river. Freshwater Biology 46: 1335–1348.

Frenken, T., M. Velthuis, L. N. de Senerpont Domis, S. Stephan, R. Aben, S. Kosten, E. van Donk, & D. B. Van de Waal, 2016. Warming accelerates termination of a phytoplankton spring bloom by fungal parasites. Global Change Biology 22: 299–309.

Gächter, R. & B. Müller. 2003. Why the phosphorus retention of lakes does not necessarily depend on the oxygen supply to the sediment surface. Limnology and Oceanography 48: 929–933.

Germer, S., K. Kaiser, O. Bens & R. F. Hüttl, 2011. Water Balance Changes and Responses of Ecosystems and Society in the Berlin-Brandenburg Region - a Review. Die Erde 142: 65–95.

Gessner, M. O., B. Schieferstein, U. Müller, S. Barkmann, & U. A. Lenfers, 1996. A partial budget of primary organic carbon flows in the littoral zone of a hardwater lake. Aquatic Botany 55: 93–105.

Glud, R. N., J. Woelfel, U. Karsten, M. Kühl, & S. Rysgaard, 2009. Benthic microalgal production in the Arctic: applied methods and status of the current database. Botanica Marina 52: 559–571.

Grabowska M., A. Górniak., E. Jekatierynczuk-Rudczyk & P. Zieliński, 2003. The influence of hydrology and water quality on phytoplankton community composition and biomass in a humoeutrophic reservoir, Siemianówka reservoir (Poland) – Ecohydrology and Hydrobiology 3: 185-196.

Granéli, W., 1979. A comparison of carbon dioxide production and oxygen uptake in sediment cores from four south Swedish lakes. Ecography 2: 51–57.

Granéli, W., Lindell, M. & Tranvik, L. 1996. Photo-oxidative production of dissolved inorganic carbon in lakes of different humic content. Limnol. Oceanogr. 41, 698–706.

Guillemette, F., & P. A. del Giorgio, 2011. Reconstructing the various facets of dissolved organic carbon bioavailability in freshwater ecosystems. Limnology and Oceanography 56: 734–748.

Gudasz, C., D. Bastviken, K. Steger, K. Premke, S. Sobek, & L. J. Tranvik, 2010. Temperature-controlled organic carbon mineralization in lake sediments. Nature 466: 478–481.

Hagerthey, S. E., J. J. Cole & D. Kilbane, 2010. Aquatic metabolism in the Everglades: Dominance of water column heterotrophy. Limnology and Oceanography 55: 653–666.

Hann, B. J. 1991. Invertebrate grazer — periphyton interactions in a eutrophic marsh pond. Freshwater Biology 26: 87–96.

Hanson, P. C., D. L. Bade, S. R. Carpenter, & T. K. Kratz, 2003. Lake metabolism: Relationships with dissolved organic carbon and phosphorus. Limnology and Oceanography 48: 1112–1119.

Hanson, P. C., S. R. Carpenter, N. Kimura, C. Wu, S. P. Cornelius & T. K. Kratz, 2008. Evaluation of metabolism models for free-water dissolved oxygen methods in lakes. Limnology and Oceanography: Methods 6: 454–465.

Hansson, L.A., 1992. Factors regulating periphytic algal biomass. Limnology and Oceanography 37: 322–328.

Heathcote, A. J., N. J. Anderson, Y. T. Prairie, D. R. Engstrom & P. A. Del Giorgio, 2016. Large increases in carbon burial in northern lakes during the Anthropocene. Nature Communications 6: 10016.

Hedström, P., D. Bystedt, J. Karlsson, F. Bokma, P. Byström, 2017. Brownification increases winter mortality in fish. Oecologia 183: 58-595.

Hilt, S., T. Wanke, K. Scharnweber, M. Brauns, J. Syväranta, S. Brothers, U. Gaedke, J. Köhler, B. Lischke, & T. Mehner, 2015. Contrasting response of two shallow eutrophic cold temperate lakes to a partial winterkill of fish. Hydrobiologia 749: 31–42.

Hilt, S., Brothers, S., Jeppesen, E., Veraart, A. & Kosten, S. 2017. Translating regime shifts in shallow lakes into changes in ecosystem functions and services. BioScience 67: 928-936.

Hladyz, S., S. C. Watkins, K. L. Whitworth, & D. S. Baldwin, 2011. Flows and hypoxic blackwater events in managed ephemeral river channels. Journal of Hydrology 401: 117–125.

Hocking, P. J., 1989. Seasonal dynamics of production, and nutrient accumulation and cycling by *Phragmites australis* (Cav.) Trin. ex Steudel in a nutrient-enriched swamp in Inland Australia. I. Whole Plants. Journal of Marine and Freshwater Research 40: 421–444.

Hoellein, T. J., D. A. Bruesewitz & D. C. Richardson, 2013. Revisiting Odum (1956): A synthesis of aquatic ecosystem metabolism. Limnology and Oceanography 58: 2089–2100.

Holgerson, M. A., 2015. Drivers of carbon dioxide and methane supersaturation in small, temporary ponds. Biogeochemistry 124: 305–318.

Holgerson, M. A. & P. A. Raymond, 2016. Large contribution to inland water CO_2 and CH_4 emissions from very small ponds. Nature Geoscience 9: 222–226.

Holt, R. D. 2008. Theoretical perspectives on resource pulses. Ecology 89: 671–681.

Isidorova, A., A. G. Bravo, G. Riise, S. Bouchait, E. Björn & S. Sobek, 2016. The effect of lake browning and respiration mode on the burial and fate of carbon in the sediment of two boreal lakes. Journal of Geophysical Research: Biogeosciences 121: 233–245.

IPCC Climate Change 2013: The Physical Science Basis in Contribution of Working Group I to the Fifth Assessment Report of the Intergovernmental Panel on Climate Change (eds. Stocker, T.F. et al.) pp. 1535 (Cambridge University Press, Cambridge, United Kingdom and New York, NY, USA, 2013).

Jeppesen, E., B. Kronvang, M. Meerhoff, M. Søndergaard, K. M. Hansen, H. E. Andersen, T. L. Lauridsen, L. Liboriussen, M. Beklioglu, A. Özen, & J. E. Olesen, 2009. Climate Change Effects on Runoff, Catchment Phosphorus Loading and Lake Ecological State, and Potential Adaptations. Journal of Environment Quality 38: 1930–1941.

Jones, J. I. & C. D. Sayer, 2003. Does the fish-invertebrate-periphyton cascade precipitate plant loss in shallow lakes? Ecology 84: 2155–2167.

Jones, S. E., & J. T. Lennon, 2015. A test of the subsidy–stability hypothesis: the effects of terrestrial carbon in aquatic ecosystems. Ecology 96(6): 1550–1560.

Jones, S. E., Solomon, C. T., & B. C. Weidel, 2012. Subsidy or Subtraction: How Do Terrestrial Inputs Influence Consumer Production in Lakes? Freshwater Reviews 5(1): 37–49.

Kairesalo, T. & I. Koskimies, 1987. Grazing by oligochaetes and snails on epiphytes. Freshwater Biology 17: 317–324.

Kalettka, T. 1996. Die Problematik der Sölle (Kleinhohlformen) im Jungmoränenland Nordostdeutschlands. In Naturschutz und Landschaftspflege in Brandenburg (Sonderheft) 4–13.

Kalettka, T. & C. Rudat, 2006. Hydrogeomorphic types of glacially created kettle holes in North-East Germany. Limnologica 36: 54–64.

Kalettka, T., C. Rudat & J. Quast, 2001. ‘‘Potholes’’ in Northeast German agro-landscapes: functions, land use impacts, and protection strategies. In Tenhunen, J. D., R. Lenz & R. Hantschel (eds), Ecosystem Approaches to Landscape Management in Central Europe. Ecological Studies 147: 291–298.

Karlsson, J., P. Byström, J. Ask, P. Ask, L. Persson & M. Jansson, 2009. Light limitation of nutrient-poor lake ecosystems. Nature 460(7254): 506–509.

Karlsson, J., A. K. Bergström, P. Byström, C. Gudasz, P. Rodríguez, & C. Hein, 2015. Terrestrial organic matter input suppresses biomass production in lake ecosystems. Ecology 96: 2870–2876.

Kazanjian, G., S. Flury, K. Attermeyer, T. Kalettka, A. Kleeberg, K. Premke, J. Köhler, & S. Hilt, 2018. Primary production in nutrient-rich kettle holes and consequences for nutrient and carbon cycling. Hydrobiologia Springer International Publishing 806: 77–93.

Kazanjian, G., M. Velthuis, R. Aben, S. Stephan, E. T. H. M. Peeters, T. Frenken, J. Touwen, F. Xue, S. Kosten, D. B. Van De Waal, L. N. De Senerpont Domis, E. Van Donk, & S. Hilt, 2018b. Impacts of warming on top-down and bottom-up controls of periphyton production. Scientific Reports 8: 9901.

Kellerman, A. M., T. Dittmar, D. N. Kothawala, and L. J. Tranvik. 2014. Chemodiversity of dissolved organic matter in lakes driven by climate and hydrology. Nat. Commun. 5: 1–8. doi:10.1038/ncomms4804

Kelly, P. T., Solomon, C. T., Weidel, B. C., & S. E. Jones, 2014. Terrestrial carbon is a resource, but not a subsidy, for lake zooplankton. Ecology 95(5): 1236–1242.

Kelly, P. T., N. Craig, C. T. Solomon, B. C. Weidel, J. A. Zwart, & S. E. Jones, 2016. Experimental whole-lake increase of dissolved organic carbon concentration produces unexpected increase in crustacean zooplankton density. Global Change Biology 22: 2766–2775.

Kenning, J. M, 2009. Carbon dioxide sequestration and heterotrophy in shallow lakes. PhD Thesis, University of Minnesota.

Kerr, J. L., D. S. Baldwin, & K. L. Whitworth, 2013. Options for managing hypoxic blackwater events in river systems: A review. Journal of Environmental Management 114: 139–147.

Koenings, J.P. & F.F. Hooper, 1976. The influence of colloidal organic matter on iron and iron-phosphorus cycling in an acid bog lake. Limnology and Oceanography 21: 684-696.

Kishi, D., Murakami, M., Nakano, S. & K. Maekawa, 2005. Water temperature determines strength of top-down control in a stream food web. Freshwater Biology 50: 1315–1322

Kleeberg, A., C. Herzog & M. Hupfer, 2013. Redox sensitivity of iron in phosphorus binding does not impede lake restoration. Water Research 47: 1491–1502.

Kleeberg, A., M. Neyen & T. Kalettka, 2016a. Element-specific downward fluxes impact the metabolism and vegetation of kettle holes. Hydrobiologia 766: 261–274.

Kleeberg, A., M. Neyen, U. K. Schkade, T. Kalettka & G. Lischeid, 2016b. Sediment cores from kettle holes in NE Germany reveal recent impacts of agriculture. Environmental Science and Pollution Research 23: 7409–7424.

Klotz, R. L., 2013. Factors driving the metabolism of two north temperate ponds. Hydrobiologia 711: 9–17.

Körner, S. & H. Kühl, 1996. Submerged macrophytes in the treated sewage channel Wuhle (Berlin, Germany). Internationale Revue der gesamten Hydrobiologie 81: 385–397.

Kosten, S., A. Kamarainen, E. Jeppesen, E. H. Van Nes, E. T. H. M. Peeters, N. Mazzeo, L. Sass, J. Hauxwell, N. Hansel-Welch, T. L. Lauridsen, M. Søndergaard, R. W. Bachmann, G. Lacerot, & M. Scheffer, 2009. Climate-related differences in the dominance of submerged macrophytes in shallow lakes. Global Change Biology 15: 2503–2517.

Kosten, S., F. Roland, D. M. L. Da Motta Marques, E. H. Van Nes, N. Mazzeo, L. D. S. L. Sternberg, M. Scheffer, & J. J. Cole, 2010. Climate-dependent CO_2 emissions from lakes. Global Biogeochemical Cycles 24: GB2007.

Kratina, P., H. S. Greig, P. L. Thompson, T. S. A. Carvalho-Pereira, & J. B. Shurin, 2012. Warming modifies trophic cascades and eutrophication in experimental freshwater communities. Ecology 93: 1421–1430.

Kritzberg, E. S., Langenheder, S. & E. S. Lindström, 2006. Influence of dissolved organic matter source on lake bacterioplankton structure and function - Implications for seasonal dynamics of community composition. FEMS Microbiology Ecology 56: 406–417.

Kritzberg, E. S. & S. M. Ekstrom, 2012. Increasing iron concentrations in surface waters - a factor behind brownification? Biogeosciences 9: 1465-1478.

Kritzberg, E. S., W. Granéli, J. Björk, C. Brönmark, P. Hallgren, A. Nicolle, A. Persson, & L. A. Hansson. 2014. Warming and Browning of Lakes: Consequences for Pelagic Carbon Metabolism and Sediment Delivery. Freshwater Biology 59: 325–336.

Lassen, M. K., Nielsen, K. D., Richardson, K., Garde, K. & L. Schlüter, 2010. The effects of temperature increases on a temperate phytoplankton community - A mesocosm climate change scenario. Journal of Experimental Marine Biology and Ecology 383: 79–88.

Lenard, T. & W. Ejankowski, 2017. Natural water brownification as a shift in the phytoplankton community in a deep hard water lake. Hydrobiologia 787: 153–166.

Liboriussen, L. & E. Jeppesen, 2003. Temporal dynamics in epipelic, pelagic and epiphytic algal production in a clear and a turbid shallow lake. Freshwater Biology 48: 418–431.

Liboriussen, L., F. Landkildehus, M. Meerhoff, M. E. Bramm, M. Søndergaard, K. Christoffersen, K. Richardson, M. Søndergaard, T. L. Lauridsen, & E. Jeppesen, 2005. Global warming: Design of a flow-through shallow lake mesocosm climate experiment. Limnology and Oceanography: Methods 3: 1–9.

Liboriussen, L., T. L. Lauridsen, M. Søndergaard, F. Landkildehus, M. Søndergaard, S. E. Larsen, & E. Jeppesen, 2011. Effects of warming and nutrients on sediment community respiration in shallow lakes: an outdoor mesocosm experiment. Freshwater Biology 56: 437–447.

Lischeid, G. & T. Kalettka, 2012. Grasping the heterogeneity of kettle hole water quality in Northeast Germany. Hydrobiologia 689: 63–77.

Lischke, B., Weithoff, G., Wickham S.A., Attermeyer, K., Grossart, H.P., Scharnweber, K., Hilt, S., & U. Gaedke, 2016. Large biomass of small feeders: Ciliates may dominate herbivory in eutrophic lakes. Journal of Plankton Research, 38: 2–15.

Lorenz, S., J. J. Rasmussen, A. Süß, T. Kalettka, B. Golla, P. Horney, M. Stähler,, B. Hommel & R. B. Schäfer, 2017. Specifics and challenges of assessing exposure and effects of pesticides in small water bodies. Hydrobiologia 793: 213-224.

Luthardt, V. & F. Dreger, 1996. Ist-Zustandsanalyse und Bewertung der Vegetation von Söllen in der Uckermark. Naturschutz und Landschaftspflege in Brandenburg. Sonderheft Sölle, UNZE, Golm, 31–38.

Mahdy, A. et al. 2015. Effects of water temperature on summer periphyton biomass in shallow lakes: a pan- European mesocosm experiment. Aquatic Science 77: 499–510.

Masclaux, H., Bec, A. & Bourdier, G. 2012. Trophic partitioning among three littoral microcrustaceans: relative importance of periphyton as food resource. Journal of Limnology 71 : 261–266.

McGowan, S., P. R. Leavitt, R. I. Hall, N. J. Anderson, E. Jeppesen, & B. V Odgaard, 2005. Controls of algal abundance and community composition during ecosystem state change. Ecology 86: 2200–2211.

McIntyre, P. B., Michel, E. & Olsgard, M. 2006. Top-down and bottom-up controls on periphyton biomass and productivity in Lake Tanganyika. Limnology and Oceanography 51: 1514–1523.

Meehl, G. A., Zwiers, F., Evans, J., Knutson, T., Mearns, L., & Whetton, P. 2000. Trends in extreme weather and climate events: issues related to modeling extremes in projections of future climate change. Bulletin of the American Meteorological Society 81: 427–436.

Meerhoff, M. et al. 2012. Environmental warming in shallow lakes: A review of potential changes in community structure as evidenced from space-for-time substitution approaches. Advances in Ecological Research 46: 259–349.

Mitchell, S. F., 1989. Primary production in a shallow eutrophic lake dominated alternately by phytoplankton and by submerged macrophytes. Aquatic Botany 33: 101–110.

Mitsch, W. J. & J. G. Gosselink, 1993. Wetlands (2nd ed.). Van Nostrand Reinhold, New York.

Moody, C. S., Worrall, F., Evans, C. D. & Jones, T. G. 2013. The rate of loss of dissolved organic carbon (DOC) through a catchment. Journal of Hydrology 492: 139–150.

Mooij, W. M., Janse, J. H., Domis, L. N. D. S., Hülsmann, S. & Ibelings, B. W. 2007. Predicting the effect of climate change on temperate shallow lakes with the ecosystem model PCLake. Hydrobiologia 584, 443–454.

Moorthi, S. D., J. A. Schmitt, A. Ryabov, I. Tsakalakis, B. Blasius, L. Prelle, M. Tiedemann, & D. Hodapp, 2016. Unifying ecological stoichiometry and metabolic theory to predict production and trophic transfer in a marine planktonic food web. Philosophical Transactions of the Royal Society B: Biological Sciences 371: 20150270.

Mouthon, J. & M. Daufresne, 2008. Population dynamics and life cycle of *Pisidium amnicum* (Müller) (Bivalvia : Sphaeriidae) and *Valvata piscinalis* (Müller) (Gastropoda : Prosobranchia) in the Saône river, a nine-year study. Annales de Limnologie - International Journal of Limnology 44: 241–251.

Nicolle, A., P. Hallgren, J. Von Einem, E. S. Kritzberg, W. Granéli, A. Persson, C. Brönmark, & L.-A. Hansson, 2012. Predicted warming and browning affect timing and magnitude of plankton phenological events in lakes: a mesocosm study. Freshwater Biology 57: 684–695.

Ning, N.P., Petrie, R., Gawne, B., Nielsen, D., & G. Rees, 2014. Hypoxic blackwater events suppress the emergence of zooplankton from wetland sediments. Aquatic Sciences, 1-10.

Nitzsche, K., V. Verch, K. Premke, A. Gessler & Z. E. Kayler, 2016. Visualizing land-use and management complexity within biogeochemical cycles of an agricultural landscape. Ecosphere 7: e01282.

Obernosterer, I. & R. Benner, 2004. Competition between biological and photochemical processes in the mineralization of dissolved organic carbon. Limnology and Oceanography 49, 117–124.

Obrador, B., P. A. Staehr & J. P. Christensen, 2014. Vertical patterns of metabolism in three contrasting stratified lakes. Limnology and Oceanography 59: 1228–1240.

Onandia, G., G. Lischeid, T. Kalettka, A. Kleeberg, M. Omari, K. Premke, & G. B. Arhonditsis, 2018. Biogeochemistry of natural ponds in agricultural landscape: Lessons learned from modeling a kettle hole in Northeast Germany. Science of The Total Environment 634: 1615–1630.

Pace, M. L., & J. J. Cole, 2002. Synchronous variation of dissolved organic carbon and color in lakes. Limnology and Oceanography 47(2): 333–342.

Pace, M. L. & Y. T. Prairie, 2005. Respiration in lakes, p. 103–122. In P. A. del Giorgio and P. J. L. B. Williams [eds.], Respiration in aquatic ecosystems. Oxford Univ. Press.

Parmesan, C. & G. Yohe, 2003. A globally coherent fingerprint of climate change impacts across natural systems. Nature 421: 37–42.

Patrick, D. A., N. Boudreau, Z. Bozic, G. S. Carpenter, D. M. Langdon, S. R. LeMay, S. M. Martin, R. M. Mourse, S. L. Prince, & K. M. Quinn, 2012. Effects of climate change on late-season growth and survival of native and non-native species of watermilfoil (*Myriophyllum* spp.): Implications for invasive potential and ecosystem change. Aquatic Botany 103: 83–88.

Pätzig, M., T. Kalettka, M. Glemnitz & G. Berger, 2012. What governs macrophyte species richness in kettle hole types? A case study from Northeast Germany. Limnologica 42: 340–354.

Peter, S., O. Agstam & S. Sobek. 2017. Widespread release of dissolved organic carbon from anoxic boreal lake sediments. Inland Waters 7: 151-163.

Pettit, N. E., D. P. Ward, M. F. Adame, D. Valdez & S. E. Bunn, 2016. Influence of aquatic plant architecture on epiphyte biomass on a tropical river floodplain. Aquatic Botany 129: 35–43.

Phillips, G. L., Eminson, D. & Moss, B. 1978. A mechanism to account for macrophyte decline in progressively eutrophicated freshwaters. Aquatic Botany 4: 103–126.

Prairie, Y. T., D. F. Bird & J. J. Cole, 2002. The summer metabolic balance in the epilimnion of southeastern Quebec lakes. Limnology and Oceanography 47: 316–321.

Premke, K., K. Attermeyer, J. Augustin, A. Cabezas, P. Casper, D. Deumlich, J. Gelbrecht, H. Gerke, A. Gessler, H. P. Grossart, S. Hilt, M. Hupfer, T. Kalettka, Z. E. Kayler, G. Lischeid, M. Sommer & D. Zak, 2016. The importance of landscape complexity for carbon fluxes on the landscape level: Small-scale heterogeneity matters. WIREs Water 3: 601–617.

R Core Team, 2017. R: A language and environment for statistical computing. R Foundation for Statistical Computing, Vienna, Austria. URL https://www.R-project.org/.

Raymond, P. A., J. Hartmann, R. Lauerwald, S. Sobek, C. McDonald & M. Hoover, 2013. Global carbon dioxide emissions from inland waters. Nature 503: 355–359.

Reeder, B. C., 2011. Assessing constructed wetland functional success using diel changes in dissolved oxygen, pH, and temperature in submerged, emergent, and open-water habitats in the Beaver Creek Wetlands Complex, Kentucky (USA). Ecological Engineering 37: 1772–1778.

Reverey, R., H. P. Grossart, K. Premke & G. Lischeid, 2016. Carbon and nutrient cycling in kettle hole sediments depending on hydrological dynamics: a review. Hydrobiologia 775: 1–20.

Revsbech, N. P., Jørgensen, B. B. & Brix, O. 1981. Primary production of microalgae in sediments measured by oxygen microprofile, $H_{14}CO_3^-$ fixation, and oxygen exchange methods. Limnology and Oceanography 26: 717–730.

Rier, S. T., Stevenson, R. J. & G. D. LaLiberte, 2006. Photo-acclimation response of benthic stream algae across experimentally manipulated light. Journal of Phycology 42: 560–567.

Roberts, E., Kroker, J., Körner, S. & A. Nicklisch, 2003. The role of periphyton during the re-colonization of a shallow lake with submerged macrophytes. Hydrobiologia 506: 525–530.

Rodríguez, P. & H. Pizarro, 2015. Phytoplankton and periphyton production and its relation to temperature in a humic lagoon. Limnologica 55: 9–12.

Rolinski, S., Horn, H., Petzoldt, T. & Paul, L. 2007. Identifying cardinal dates in phytoplankton time series to enable the analysis of long-term trends. Oecologia 153, 997–1008.

Rothe, M., A. Kleeberg, B. Grüneberg, K. Friese, M. Pérez-Mayo & M. Hupfer, 2015. Sedimentary sulphur: iron ratio indicates vivianite occurrence: A study from two contrasting freshwater systems. PLoS ONE 10: e0143737.

Roulet, N. & T. R. Moore, 2006. Environmental chemistry - Browning the waters. Nature 444: 283-284.

Sadro, S., & J.M. Melack. 2012. The effect of an extreme rain event on the biogeochemistry and ecosystem metabolism of an oligotrophic high-elevation lake. Arctic, Antarctic, and Alpine Research 44: 222–231.

Sand-Jensen, K. & P. A. Staehr, 2009. Net heterotrophy in small Danish lakes: A widespread feature over gradients in trophic status and land cover. Ecosystems 12: 336–348.

Sasser, C. E. & J. G. Gosselink, 1984. Vegetation and primary production in a floating freshwater marsh in Louisiana. Aquatic Botany 20: 245–255.

Scharnweber, K., Syväranta, J., Hilt, S., Brauns, M., Vanni, M.J. Brothers, S., Köhler, J., Knežević-Jarić, J. & Mehner T. 2014. Whole-lake experiments reveal the fate of terrestrial particulate organic carbon in benthic food webs of shallow lakes. Ecology 95: 1496–1505.

Scheffer, M., S. H. Hosper, M. L. Meijer, B. Moss & E. Jeppesen, 1993. Alternative equilibria in shallow lakes. Trends in Ecology and Evolution 8: 275–279.

Scheffer, M., S. Szabó, A. Gragnani, E. H. Van Nes, S. Rinaldi, N. Kautsky, J. Norberg, R. M. M. Roijackers & R. J. M. Franken, 2003. Floating plant dominance as a stable state. Proceedings of the National Academy of Sciences of the United States of America 100: 4040–4045.

Seekell DA, Lapierre JF, Ask J, Bergström AK, Deininger A, Rodriguez P, Karlsson J. 2015. The influence of dissolved organic carbon on primary production in northern lakes. Limnology and Oceanography 60: 1276–85.

Shatwell, T., A. Nicklisch, & J. Köhler, 2012. Temperature and photoperiod effects on phytoplankton growing under simulated mixed layer light fluctuations. Limnology and Oceanography 57: 541–553.

Shurin, J. B., Clasen, J. L., Greig, H. S., Kratina, P. & Thompson, P. L. 2012. Warming shifts top-down and bottom-up control of pond food web structure and function. Philosophical Transactions of the Royal Society B 367: 3008–17.

Skoog, A.C., and V.A. Arias-Esquivel. 2009. The effect of induced anoxia and reoxygenation on benthic fluxes of organic carbon, phosphate, iron, and manganese. Science of the Total Environment 407: 6085–6092.

Sobek, S., E. Durisch-Kaiser, R. Zurbrügg, N. Wongfun, M. Wessels, N. Pasche & B. Wehrli, 2009. Organic carbon burial efficiency in lake sediments controlled by oxygen exposure time and sediment source. Limnology and Oceanography 54: 2243–2254.

Solomon, C. T., S. R. Carpenter, M. K. Clayton, J. J. Cole, J. J. Coloso, M. L. Pace, M. J. Vander Zanden, and B. C. Weidel. 2011. Terrestrial, benthic, and pelagic resource use in lakes: Results from a three-isotope Bayesian mixing model. Ecology 92: 1115–1125.

Solomon, C.T., Jones, S.E., Weidel, B.C. et al. 2015. Ecosystem Consequences of Changing Inputs of Terrestrial Dissolved Organic Matter to Lakes: Current Knowledge and Future Challenges. Ecosystems 18: 376–389.

Sommer, U., Adrian, R., Bauer, B. & Winder, M. 2012. The response of temperate aquatic ecosystems to global warming: Novel insights from a multidisciplinary project. Marine Biology 159: 2367–2377.

Spence, D. H. N. & J. Chrystal, 1970. Photosynthesis and Zonation of Freshwater Macrophytes: I. Depth Distribution And Shade Tolerance. New Phytologist 69: 205–215.

Staehr, P. A., D. Bade, G. R. Koch, C. Williamson, P. Hanson, J. J. Cole & T. Kratz, 2010. Lake metabolism and the diel oxygen technique: State of the science. Limnology and Oceanography: Methods 8: 628–644.

Staehr, P.A., J. M. Testa, W. M. Kemp, J. J. Cole, K. Sand-Jensen & S. V. Smith, 2011. The metabolism of aquatic ecosystems: history, applications, and future challenges. Aquatic Sciences 74: 15–29.

Stallard, R. F., 1998. Terrestrial sedimentation and the carbon cycle: Coupling weathering and erosion to carbon burial. Global Biogeochemical Cycles 12: 231–257.

Sterner, R. W. & Elser, J. J. 2002. Ecological stoichiometry: The biology of elements from molecules to the biosphere. Princeton Univ. Press, New Jersey, United States.

Stewart, R. I. A., M. Dossena, D. A. Bohan, E. Jeppesen, R. L. Kordas, M. E. Ledger, M. Meerhoff, B. Moss, C. Mulder, J. B. Shurin, B. Suttle, R. Thompson, M. Trimmer, & G. Woodward, 2013. Mesocosm Experiments as a Tool for Ecological Climate-Change Research. Advances in Ecological Research 3(48): 71–181.

Thrane J, Hessen DO, Andersen T. 2014. The Absorption of Light in Lakes: Negative Impact of Dissolved Organic Carbon on Primary Productivity. Ecosystems 17: 1040–52.

Tranvik, L., and Bertilsson, S., 2001. Contrasting effects of solar UV radiation on dissolved organic sources for bacterial growth. Ecology Letters 4: 458-463.

Tranvik, L. J., J. A. Downing, J. B. Cotner, and others. 2009. Lakes and reservoirs as regulators of carbon cycling and climate. Limnology and Oceanography 54: 2298–2314.

Tsai, J. W., T. K. Kratz, P. C. Hanson, and others. 2011. Metabolic changes and the resistance and resilience of a subtropical heterotrophic lake to typhoon disturbance. Canadian Journal of Fisheries and Aquatic 68: 768–780.

Twilley, R. R., L. R. Blanton, M. M. Brinson & G. J. Davis, 1985. Biomass production and nutrient cycling in aquatic macrophyte communities of the Chowan River, North Carolina. Aquatic Botany 22: 231–252.

Urrutia-Cordero, P., M. K. Ekvall, J. Ratcovich, M. Soares, S. Wilken, H. Zhang, and L. A. Hansson. 2017. Phytoplankton diversity loss along a gradient of future warming and brownification in freshwater mesocosms. Freshwater Biology 62: 1869–1878.

Vadeboncoeur, Y. & D. M. Lodge, 2000. Periphyton production on wood and sediment: substratum-specific response to laboratory and whole-lake nutrient manipulations. Journal of the North American Benthological Society 19: 68–81.

Vadeboncoeur, Y., E. Jeppesen, J. V. M. Zanden, H. Schierup, K. Christoffersen & D. M. Lodge, 2003. From Greenland to green lakes: Cultural eutrophication and the loss of benthic pathways in lakes. Limnology and Oceanography 4: 1408–1418.

Vadeboncoeur, Y., Vander Zanden, M. J. & Lodge, D. M. 2002. Putting the lake back together: Reintegrating benthic pathways into lake food web models. Bioscience 52: 44–54.

Van de Bogert, M. C., D. L. Bade, S. R. Carpenter, J. J. Cole, M. L. Pace, P. C. Hanson & O. C. Langman, 2012. Spatial heterogeneity strongly affects estimates of ecosystem metabolism in two north temperate lakes. Limnology and Oceanography 57: 1689–1700.

van den Besselaar, E. J. M., A. M. G. Klein Tank & T. A. Buishand, 2012. Trends in European precipitation extremes over 1951–2010. International Journal of Climatology 33: 2682–2689.

Vasconcelos, F. R., Diehl, S., Rodríguez, P., Hedström, P., Karlsson, J., & P. Byström, 2016. Asymmetrical competition between aquatic primary producers in a warmer and browner world. Ecology 97(10): 2580–2592.

Velthuis, M., L. N. de Senerpont Domis, T. Frenken, S. Stephan, G. Kazanjian, R. Aben, S. Hilt, S. Kosten, E. van Donk, & D. B. Van de Waal, 2017. Warming advances top-down control and reduces producer biomass in a freshwater plankton community. Ecosphere 8: e01651,

Velthuis, M., S. Kosten, R. Aben, G. Kazanjian, S. Hilt, E. T. H. M. Peeters, E. van Donk, & E. S. Bakker, 2018. Warming enhances sedimentation and decomposition of organic carbon in shallow macrophyte-dominated systems with zero net effect on carbon burial. Global Change Biology 24: 5231–5242.

Veraart, A. J., de Klein, J. J. M. & Scheffer, M. 2011. Warming can boost denitrification disproportionately due to altered oxygen dynamics. PLoS One 6: 2–7.

Verschoor, A. M., Takken, J., Massieux, B. & Vijverberg, J. 2003. The Limnotrons: a facility for experimental community and food web research. Hydrobiologia 491: 357–377.

Vis C., C. Hudon, R. Carignan & P. Gagnon, 2007. Spatial analysis of production by macrophytes, phytoplankton and epiphyton in a large river system under different water-level conditions. Ecosystems 10: 293–310.

Von Wachenfeldt, E., & L. J. Tranvik, 2008. Sedimentation in boreal lakes - The role of flocculation of allochthonous dissolved organic matter in the water column. Ecosystems 11: 803–814.

Wagle, P., X. Xiao, M. S. Torn, D. R. Cook, R. Matamala, M. L. Fischer, C. Jin, J. Dong & C. Biradar, 2014. Sensitivity of vegetation indices and gross primary production of tallgrass prairie to severe drought. Remote Sensing of Environment 152: 1–14.

Westlake, D.F., 1982. The primary productivity of water plants. In Symoens, J.J., Hooper, S.S., Compére, P. (Eds.), Studies on Aquatic Vascular Plants. Royal Botanical Society of Belgium, Brussels, 165–180.

Wetzel, R. G., 1964. Primary productivity of aquatic macrophytes. Verhandlungen der Internationalen Vereinigung für Theoretische und Angewandte Limnologie 15: 426–436.

Wetzel, R. G., 2001. Limnology: Lake and River Ecosystems. Academic Press.

Whitworth, K.L., Baldwin, D.S., Kerr, J.L., 2012. Drought, floods and water quality: drivers of a severe hypoxic blackwater event in a major river system (the southern Murray–Darling Basin, Australia). Journal of Hydrology 450–451: 190–198.

Wilkinson, G. M., Carpenter, S. R., Cole, J. J., Pace, M. L., & Yang, C. 2013. Terrestrial support of pelagic consumers: patterns and variability revealed by a multilake study. Freshwater Biology 58(10): 2037–2049.

Yvon-Durocher, G., Montoya, J. M., Woodward, G., Jones, J. I. & Trimmer, M. 2011. Warming increases the proportion of primary production emitted as methane from freshwater mesocosms. Global Change Biology 17: 1225–1234.

Yvon-Durocher, G. et al. 2015a. Five Years of Experimental Warming Increases the Biodiversity and Productivity of Phytoplankton. PLoS Biology 13: 1–22.

Yvon-Durocher, G., Dossena, M., Trimmer, M., Woodward, G. & Allen, A. P. 2015b. Temperature and the biogeography of algal stoichiometry. Global Ecology and Biogeography 24: 562–570.

Zimmer, K. D., W. O. Hobbs, L. M. Domine, B. R. Herwig, M. A. Hanson & J. B. Cotner, 2016. Uniform carbon fluxes in shallow lakes in alternative stable states. Limnology and Oceanography 61: 330-340.

Zwart, J. A., N. Craig, P. T. Kelly, S. D. Sebestyen, C. T. Solomon, B. C. Weidel, & S. E. Jones, 2016. Metabolic and physiochemical responses to a whole-lake experimental increase in dissolved organic carbon in a north-temperate lake. Limnology and Oceanography 61: 723–734.